Expression and Function of the *Nicotiana tabacum* Aquaporin *Nt*AQP1

Dissertation zur Erlangung des
naturwissenschaftlichen Doktorgrades
der Bayerischen Julius-Maximilians-Universität Würzburg

vorgelegt von

Franka Siefritz

aus

Schweinfurt

Würzburg 2002

Eingereicht am: .....

Mitglieder der Promotionskommission:

Vorsitzender: Prof. Dr. Rainer Hedrich

Gutachter: Prof. Dr. Ralf Kaldenhoff

Gutachter: Prof. Dr. Ulrich Zimmermann

Tag des Promotionskolloquiums: .....

Doktorurkunde ausgehändigt am: .....

MEIN DANK GILT...

besonders Prof. Dr. Ralf Kaldenhoff, der mir das Thema überlassen und diese Arbeit durch seine Ideen und seine Unterstützung ermöglicht hat,

Prof. Dr. Ulrich Zimmermann für die Bereitschaft sich als Gutachter meiner Arbeit zur Verfügung zu stellen,

Dr. Menachem Moshelion, Markus Albert, Norbert Uehlein für die Hilfe beim Aufbau des Protoplasten Schwellungsassays,

Prof. Dr. Melvin T. Tyree für die Messungen mit dem HPFM,

Dr. Claudio Lovisolo und Prof. Dr. Andrea Schubert für die Unterstützung und die Möglichkeit der Gaswechsel-Untersuchungen in Turin,

Prof. Dr. Christophe Maurel, Marc Bots, Prof. Dr. Titti Mariani, für die Bereitstellung wichtiger Klone und Sequenzen,

der Arbeitsgruppe Kaldenhoff, insbesondere auch den "Leihdoktoranden" anderer Lehrstühle, für den Beistand in Rat und Tat,

den Arbeitsgruppen Hedrich, Hartung und Kaiser für den Beistand in wissenschaftlichen Fragen und die Bereitstellung von Geräten,

Dr. Hilde Zimmermann für die Einführung in elegante Färbemethoden,

meiner Familie und Andreas Syfonios für den Beistand und die unendliche Geduld in allen Fragen,

den Korrekturlesern dieser Arbeit und

nicht zuletzt der Deutschen Forschungsgemeinschaft (SFB 251, 176, 567) für die finanzielle Unterstützung.

CONTENTS

ZUSAMMENFASSUNG

Hintergrund:

Nicotiana tabacum AQP1 (*Nt*AQP1) ist ein Aquaporin der Plasmamembran, das im heterologen *Xenopus laevis* Oozyten System charakterisiert wurde (Biela et al, 1999). *Nt*AQP1 erleichtert den dem Wasserpotentialgefälle folgenden Wasserfluss und ist außerdem permeabel für Harnstoff und Glycerin.

Aufgrund von Sequenzvergleichen konnte *Nt*AQP1 als Mitglied der PIP1- Familie klassifiziert werden und ist hoch homolog (91,6 % auf Proteinebene) zu *Arabidopsis thaliana* PIP1b (*At*PIP1b). Northern-Analysen zeigten *Nt*AQP1-Expression in fast allen Tabakorganen mit höchstem Niveau in der Wurzel.

Zielsetzung:

Analyse der Korrelation zwischen räumlichem und zeitlichem Expressionsmuster von *Nt*AQP1 und seiner Funktion im Wasserhaushalt *in planta.*

Ergebnisse:

Expressionsstudien:

- Morphologische Studien identifizierten apoplastische Barrieren für den Wassertransport in den Tabakwurzeln. Damit wurden Orte angezeigt, an denen erhöhte Aquaporin-Expression nötig ist, um für den Wassertransport über die Plasmamembran aufzukommen.
- Immunologische *in situ*-Studien deuteten auf eine *Nt*AQP1-Protein-Akkumulation in der Wurzelexodermis und -endodermis, im Cortex, in der Nähe der Leitbündel, im Xylemparenchym und in Zellen der Atemhöhle hin. Das Aquaporin wurde auch in longitudinalen Zellreihen der Petiolen in erhöhten Mengen gefunden (Otto et al, 2000).
- Expressionsstudien mit transgenen Pflanzen, die mit Konstrukten aus dem *Nt*aqp1-Promotor und dem stabilen Reportergen β-Glucuronidase (gus) oder dem Echtzeit-Reporter Luciferase (luc) transformiert wurden, bestätigten die *Nt*AQP1-Akkumulation in der Wurzel, dem Spross und den Petiolen, lokalisierten dessen Expression aber auch in Pollen, Adventivwurzel und Blatthaaren.
- Die *Nt*aqp1-Expression wurde während Wachstumsprozessen wie Sprossorientierung nach Gravistimulation oder Photostimulation, Samenkeimung, aber auch während der vergleichsweise schnellen circadianen Blattbewegung induziert. Die Expression wurde weiterhin durch Phytohormone, im Speziellen durch Gibberellinsäure (GA) und osmotischen Stress stimuliert.
- Northern-Analysen, LightCycler-Experimente und die Luciferase-Versuche hoben eine diurnale und sogar circadiane Expression von *Nt*aqp1 in Wurzeln und Petiolen hervor.

Funktionelle Analyse: Reverse Genetik und biophysikalische Studien

- Die Antisense-Technik wurde benutzt, um die *Nt*AQP1-Expression in Tabakpflanzen zu reduzieren. Transgene Pflanzen wurden hergestellt, verifiziert und mit Kontrollpflanzen verglichen. Die Antisense (AS)-Pflanzen zeigten eine starke Verringerung (80-95 %) der *Nt*aqp1-mRNA, eine weniger ausgeprägte Verminderung der hoch homologen *Nt*PIP1a-mRNA und keinen Effekt auf die Expression anderer Aquaporin-Genfamilien (PIP2, TIP).

Funktion von *Nt*AQP1 auf zellulärer Ebene

- Die zelluläre Membranwasserpermeabilität wurde mit einer hierfür neuentwickelten Apparatur untersucht. Der experimentelle Aufbau ermöglichte die Aufzeichnung der Protoplasten-Volumenzunahme (Schwellung), die durch einen starken osmotischen Gradienten über der Zellmembran ausgelöst wurde. Die Ergebnisse der Schwellungs-experimente sind als osmotische Membranwasserpermeabilität (P_{os}) dargestellt.
- Die Reduktion von *Nt*AQP1 durch die Antisense-Expression verminderte die zelluläre Wasserpermeabilität um mehr als 50 %.

Funktion von *Nt*AQP1 in der Gesamtpflanze

- Die hydraulische Wurzelleitfähigkeit pro Wurzeloberflächeneinheit (K_{RA}) wurde durch die "High-pressure flow meter" Methode gemessen. Die K_{RA} der Wurzeln der Antisense-Linien erreichte nur 45 % der der Kontrollen.
- Nach zwei Gefrier-Auftauzyklen des Wurzelsystems, welche eine mechanische Perforation der Zellmembranen durch Wasserkristalle zur Folge hatte, war die K_{RA} in AS- und Kontrollpflanzen nahezu identisch.
- Die K_{RA} wies eine starke diurnale und circadiane Schwankung (270 %) auf, mit einem Maximum in der Mitte der Lichtperiode, ähnlich dem Verlauf des Expressionsmusters von *Nt*aqp1 in Wurzeln.
- Unter gut gewässerten Bedingungen ergaben Gaswechsel-, Spross- (Ψ_{stem}) und Blatt-Wasserpotenial (Ψ_{leaf})-Messungen unterschiedliche Werte in AS- und Kontrollpflanzen. In wasserlimitierender Umgebung verringerte sich Ψ_{stem} und Ψ_{leaf} in beiden Pflanzenlinien. AS-Pflanzen jedoch zeigten ein negativeres Wasserpotenial als Kontrollpflanzen, obwohl eine weitere Abnahme der Transpiration in AS-Pflanzen beobachtet werden konnte.
- Tabakpflanzen, die einem stärkeren Trockenstress ausgesetzt wurden, welkten nach einigen Stunden. Quantitative Analysen belegten eine stärker ausgeprägte Welkreaktion in den AS- als in den Kontrollpflanzen.

Weitere Funktionen von *Nt*AQP1

- Der Luciferase-Assay ließ eine Korrelation der *Nt*aqp1-Expression und der relativ schnellen circadianen Tabak Blattbewegung erkennen. Die ebenfalls circadiane Expression von *Nt*AQP1 wurde durch Northern-Experimente mit RNA aus Petiolen bestätigt.
- Quantitative Studien der Blattbewegung von AS- verglichen mit Kontrollpflanzen hoben eine drastische Reduktion in Geschwindigkeit und Ausmaß der Reaktion hervor. Die extremen Unterschiede zwischen AS- und Kontrollpflanzen verringerten sich während weiterer Zyklen in Schwachlicht aufgrund der eingeschränkteren Bewegungen der Kontrollpflanzen.

Schlussfolgerungen:

- *Nt*AQP1 wurde an Orten mit erwartet hohem Wasserfluss von und zum Apoplasten oder Symplasten exprimiert. Außerdem deuteten das spezifische Verteilungsmuster und die zeitliche Expression von *Nt*AQP1 in Petiolen und dem sich biegenden Spross auf eine Beteiligung in der transzellulären Wasserbewegung hin.
- Die Reduktion von *Nt*AQP1 durch die Antisense-Expression verringerte die zelluläre P_{os}. Die *Nt*AQP1-Funktion erhöht also eindeutig die Membranwasserpermeabilität von Tabak-Wurzelprotoplasten.
- Die Abnahme der spezifischen hydraulischen Wurzelleitfähigkeit (K_{RA}) befand sich in der gleichen Größenordnung wie die Verringerung der mittleren zellulären Wasserpermeabilität. Dies weist darauf hin, dass die Aquaporin-Expression essentiell für die Aufrechterhaltung der natürlichen Wurzelleitfähigkeit ist.
- Die Verringerung von K_{RA} in AS-Pflanzen könnte der erste sichere Beweis dafür sein, dass der Weg der Wasseraufnahme von der Wurzeloberfläche in das Xylem den Übergang über Membranen, z.B. der Plasmamembran von Zellen mit Casparischem Streifen, einschließt.
- K_{RA}-Messungen vor und nach zwei Gefrier-Auftauzyklen bestätigten, dass die Funktion und Morphologie des vaskulären Systems in AS- und Kontrollpflanzen sehr ähnlich ist.
- Die Reduktion von *Nt*AQP1 resultierte in einem Wasserstresssignal, das ein Schließen der Stomata zur Folge hatte. *Nt*AQP1 scheint an der Vermeidung von Wasserstress in Tabak beteiligt zu sein.
- Die *Nt*AQP1-Funktion ist also notwendig für den Widerstand gegen extreme Wassermangel-effekte.
- *Nt*AQP1 spielt eine essentielle Rolle bei schnellen Pflanzenbewegungen und der transzellulären Wasserverschiebung.

SUMMARY

Background:

Nicotiana tabacum AQP1 (*Nt*AQP1) is a plasma membrane located aquaporin, that has been characterized in the heterologous *Xenopus laevis* oocyte system (Biela et al, 1999). It facilitates water flux towards a lower water potential and is also permeable to glycerol and urea.

Based on sequence comparisons *Nt*AQP1 was classified as a member of the PIP1- family and is highly homologous (91.6 % on protein level) to the *Arabidopsis thaliana* PIP1b (*At*PIP1b). Northern blot analysis displayed *Nt*aqp1-expression in almost all organs of tobacco, with highest levels in the root.

Objective:

Analysis of the Correlation between the Spatial and Temporal Expression Pattern of *Nt*AQP1 and its Function in Water Relation *in planta*.

Results:

Expression Studies:

- Morphological studies identified apoplastic barriers for water transport in the tobacco roots, indicating locations where increased aquaporin expression may be necessary to account for the transport of water across the plasma membrane.
- *In situ* immunological studies indicated *Nt*AQP1-protein accumulation in the root exodermis and endodermis, in the cortex, close to vascular bundles, in the xylem parenchyma and in cells of the stomatal cavities. The aquaporin was also found to be abundant in longitudinal cell-rows in the petioles (Otto et al, 2000).
- Expression studies with generated transgenic plants containing the *Nt*aqp1-promoter and the stable reporter gene β-glucuronidase (gus) or real-time reporter luciferase (luc) confirmed the *Nt*aqp1 accumulation in the root, stem and petioles but also revealed further localization in pollen grains, adventitious roots and leaf glandular hairs.
- *Nt*aqp1-expression was induced during growth processes, like stem bending after gravistimulation or photostimulation, seed germination and hypocotyl elongation as well as during the comparatively fast circadian leaf movement. The expression was further stimulated by phytohormones, especially gibberellic acid (GA) and osmotic stress.
- Northern blots, LightCycler experiments and luciferase assays displayed a diurnal and even circadian expression of *Nt*aqp1 in roots and petioles.

Functional Analysis: Reverse Genetics and Biophysical Studies

- The antisense technique was used to reduce *NtAQP*1-expression in tobacco plants. Transgenic plants were generated, verified and compared to control plants. The antisense (AS) plants exhibited a severe reduction (80-95 %) of *Nt*aqp1-mRNA, less reduction of the highly homologous *Nt*PIP1a RNA and no effect on expression of other aquaporin family genes (PIP2, TIP).

Function of *Nt*AQP1 at the Cellular Level

- The cellular membrane water permeability was investigated by a newly developed experimental setup to record the increase in protoplast volume (swelling) in response to a steep osmotic gradient. Results of the swelling assay displayed the osmotic membrane water permeability (P_{os}).
- The reduction of *Nt*AQP1 by the antisense expression decreased the overall cellular P_{os} for more than 50 %.

Function of *Nt*AQP1 at the Whole Plant Level

- The root hydraulic conductivity per unit root surface area (K_{RA}) was measured by the high-pressure flow meter method. The K_{RA} of roots from the antisense lines was about 45 % compared to controls.
- K_{RA} after two freeze-thaw cycles of the root system, which cause mechanical perforation of the cell membranes by water crystals, was almost identical in AS and control plants.
- K_{RA} displayed a strong diurnal and circadian variation with a maximum in the middle of the light period, similar to the expression pattern of *Nt*aqp1 in roots.
- Gas exchange-, stem (Ψ_{stem}) and leaf (Ψ_{leaf}) water potential measurement gave dissimilar values in AS and control plants under well-watered conditions. Under a water-limiting environment Ψ_{stem} and Ψ_{leaf} decreased in both plant lines but the AS remained at more negative water potentials than the control plants, even though a further decrease in transpiration of antisense plants was detected.
- Tobacco plants subjected to a more severe drought stress wilted after several hours. Quantitative analysis displayed a much stronger wilting reaction in the AS than in the control plants.

Further Functions of *Nt*AQP1

- The luciferase assay clearly showed a correlation of *Nt*aqp1-expression and the relatively fast circadian tobacco leaf movement. The likewise circadian expression of *Nt*aqp1 was confirmed by Northern experiments with petiole RNA.

- Quantitative studies of the leaf movement in AS compared to control plants exhibited a dramatic reduction in velocity and also in the extent of the process. The extreme differences between AS and control plants diminished during further cycles in dimmed light due to reduced movement in control plants.

Conclusions:

- *Nt*AQP1 was expressed at sites of anticipated high water fluxes from and to the apoplast or symplast. Additionally, the specific distribution pattern and temporal expression of *Nt*AQP1 in petioles and the bending stem strongly indicate a role in transcellular movement of water.
- The reduction of *Nt*AQP1 by the antisense expression decreased the overall cellular P_{os}. Conclusively, *Nt*AQP1-function increases membrane water permeability of tobacco root protoplasts.
- The decrease of the specific root hydraulic conductivity (K_{RA}) was in the same order of magnitude as the mean cellular water permeability reduction, indicating that aquaporin expression is essential in maintaining a natural root hydraulic conductance.
- Reduction of K_{RA} in AS plants might be the first definitive proof that the pathway of water uptake from the root surface to the xylem involves passage across membranes, e.g. the plasma membranes of cells in the *Casparian Band*.
- K_{RA} measurements before and after two freeze-thaw cycles confirmed that the function and morphology of the vascular system is very similar in control and antisense plants.
- The absence of *Nt*AQP1 resulted in a water stress signal, causing a certain stomatal closure. *Nt*AQP1 seems to contribute to water stress avoidance in tobacco.
- *Nt*AQP1-function is required for the resistance to extreme water depletion effects.
- *Nt*AQP1 plays an essential role in fast plant movements and transcellular water shift.

A INTRODUCTION

1 Water Uptake and Movement in Higher Plants

Water is an essential component for maintaining plant metabolism and structure. From all resources that plants need to grow and function, water is the most limiting for productivity of natural ecosystems and agriculture. For every gram of organic material made by the plant, about 500 g of water is absorbed by the roots. Water is moved from the soil through the plant, across membranes, through cells and cell walls before it escapes as vapor into the air spaces inside the leaf and diffuses to the outside atmosphere. The understanding of the uptake and loss of water by plants is very important.

Different driving forces are involved in this pathway: differences in water vapor concentration (Δc_{wv}), hydrostatic pressure ($\Delta\Psi_p$), and water potential ($\Delta\Psi_w$) (Figure A.1).

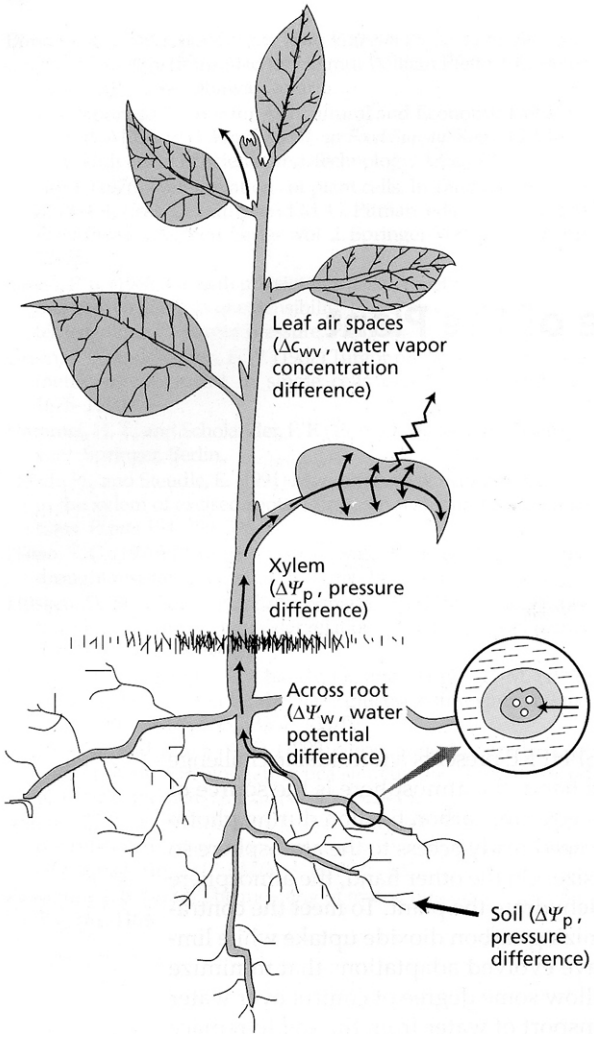

Figure A.1: Main driving forces for water flow from the soil through the plant to the atmosphere: Differences in water vapor concentration (Δcwv), hydrostatic pressure ($\Delta\Psi_p$), and water potential ($\Delta\Psi_w$).

Water potential and its components: (Taiz and Zeiger, 1998)

Location	Ψ_w	Ψ_p	Ψ_s	Ψ_g	Ψ_w gas phase
Outside air (RH=50%)	-95.2				-95.2
Internal leaf air space	-0.8				-0.8
Cell wall of mesophyll (at 2m)	-0.88	-0.7	-0.2	0.02	
Vacuole of mesophyll (at 2m)	-0.88	0.2	-1.1	0.02	
Leaf xylem (at 2m)	-0.68	-0.8	-0.1	0.02	
Root xylem	-0.6	-0.5	-0.1	0.0	
Root cell vacuole	-0.6	0.5	-1.1	0.0	
soil	-0.5	-0.4	-0.1	0.0	

The water potential $\Delta\Psi_w$ may be dissected in Ψ_s(solute) + Ψ_p(pressure) + Ψ_g(gravity). It decreases consistently from the soil to the leaves (Figure A.1). In the soil and the xylem the water moves by bulk flow in response to a pressure gradient. In the vapor phase, water moves preliminarily by diffusion, until it reaches the outside air. When water moves across membranes, the driving force is the water potential difference across the membrane. Such osmotic flow occurs when cells absorb water and when roots transport water from the soil to the xylem. In all the described situations, water moves towards regions of lower water potential or free energy.

To minimize uncontrolled water loss, the plant is protected by a water impermeable cuticle which covers almost the whole surface. Stomata in the leaves regulate the hydraulic resistance.

The root which is the organ for water uptake is protected against water loss as well. It is therefore composed of different tissues (Figure A.2): The rhizodermis, which has thin walls and lacks a cuticle to facilitate water uptake. It dies and disintegrates to default to a more persistent outer cortical layer, the exodermis. The development of the exodermis involves suberization and lignification, to protect moderately against water loss. The next zones are the root cortex and the inner most cortical cell layer, the endodermis. The endodermis contains lignified and suberized *Casparian Bands*, which form a barrier for water loss but also for apoplastic water transport (Steudle et al, 1997). The central part of the root is the stele, which mainly contains the long distance water transport vessels and the parenchyma.

For the uptake and distribution of water in the plant it has to enter the root and to surmount the tissues mentioned above to end up in the conducting tissue.

This is accomplished by three different ways (Figure A.2): (a) The apoplastic path, where water flows across cell walls and intercellular spaces, (b) the symplastic path, mediated by plasmodesmata, which involves water movement within the cytoplasmatic continuum, and (c) the transcellular pathway, where the water has to cross membranes (plasma membrane and/or tonoplast). Precise data about the relation of apoplastic or symplastic water transport to the overall water movement were not available until today (Steudle and Frensch, 1996).

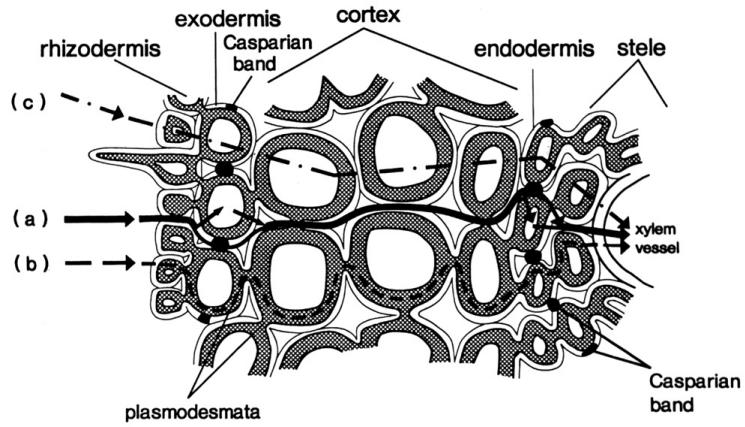

Figure A.2: Uptake of water across the root cylinder. Apoplastic barriers occur in the exo- and endodermis (Casparian Bands), which tends to interrupt the water flow across the apoplast (a). The symplastic (b) and transcellular (c) water flow can be summarized as cell to cell pathway (after Steudle, 1997).

2 Water Transport across Membranes

The passive transport of water (along the osmotic gradient) across the lipid bilayer can be accomplished by diffusion, co-transporters or aquaporins. The overall permeability of a membrane is a composition of the three distinct processes. They can be distinguished by their activation energy E_{act} and the dependence or independence of the mediated transport on the nature of the chemical gradient (Table A.1).

Table A.1: Characteristics of passive water transport across membranes mediated by diffusion, co-transporters and aquaporins.

	Diffusion	Co-transporter	Aquaporins
Activation energy (E_{act})	11-14 kcal·mol^{-1}	18 kcal·mol^{-1}	5 kcal·mol^{-1}
Dependent on nature of the chemical gradient	-	+	-

Active movement of water, necessary for transport against the water potential gradient, is achieved by co-transporters. An electrochemical potential difference is build up by an energy consuming process of active ion transport. Secondary active ion transport of co-transporters is coupled with the water transport against the water potential gradient.

Water transport across membranes plays an important role in plant water uptake and bypass of water around apoplastic barriers in the root. It is necessary for translocation of water from the cells into and out of the xylem, as well as for water release from the cells surrounding the stomatal cavity to the atmosphere in the process of transpiration. But it is also essential during cell expansion and elongation, stomatal movement or other hydronastic actions to fulfill the needs of individual cells in order to change their size, turgor and/or osmolarity.

Aquaporins which facilitate the rapid water transport across the membrane account for the high water flux which can't be explained by simple diffusion. In plant cells aquaporins have been found in the plasma membrane and the tonoplast. The integration of these proteins contributes to the control of water flux by regulation of water permeability of these membranes.

3 Aquaporins

Aquaporins are conserved membrane spanning proteins forming aqueous pores. They belong to an ancient family of major intrinsic proteins (MIP) and are highly selective for water but some are also permeable to other small solutes like glycerol (AQP0, Kushmerick et al, 1998; *Nt*AQP1, Biela et al, 1999). They facilitate the rapid water flux towards lower water potential, independent

of the gradient's chemical nature (reviews Maurel et al, 1997; Kaldenhoff et al, 1999; Eckert et al, 1999; Santoni et al, 2000).

Aquaporins were found in the animal system first (MIP26, Gorin et al, 1984) and later in virtually all organisms from bacteria to plants. Five subfamilies can be distinguished with regard to sequence homology: (a) Animal aquaporins, (b) aquaglyceroporins, (c) plant aquaporins of the plasma membrane (plasma membrane intrinsic proteins, PIPs), divided into the subfamilies PIP1 and PIP2, (d) tonoplast aquaporins (tonoplast intrinsic proteins, TIPs), and (e) nodulin-like membrane proteins.

In mammals, the significance of these aquaporins was rapidly conceived and rather obvious for specialized tissues such as the renal descending limb of Henle's Loop (Knepper et al, 1996). Water absorption rates of up to 170 $l \cdot d^{-1}$ and the fact that in renal collecting tubes the cellular water permeability can be increased by a hormone (vasopressin) led early to the suggestion of molecules responsible for water transport.

The molecular weight of most of the aquaporins characterized until today is between 25-30 kDa (van Os et al, 1994, Verkmann et al, 1996). The functional unit is the tetramer with each monomer providing an independent water channel. The spatial dimensions of the monomer are about 40 Å across and 60 Å in length (Sui et al, 2001). Sequence analysis showed that the amino and carboxy-terminal half of an aquaporin sequence exhibits a high degree of similarity and each half contains the highly conserved MIP-family NPA motif (asparagine, proline, alanine) which can be attributed to an intragenic duplication (Reizer et al, 1993). The database Prosite (http://www.expasy.ch/tools/scnpsite.html) reveals the motif [HNQA]-x-N-P-[STA]-[LIVMF]-[ST]-[LIVMF]-[GSTAFY] as MIP-characteristic for the region of the first NPA-box.

The tertiary structure of an aquaporin is composed of six transmembrane helices forming a trapezoid-like structure partially enclosing two membrane-inserted non-membrane spanning helices and two loops dipping into the membrane (Cheng et al, 1997; Walz et al, 1997; Murata et al, 2000; Ren et al, 2001) (Figure A.3). The amino as well as the carboxy terminus are orientated towards the cytoplasm (Preston et al, 1994).

The channel pore itself is dumb-bell-like when viewed in profile and consists of three topological elements: An extra cellular vestibule with a diameter of 15 Å, with polar and partially charged amino acid side chains, a constriction region or selectivity filter through the membrane of 20 Å in length and a diameter of 2.8 Å. The pore is formed by membrane-inserted non-membrane spanning helices and the two loops containing the NPA- motif, and a cytoplasmic vestibule with positively charged side chains (Heymann and Engel, 1999).

The unusual combination of a long hydrophobic pore and a minimal number of solute binding sites facilitates rapid water movement along a single file transport. Hence, the mechanism of water selectivity is a combination of channel steric and solute binding sites.

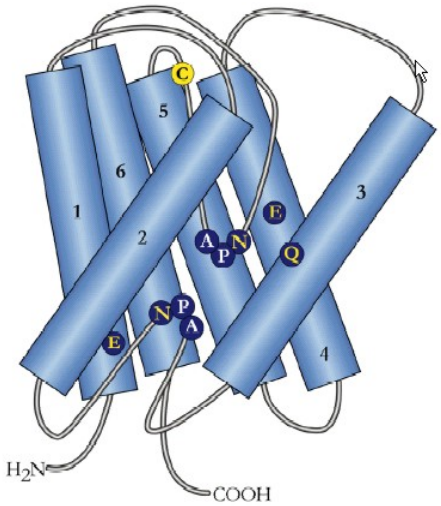

Figure A.3: Topology of a single membrane spanning MIP. Six right-hand tilted alpha helices (1-6) cross the membrane. They are linked by hydrophilic loops, two of which are slightly hydrophobic and bend inward into the protein, giving shape to a pore. These loops contain the highly conserved NPA boxes. The amino- and carboxy-terminus are localized in the cytosol. (Illustration taken from Heymann, 1998, modified).

Most evidence for aquaporin function comes from experiments in which channels have been characterized after expressing the corresponding cRNA in *Xenopus laevis* oocytes (Preston et al, 1992). Cell swelling assays in hypotonic bath solution are used to determine the membrane water permeability of the oocyte. This technique has also been applied for the identification of the first aquaporin in plants (Maurel et al, 1993).

Despite the molecular characterization of several plant aquaporins in the heterologous expression system, the question about physiological function of aquaporins in plants arises. Extensive expression studies gave first hints about the physiological processes, with a possible contribution of an aquaporin (Kaldenhoff et al, 1995 and 1996; Yamada et al, 1997).

3.1 Expression in Plants

Aquaporins display an organ-, tissue- and cell specific as well as developmental expression. For example δ-TIP, a tonoplast intrinsic protein of *Arabidopsis thaliana* is expressed in developing vascular tissues of the shoot but not in roots, while the Arabidopsis PIP1b is also expressed in roots (Daniels et al, 1996, Kaldenhoff et al, 1995). The *Nicotiana* TobRB7 is found in the root stele and the *Mesembryanthemum* MIP-A in the meristem and the xylem parenchyma (Yamamoto et al, 1991, Yamada et al, 1997). Both SunTIP-7 and SunTIP-20 of *Helianthus* are expressed in guard cells (Sarda et al, 1997).

Changes in aquaporin gene activity have been observed in various physiological and developmental processes, which may account for transient rapid translocation of relatively large volumes of water, e.g., during cell expansion and elongation (Ludevid et al, 1992; Kaldenhoff et

al, 1995 and 1996) and stomatal movement or other hydronastic actions like in motor cells of *Mimosa pudica* (Fleurat-Lessard et al, 1997; Moshelion et al, 2002) or as a strategy against osmotic or drought stress (Sarda et al, 1999).

The requirement for increased permeability on one hand and the risk of extensive water loss implicates a strong regulation of AQPs.

3.2 Regulation of Plant Aquaporins

Changes in environmental conditions as well as developmental stage specific processes like growth or differentiation require adaptation of water permeability of cellular membranes. An insufficient control of the aquaporin expression would lead to the loss of plant water balance or even to the disturbance of growth and development. This implies a stringent control of the aquaporins which can be accomplished at different levels:

- Transcriptional control, where the expression of the gene is regulated by the activity of its promoter. This mechanism includes the contribution of transcription factors which are also regulated in their synthesis, concentration, and activity. Depending on the combination of different transcription factors, the transcription is in- or decreased.

Regulation at the transcription level was shown e.g. by dramatic changes in promoter reporter gene activity for tonoplast as well as plasma membrane aquaporins (Ludevid et al, 1992; Yamada et al, 1997; Kaldenhoff et al, 1995).

- Subsequent translation of the produced mRNA is influenced by the stability and processing of the RNA.
- Control at the protein level includes protein decaying or modifying enzymes required for posttranslational modifications. Those enzymes are also regulated by factors changing their activity or stability.

Up to now two aquaporins were described to be regulated on protein level. *Vicia faba* α-TIP was shown to be *in vivo* phosphorylated by a Ca^{2+}-dependent protein kinase (Johnson et al, 1992). An identical result was achieved for PM28A, a plasma membrane aquaporin from spinach (Johansson et al, 1998). Phosphorlylation and dephosphorylation shifts aquaporins from the activated to the inactivated, less permeable state. The existence of multiple phosphorylation sites in MIPs (Reizer et al, 1993) was the first argument for this hypothesis until reports of increased permeability of α-TIP expressing *Xenopus* oocytes after addition of cAMP, adenylate cyclase activator forskolin and phosphatase inhibitor were used to verify the hypothesis (Maurel et al, 1995).

As already mentioned most of the plant aquaporins under investigation display an organ-, tissue- and cell specific as well as developmental stage specific expression. These specificities often result from the recruitment of a specific initiation complex and therefore point to a transcriptional regulation of the gene activity. The transcriptional regulation may therefore be an

important mechanism to control water balance in the plant. The promoters of these genes have to be activated or deactivated by corresponding signal transduction pathways. To date, a number of exogenous and endogenous stimuli are described to have an influence on aquaporin expression, e.g. drought, salinity, hormones and blue light (Yamaguchi-Shinozaki et al, 1992; Martinez-Ballesta et al, 2000; Philips et al, 1994; Kaldenhoff et al, 1993, 1996). The close relation between stress factors and changes in the expression of aquaporins led to the assumption that phytohormones are involved in the regulation process. This could be mainly shown for the phytohormones ABA and GA. In *Lycopersicon*, *Oryza*, *Pisum*, *Arabidopsis*, and *Craterostigma* stress treatment or changes in phytohormone concentration were shown to be correlated with alterations in aquaporin expression (Mariaux et al, 1998; Daniels et al, 1994; Kaldenhoff et al, 1996).

3.3 Plasma membrane Intrinsic Proteins (PIPs)

The number of newly found MIP sequences is still increasing very fast. About 300 are already known until today, but the majority of corresponding proteins were not further characterized by physiological and functional studies.

*At*PIP1b (AthH2) was one of the first cloned plasma membrane intrinsic proteins (Kaldenhoff et al, 1993) of *Arabidopsis thaliana*. The 30.5 kDa polypeptide is encoded by a single copy gene composed of four exons. Its promoter region contains several potential regulatory sequences including GA- and ABA-responsive elements. *At*PIP1 promoter reporter (GUS) and other studies showed that the PIP1b gene is active in virtually all tissues of young seedlings but the expression in older plants is restricted to cells which are in the process of elongation. It is activated by light and the phytohormones ABA and GA (Kaldenhoff et al, 1996).

*At*PIP1b was functionally characterized as a water channel in the heterologous *Xenopus* oocytes expression system (Kammerloher et al, 1994). In order to provide direct evidence for the aquaporin function of *At*PIP1b *in planta*, transgenic plants were generated and characterized. Antisense PIP1b-constructs were used for transformation which resulted in a dramatic decrease of PIP1b and the closely related PIP1c aquaporin expression (Kaldenhoff et al, 1998). The physiological consequence of aquaporin reduction became evident after measurement of cellular water permeability of mesophyll protoplasts. The average water permeability decreased by a factor of about three in comparison to control plants. Besides the change at the cellular level, the antisense plants developed a larger, more branched root system, which was apparently a reaction to the reduced water permeability. Despite all the advantages, the model plant Arabidopsis offers some small but crucial limitations, which led to decision to continue the aquaporin studies on another plant. One of the major reasons was the overall small size which limits the interpretation of many data obtained by physiological and biophysical experimental techniques. Among numerous possible plants, tobacco was selected for future work on plasma membrane intrinsic aquaporins because it is large enough, for example, for water flux or root pressure measurements, it is easy to transform and several tissue culture lines are available.

3.4 *Nt*AQP1 – PIP of *Nicotiana Tabacum* – Previous Work

Biela et al (1999) isolated an *At*PIP1b homologue from a tobacco cDNA library and functionally characterized it in the heterologous *Xenopus* oocyte system.

This tobacco aquaporin, named *Nt*AQP1 (*Nicotiana tabacum* Aquaporin 1) was selective for water but also permeable to glycerol and urea (Eckert et al, 1999). Patch clamp analysis of the respective oocytes clearly demonstrated *Nt*AQP1 to be impermeable for ions. Its water permeability was only moderately influenced by heavy metal ions. It displayed a water permeability coefficient (P_f) in the oocyte system of 14.5 ± 0.9 cm·s^{-1}·10^{-4} (n = 11) compared to 6.4 ± 2.4 cm·s^{-1}·10^{-4} of controls (n = 28).

Table A.2: Characteristics of water transport mediated by plant aquaporins expressed in the heterologous Xenopus oocyte system.

	P_f (cm·s^{-1}·10^{-4})	**other solutes**	**heavy metal sensitive**
Control	6.4 ± 2.4	-	-
***Nt*AQP1**	14.5 ± 0.9	glycerol, urea	-
***At*PIP2**	30.6 ± 4.9	-	+

The tissue-specific expression of *Nt*AQP1 could be shown by Northern analysis with RNA from different tissues. The studies revealed a low mRNA concentration in stems and leaves, and a high concentration in flowers and roots.

Since it is known from the studies of the *At*PIP1b promoter regulation, that aquaporins may be dramatically regulated at the level of transcription, an about 1400 bp promoter region of *Nt*aqp1 was isolated (Siefritz, 1998). Sequence analysis of the 5'-upstream region and comparison with known cis-acting elements revealed the presence of elements that activate transcription depending on the development or the phytohormones gibberrillic acid (GA) and abscisic acid (ABA). The activity of these elements was analyzed by protoplast transformation with a bicistronic construct. A region between -1374 and -1037, which encompasses the mentioned elements, is responsible for the phytohormone dependent gene regulation. The subcellular localization of *Nt*AQP1 could be shown by means of protoplast transformation, too. *Nt*AQP1 translational fusion to the green fluorescent protein (GFP) revealed that it is located in the plasma membrane and in not yet identified vesicles, reflecting the possible routing of *Nt*AQP1 from synthesis site to the integration in the membrane (Siefritz et al, 2001).

4 Objective of this Thesis

Objective: Correlation between the Spatial and Temporal Expression Pattern of *Nt*AQP1 and its Function for the Whole Plant Water Relation.

Evidence for aquaporin function comes from experiments in which channels have been characterized after expressing the corresponding cRNA in the heterologous *Xenopus laevis* oocytes system. However, their significance for the water transport physiology of multicellular organisms is still uncertain in many cases.

***Nt*AQP1 – an aquaporin from *Nicotiana tabacum* – was used to elucidate this issue.**

In order to identify apolastic barriers for water transport and thus identify sites of high water fluxes different staining methods were applied. The results can indicate locations where increased aquaporin expression may be necessary to account for the transport of water across the plasma membrane.

Expression studies of *Nt*AQP1 were performed to elucidate where and when the aquaporin is expressed and to address the question if this aquaporin may contribute to the processes of water uptake and transport.

The goal was to analyze the aquaporin function in tobacco plants at the cellular, organ, and the whole plant level.

4.1 Where and when is *Nt*AQP1 expressed in the Tobacco Plant?

Spatial and temporal expression of *Nt*AQP1 was studied in detail to get hints about possible aquaporin functions and regulation.

Transgenic tobacco plants containing the *Nt*aqp1-promoter fused to different reporter genes (gus, luc) were generated and analyzed. Additional *Nt*aqp1-mRNA and cDNA levels were studied. *In situ* immunological studies were performed to get a complete picture of the aquaporin expression.

4.2 What is the Function of *Nt*AQP1 in Water Relation?

*Nt*AQP1 was shown to be a plasma membrane intrinsic aquaporin expressed in almost all organs, with highest levels in the root. From the location of the aquaporin in the root a function in water uptake, transport and/or loading into the conducting tissue may be assumed.

In order to analyze the cellular function of an aquaporin it is important to perform assays on plant protoplasts and to determine the membrane water permeability.

In the past such measurements often relied on mercurials to perturb aquaporin function. However it can not be excluded that these heavy metals act in a nonspecific way on metabolism, membranes and proteins. Therefore, this approach is not suitable to investigate the function of one specific aquaporin, in this case *Nt*AQP1. An additional argument against the use of mercurials is the observation that *Nt*AQP1 is mercury-insensitive. Consequently a practicable way to elucidate the *Nt*AQP1-function is to knock out the aquaporin in the plant and determine the difference to the unmodified ones.

Reverse Genetics and Plant Physiology.

Tobacco plants impaired in *Nt*aqp1-expression should be used to elucidate the function of the aquaporin by comparison of physiological parameters with wild type (control) plants. Intensive but unsuccessful search for aquaporin T-DNA insertion mutants (Feldmann Lines, http://www.arabidopsis.org/abrc/feldmann.html) or *en*1-transposon tagged aquaporins (AMAZE, Max-Planck-Institut für Züchtungsforschung, Cologne) of *Arabidopsis* PIPs led to the assumption that the loss of these proteins might be lethal to the plants. Due to this fact *Nt*AQP1-deficient tobacco plants should be generated by an antisense technique which only reduces the level of the target gene expression. The *Nt*aqp1-antisense (AS) lines should subsequently be compared to control plants to answer the following questions:

4.2.1 What is the *Nt*AQP1 Function at the Cellular Level?

Since *Nt*AQP1 is a plasma membrane intrinsic aquaporin the conclusion was drawn that it may increase the cellular water permeability.

In order to prove this hypothesis the osmotic membrane water permeability (P_{os}) of AS and control protoplasts should be determined. A new protoplast swelling assay was necessary to be developed to follow the swelling kinetics of several cells at the same time without further manipulating them. Because *Nt*aqp1-expression was highest in roots and the effect in the AS expression was expected to be most evident in cells with abundant *Nt*aqp1-RNA level, root-cells were chosen for these studies.

4.2.2 What is the Function of the Aquaporin in Whole Plant Water Flux and Transport?

The working hypothesis for this part of the thesis was: *Nt*AQP1 may be involved in water uptake and transport processes by lowering the resistance to water flux.

To verify these assumptions studies were first focused on the organ level: Root hydraulic conductivity should be measured in AS and control plants. Investigations will then be extended to the whole plant level by measuring the transpiration rate, stem and leaf water potential of AS and control plants.

4.3 Are there Other Functions of *Nt*AQP1?

*Nt*aqp1-expression is not restricted to sites of water uptake. In these studies it could be shown, that *Nt*AQP1 displayed a specific pattern of distribution, e.g. in petioles and in bending stems.

In addition tobacco leaves perform a circadian sleep movement by placing the petioles from a nearly horizontal to an almost vertical position and vice versa. These hydronastic movements of plant organs involve a shift of high amounts of water in the elevating tissue.

The location in correlation with this observation strongly indicates a role of *Nt*AQP1 in transcellular movement of water, necessary in the hydronastic movement.

This hypothesis should be tested by investigation of the leaf movement of the AS and control plants.

B RESULTS

1 Expression and Function of *Nt*AQP1 in Water Uptake and Transport in Roots

1.1 Anatomy of Tobacco Roots

All plant parts exposed to the atmosphere are coated with layers of lipid material that reduce water loss and help to block the entry of pathogenic fungi and bacteria. The principal types of coating material are cutin, suberin, and waxes. Cutin can be found on most aboveground parts, while suberin is present on underground parts, woody stems, and healed wounds. Anatomic investigations of tobacco roots should reveal if there are apoplastic barriers to water transport, especially *Casparian Bands*, which increases the water transport via the cell to cell pathway.

Staining of Cross Sections of Roots and Petioles

Freehand cross sections of roots from tobacco plants (grown in hydroponic culture) were stained with different dyes to detect suberin, lignin and *Casparian Bands*.

The development of the *Casparian Bands* and suberin lamellae was observed by Berberine-Aniline Blue and Sudan Red 7B. Berberine-Aniline Blue stained structures containing the *Casparian Band*, suberin or lignin in bright yellow upon excitation with UV-light. As depicted in Figure B.1, cross sections of roots showed the stele and two rims of yellow endo- and exodermis overlaid with bluish color, typically for the quenching by the Aniline Blue of lamellar suberin staining. The endo- and exodermis contained *Casparian Bands* indicated in the pictures.

Tobacco roots grown in hydroponic culture developed a primary endodermis with a *Casparian Band* in the radial cell walls at a distance of 45-25 mm from the root tip (Figure B.1, I). At larger distances of 50-70 mm, fluorescent suberin deposits could be observed in the whole cell walls of the endodermis (Figure B.1, G). The roots also developed a continuous exodermis (hypodermis with *Casparian Band*, Figure B.1, I, F, A) with suberized walls (Figure B.1, E and I) some cells without suberin towards the cortex. At a larger distance even several suberized cell layers below the exodermis could be found (Figure B.1, A). Lateral roots could be observed (Figure B.1, J and K) about 80 mm from the root tip.

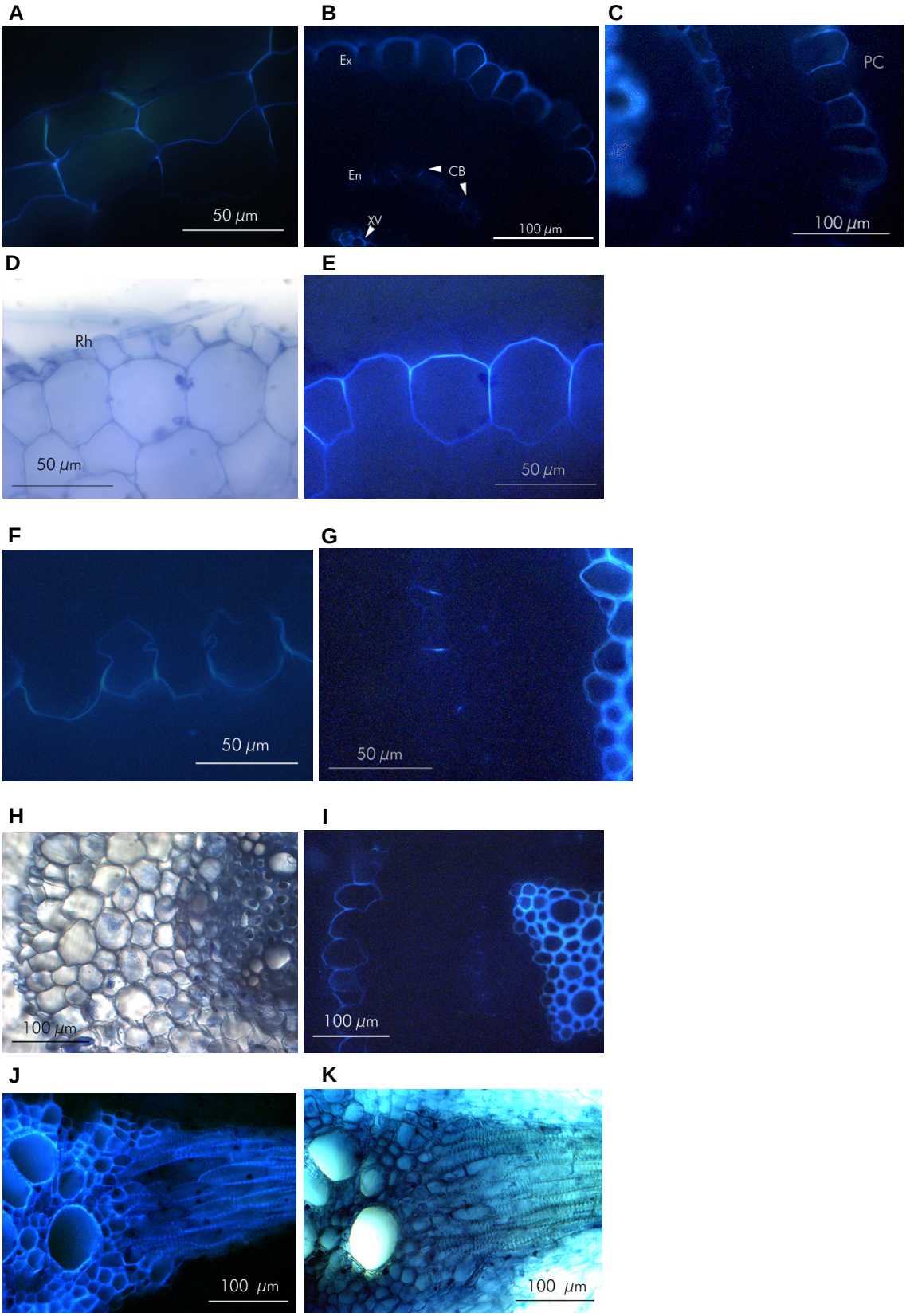

Figure B.1: Freehand root sections from different positions stained with Berberine-Aniline Blue. Sections A-I were taken from a 95 mm long tobacco root: Section A taken 70 mm from the root tip, B and C 45-65 mm from the root tip, sections D and E, 40 mm from the tip, and sections F, G, H, and I, 25-45 mm from the tip. Sections J and K depict a side root from a 40 cm long root. (Ex) Exodermis, (CB) *Casparian Band*, (En) endodermis, (XV) xylem vessels. Scale is given in every picture.

TBO stained cell walls, impregnated with lignin or other phenols, blue (Figure B.2). The pink or reddish stain of polysaccharides rich in carboxyl groups (e.g. pectic acid, alginic acid) or sulfate groups could hardly be detected. Only slight pink color could be found in the endodermis. The root sections contained lignin in the walls mainly of tracheids and vessel elements of the xylem but hardly any pectin. Lignin was deposited in the thickened secondary wall but could also occur in the primary wall and the middle lamella in close contact with the celluloses and hemicelluloses already present which explains the overall bluish staining.

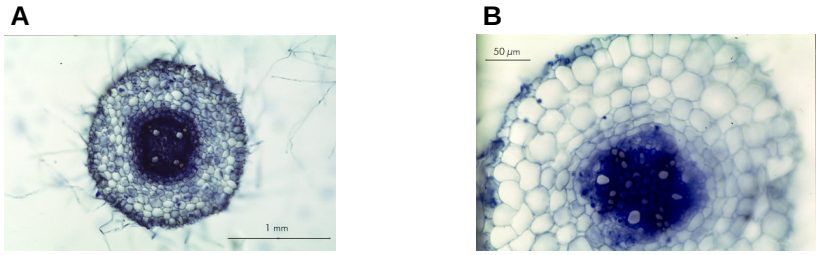

Figure B.2: A. Cross section of middle root, 80 mm from apex. B. Young root close to the apex stained with TBO. Scales are given in the pictures (A. 1 mm, B. 50 µm).

Sudan Red 7B stained the suberin lamellae (but not *Casparian Band*s) bright red. It could be detected in the endo- and exodermis of cross sections up to 5 mm from the tip (Figure B.3).

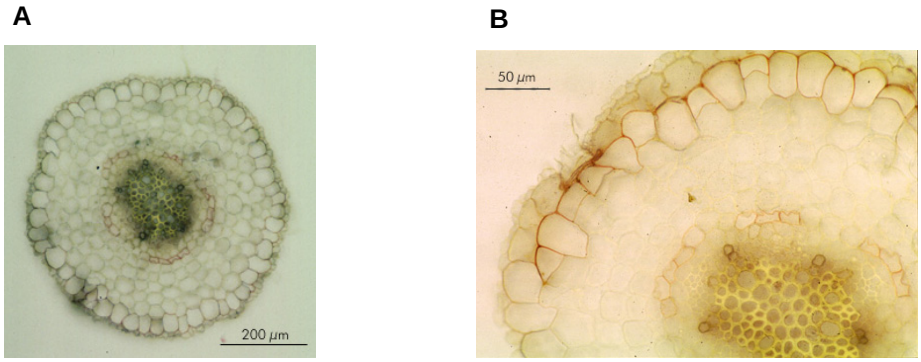

Figure B.3: Cross sections of middle root 80 mm from the apex stained with Sudan Red 7B. The suberin lamellae (but not *Casparian Band*s) are stained bright red. A. Low magnification, bar marks a distance of 200 µm. B. Higher magnification, bar marks a distance of 50 µm.

It could be seen, that tobacco plants, even grown in hydroponic culture, build up apoplastic barriers, like *Casparian Bands*. These findings showed that tobacco is suitable to work on cell to cell water transport.

1.2 NtAQP1-Expression in Roots

Northern analysis of total RNA revealed that *Nt*aqp1-mRNA was present in roots, stems and leaves (Siefritz et al, 2001). The relative concentration was highest in roots, lower in stem and comparably low in leaves. *In situ* whole mount hybridization showed a hybridization signal restricted to the foremost part of the root, which matches the apex, the elongation and differentiation zone. In older parts of the root, *Nt*aqp1-RNA was barely detectable in contrast to the protein, which could be observed by *in situ* immuno-localization in specific tissues of lignified roots (Otto and Kaldenhoff, 2000). In younger roots and at a higher magnification the tight association of *Nt*AQP1-containing cells to tracheary elements was evident. The location in older roots was found all over the root cross section with higher protein concentration at the outer border of the xylem and the cell layers of the hypodermis.

These expression studies suggested that *Nt*AQP1 occurs mainly in cells which control water flow between symplast and apoplast.

Further expression studies with tobacco plants containing *Nt*aqp1-promoter reporter constructs, Northern hybridization, LightCycler analysis and functional studies with *Nt*AQP1-antisense plants should give deeper insights in the temporal expression and the function of this aquaporin in roots. Is *Nt*AQP1, as hypothesized, involved in water uptake and in the regulation of water flux?

1.3 Further Expression Studies

The requirement for high water flux varies during the light/dark phase, but also in different developmental stages. The water flux is maintained by different driving forces, e.g. the transpirational flux, which is high in the light period and low in the dark. The transpiration is regulated by the circadian opening and closing of the stomata. Stomatal aperture is influenced by physiological properties of the plant such as the degree of water deficit or the concentration and location of plant hormones such as ABA, IAA and cytokinins. The temporal dynamics of the circadian control of stomatal movement increases the plant water-use-efficiency (carbon uptake/water loss).

The water supply for the transpirational water flux is accomplished by the root. The question arises now, if the water flux may be regulated in a diurnal way by aquaporins. Further expression studies of *Nt*AQP1 should show if this aquaporin expression is regulated in a time dependent manner and if *Nt*AQP1-expression studies on phytohormone influence on tobacco protoplasts can be confirmed *in planta* (Siefritz et al, 2001).

1.3.1 Promoter Studies at Sequence Level

Sequence analysis of the isolated *Nt*aqp1-promoter sequence (Siefritz, 1998) and comparison with gene-regulating elements of free available web databases (e.g. PLACE, http://www.dna.affrc.go.jp/htdocs/PLACE/signalscan.html) revealed the presence of putative features that regulate tissue-specific, developmental, environment and phytohormone dependent expression.

Tissue-Specificity

Root-specific sequences were highly accumulated in the *Nt*aqp1-promoter region (ROOTMOTIFTAPOX1, Elmayan and Tepfer (1995), see F4.1) only some are depicted in Figure B.4. Elmayan and Tepfer (1995) could show that this motif strongly directs expression to roots, and much less to stems and leaves.

Another putative tissue-specificity was discovered: The *Nt*aqp1-promoter showed similarities to the Lat52-promoter (late anther tomato 52, POLLEN1LELAT52, see F4.1). Lat52 encodes an abundant cysteine-rich protein and plays an essential gametophytic role in pollen hydration and tube growth demonstrated by AS down regulation in tomato (Muschietti et al, 1994). Twell showed already in 1994 that the Lat52 5'-UTR acts as tissue-specific translational activator. Taylor and Hepler (1997) suggested that germination and initial tube growth depends on translation of stored mRNAs, produced in the late stages of pollen development. Additionally, the *Nt*aqp1-promoter contained the GTGANTG10 motif (Rogers et al, 2001) at the positions -1228 (+), -850 (+), -198 (+),-936 (-), +64 (+), +278 (-). The function of the conserved GTGA motif shared between the tobacco g10 and tomato lat56 promoters was demonstrated in g10. The tobacco gene g10 is preferentially and maximally expressed in mature pollen.

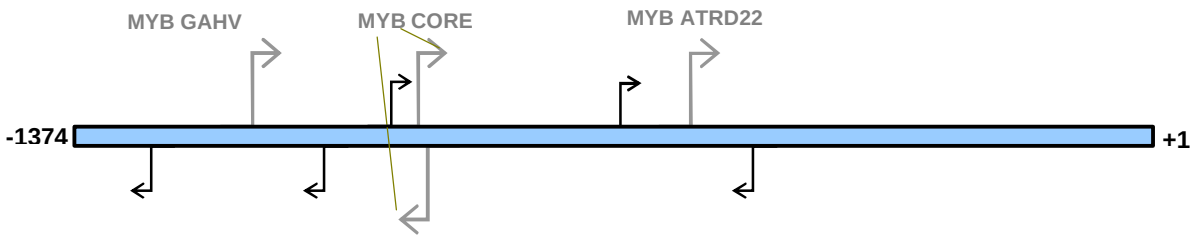

Figure B.4: Schematic presentation of the *Nt*aqp1-promoter with putative tissue-specific sequences and regulatory protein binding sites. MYB binding sites are marked in grey (specific names in the scheme), pollen-specific sites (POLLEN_LE_LAT52) are given as black arrows and root-specific sites (ROOT_MOTIF_TAPOX1) in black dotted arrows. Orientation of the motifs corresponds with the orientation of the arrows.

Environmental Regulation

Light is one of the most important factors regulating plant growth. Some of the important cis-acting elements present in light-regulated genes include GT-1 core (GGTTAA) or consensus sites (GRWAAW), I-Boxes (GATAA) and G-Boxes. None of these elements alone is able to confer light-regulation onto a non-light-regulated gene. Light-regulation arises from various combinations of different elements. Combination in pairs is required (Puente et al, 1996). The *Nt*aqp1-promoter contained all of the above mentioned motifs, except the G-BOX, in multiple copies (see appendix, F4.1).

Circadian Expression

The *Nt*aqp1-promoter region included a 'CAANNNNATC' motif (see appendix, F4.1). This motif is conserved in 5'-upstream regions of clock controlled Lhc genes and overlaps with a sequence relevant in phytochrome mediated gene expression.

To investigate the possible transcriptional regulation by the above mentioned elements, promoter reporter studies with glucuronidase (GUS) and luciferase (LUC) as well as Northern experiments and LightCycler studies were performed.

1.3.2 Glucuronidase Assay (GUS)

The GUS system is a reliable method to monitor the plant promoter activity in response to different treatments. Transgenic plants with a construct of the *Nt*aqp1-promoter (p*Nt*aqp1) fused to the functional gus gene with a nopaline-synthetase terminus (nosT) and a kanamycin resistance (nptII) were produced by Agrobacterium leaf disk transformation. The construct was produced in several subcloning steps: The 1.4 kb *Nt*aqp1-promoter fragment (sequence, see F4) was amplified by PCR with the primers *AP2* (Adapter Primer2, see F3) and *GSP-P2* (including a *Bam*HI restriction site, see F3) and cloned into pCR2.1 TOPO (F5.2). The promoter sequence was removed by *Sal*I/*Bam*HI restriction and fused into pUC 18. The linearized plasmid was fused with the 2.2 kb gus/nosT reporter gene (originating from pBI221, F5.4) via *Bam*HI/*Eco*RI restriction sites. The new p*Nt*aqp1::gus construct was transferred into the binary vector pGPTV via *Hind*III/*Eco*RI restriction sites (Figure B.5).

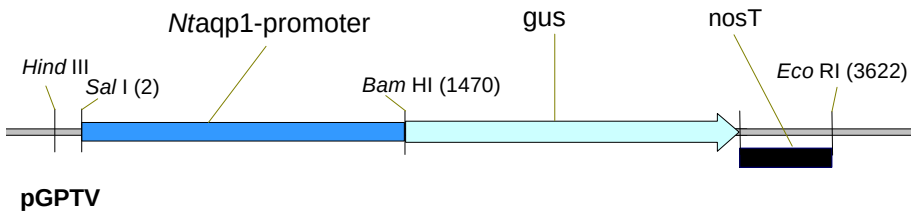

Figure B.5: Schematic representation of the p*Nt*aqp1::gus construct with nopaline-synthetase terminus (nosT) in the binary vector pGPTV (only partially shown).

Treatment with Osmoticum

Salt Treatment

Soil-grown plants were watered with a 250 mM NaCl solution for 24 h, to induce an osmotic change in the soil. Roots were isolated and subjected to GUS staining in order to monitor the response of the *Nt*aqp1-promoter on this treatment. p*Nt*aqp1::gus plants always displayed some slight expression of GUS in the roots, mainly around the root tip and in the root hair zone, less in the older parts (Figure B.6, A). Roots of the plants subjected to the osmotic treatment, exhibited increased GUS-expression all over the root (Figure B.6, C and D). A special picture could be found for short side roots, where the tips were not stained at all, but high activity could be detected all over the side roots and the main root (Figure B.6, D).

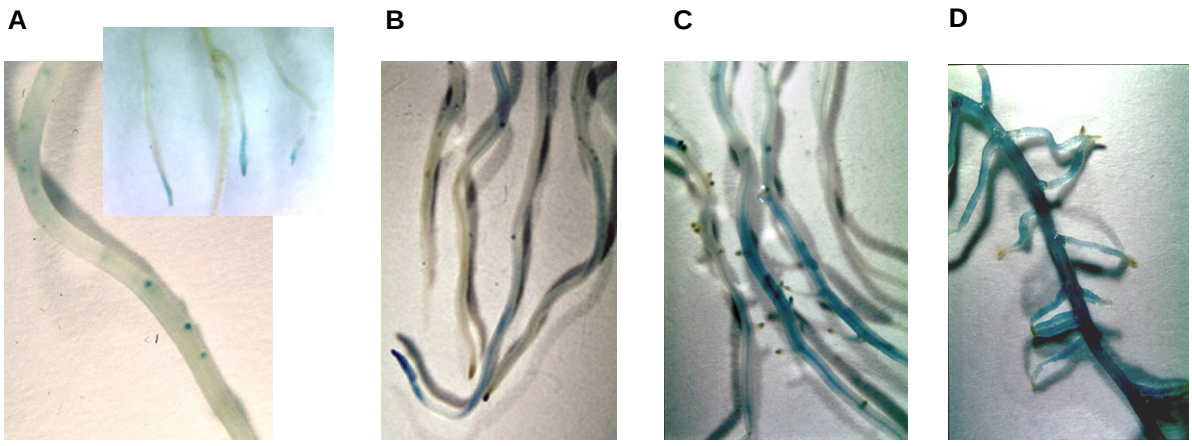

Figure B.6: GUS assay results of the salt experiment with soil grown *Nt*aqp1-promoter::gus plants. A. Roots of untreated tobacco plant. B., C., and D. Roots from tobacco plant watered with 250 mM NaCl solution.

The increased expression of *Nt*aqp1 after the addition of NaCl may lead to the conclusion that *Nt*AQP1 has an impact on osmoregulation. Or it may be a special reaction on increased Na^+- or Cl^-- ions. The exact concentration of NaCl around the root was not known, thus reliable

conclusions can only be drawn after more detailed studies. p*Nt*aqp1::gus plants were subjected to another osmotic change. They were watered with a PEG solution, to test the reaction on nonionic osmotic substances.

Further Observations

In treated as well as untreated plants a clear GUS signal could be detected at buds of lateral root (Figure B.6, A, B, C). Lateral roots were found above the elongation and root hair zone and originate from small groups of cells in the pericycle. The dividing cells gradually formed into a root apex, and the lateral root grew through the root cortex and epidermis.

*Nt*aqp1-expression seems to be involved in this developmental process.

PEG (polyethylene glycol 6000) Treatment

p*Nt*aqp1::gus plants were watered with a PEG solution of -0.35 MPa osmotic pressure for 20 h. An untreated p*Nt*aqp1::gus plant was used as control. The staining of control plants was restricted to the root hair zone (Figure B.7, A), while PEG-treated plants displayed a continuous staining at some roots except the side roots. The staining was extended from the foremost part of the tip to the base of the root (Figure B.7, B). But not all roots showed a consistent picture.

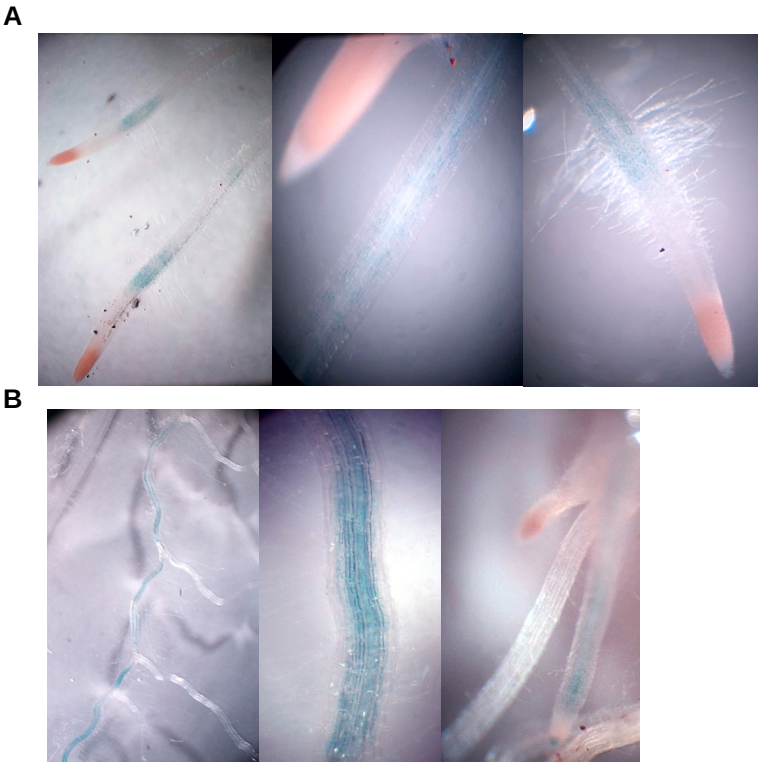

Figure B.7: GUS assay results of PEG experiment with *Nt*aqp1-promoter::gus transformed tobacco plants.

A. Untreated control and B. 20 h PEG-treated plants.

The increased expression of *Nt*aqp1 after the nonionic osmotic change led to the conclusion that *Nt*AQP1 is indeed involved in osmoregulation.

Phytohormone Influence

Sequence analysis of the *Nt*aqp1-5'-upstream region and comparison with known *cis*-acting regulatory DNA elements revealed the presence of elements that activate transcription depending on developmental stage or phytohormones gibberellic acid (TAACAAA, Skiver et al, 1991) and abscisic acid (CTAACCA, Abe et al, 1997). First results about the activity of the elements were obtained by protoplast transformation with bicistronic deletion constructs of the *Nt*aqp1-promoter in comparison to a 35SCaMV (Siefritz et al, 2001). Investigation of stable transformations of tobacco with *Nt*aqp1-promoter::gus constructs should show the activity *in planta*.

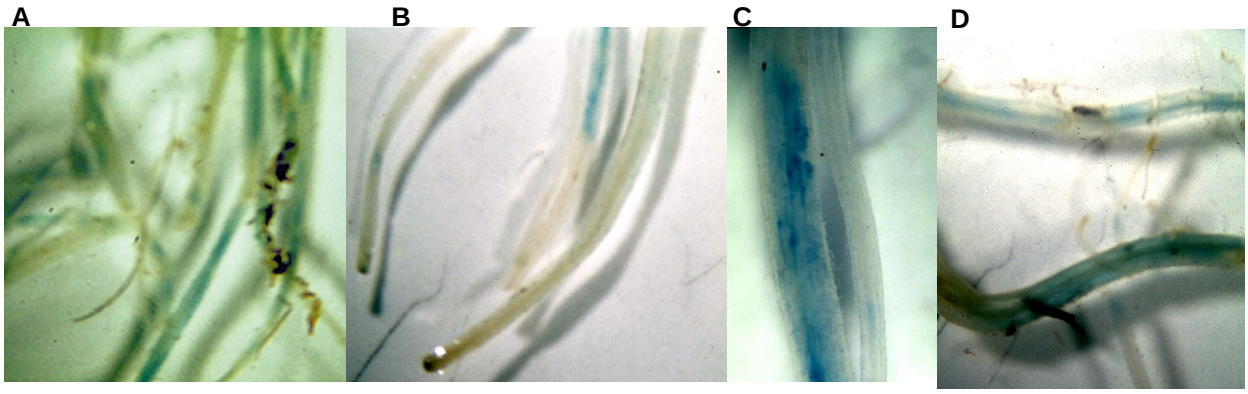

Figure B.8: GUS assay results of the phytohormone experiment on isolated roots of *Nt*aqp1-promoter:: gus plants. A. 100 nM GA, B. 100 nM ABA, C. 100 nM ABA, detailed, D 100 nM ABA, showed an induction of GUS staining.

Roots of p*Nt*aqp1::gus plants were incubated in solutions of ABA and GA. Concentrations of 10 nM, 100 nM and 10 µM were used. Untreated control roots showed GUS staining in the root tip and the root hair zone and only slight in older parts of the root (Figure B.6, Figure B.7). The treatment with the phytohormones displayed an increased expression all over the root or more concentrated in the middle parts (Figure B.8, A-D). The expression response was dose dependent. 10 nM of the phytohormones evoked only slight GUS staining, even less than in controls. This may be due to inhibitory effect on the *Nt*aqp1-expression. 100 nM and 10 µM concentration of GA exhibited the above described increase of expression, like the 100 nM ABA, while the 10 µM ABA showed less expression than the 100 nM concentration, but still higher than without phytohormone at all. Since the expression is very variable from root to root, these results are only preliminary and have to be confirmed by other methods of higher temporal resolution.

Studies with the luciferase reporter could give clearer results of the time point of the expression and the impact of phytohormones.

1.3.3 Luciferase Assay (LUC)

Luciferase catalyzes the oxidative decarboxylation of luciferin. A photon is released in the catalytic cycle with the substrate. The luciferase is blocked after the reaction, because of the slow release of oxyluciferin from the enzyme complex (chapter D, Figure D.6). Therefore, luciferase as a reporter represents gene expression as the flux of protein molecules (LUC) made in the cell (LUC/sec), while more stable reporter genes only show the accumulation of protein molecules as an indication of gene expression (total amount of reporter protein in the cell at any given time point). Consequently, luciferase can be used as a non-invasive reporter in plants to accurately mark qualitative differences (spatial and temporal variations) in transgene expression.

Transgenic plants containing the *Nt*aqp1-promoter fused to the functional luc^{+}-cDNA with a 35SCaMV terminus (35Ster) and a kanamycin resistance (nptII) were produced by Agrobacteria leaf disk transformation (D10.1). The construct was produced in several subcloning steps: The 1.4 kb *Nt*aqp1-promoter fragment was amplified by PCR with the antisense primer *NtAQP1prom as XhoI* (including a *Xho*I restriction site, see F3) and the sense primer *NtAQP1prom s Kpn I* (including a *Kpn*I restriction site, see F3) and cloned into pCR2.1 TOPO. The promoter sequence was removed by *Xho*I/*Kpn*I restriction and ligated 5' to the luc-cDNA contained in pBlueskriptSKL (Eckert 2000) substituting the 35SCaMV promoter (removed by *Xho*I/*Kpn*I restriction). The p*Nt*aqp1::luc 35Ster construct was ligated into pUC 18 by the *Bam*HI/*Kpn*I restriction sites. The new p*Nt*aqp1::luc construct was transferred into the binary vector pGPTV via *Hind*III/*Eco*RI restriction sites.

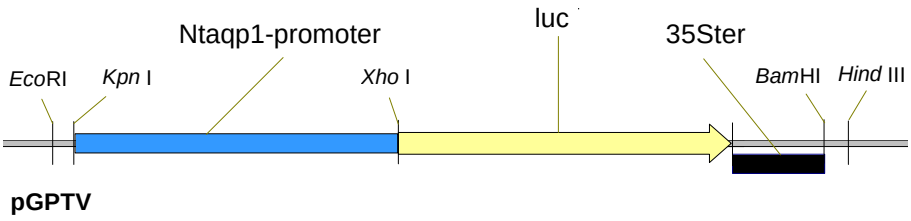

Figure B.9: Schematic representation of the p*Nt*aqp1::luc construct with 35SCaMV terminus (35Ster) in the binary vector pGPTV (only partially shown).

p*Nt*aqp1::luc transformants were tested for luciferase activity with the *in vitro* luciferase assay (D11.2.2).

GA Treatment

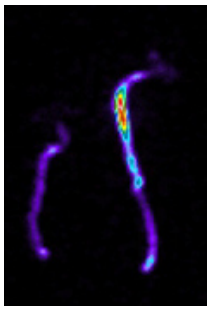

Figure B.9a: Result of the luciferase assay on p*Nt*aqp1::luc seedlings grown on wet filter paper without phytohormone (left seedling) and on plates containing 50 nM GA (right seedling). Image of luciferase activity is depicted with false color scales (blue indicating low activity, red indicating high activity, white shows overload).

p*Nt*aqp1::luc seedlings were grown on filter paper wet with water containing 50 nM GA or without phytohormone. Luciferin was added to the medium and the luciferase activity was monitored with the luminometer. Transgenic plants exhibited an increased expression in the hypocotyl of GA-treated tobacco seedlings (Figure B.9a). This phytohormone induced the *Nt*aqp1-expression.

*Nt*AQP1 seems to be involved in the phytohormone induced cell elongation during seedling development. Further investigations were done on the temporal expression of *Nt*aqp1 during germination a process where GA plays an essential role.

Germination

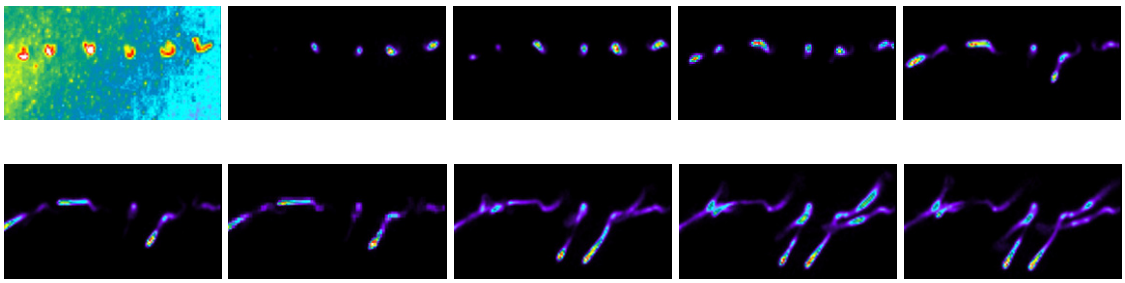

Figure B.10: Time course of luciferase assay on p*Nt*aqp1::luc seeds, germinating on filter paper, subjected to luciferin in the medium. Images of luciferase activity are depicted with false color scales (blue indicating low activity, red indicating high activity, white shows overload).

p*Nt*aqp1::luc seeds were germinated on wet filter paper and supported by luciferin in the water. As depicted in Figure B.10, four of the six transgenic seeds showed expression, while two didn't present any luminescence. During the process of germination the luciferase activity increased in the four seeds and was also turned on in the two other ones. The *Nt*aqp1-expression was highly regulated during this process. It was turned on with hydration, increased during breaking of the radicle through the seed coat, decreased afterwards and turned on again in a defined moment in the root tip when highest water uptake is required. *Nt*AQP1 seemed to be involved in seedling expansion and development and in the uptake of increasing amounts of water.

1.3.4 Northern Analysis

Diurnal and Circadian Expression

Root RNA was isolated from plants, subjected to either a continuous day/night (12 h/12 h) rhythm or to day/night and subsequent darkness. For each time point three plants of each treatment were used. Northern blot was performed with [α-^{32}P]dCTP probes against *Nt*aqp1 and 28S RNA.

The level of *Nt*aqp1-RNA content, correlated to the highest 28S-hybridization signal, ranged between 35-84 % (Figure B.11, A C) in day/night treatment, and between 45-83 % in continuous darkness (Figure B.11 B, D). The maximum *Nt*aqp1-expression in day/night cycle was found at 10:00 AM, while in continuous darkness it was shifted to 2:00 AM. Also the minimum was shifted for 4 h, from 6:00 PM to 10:00 PM.

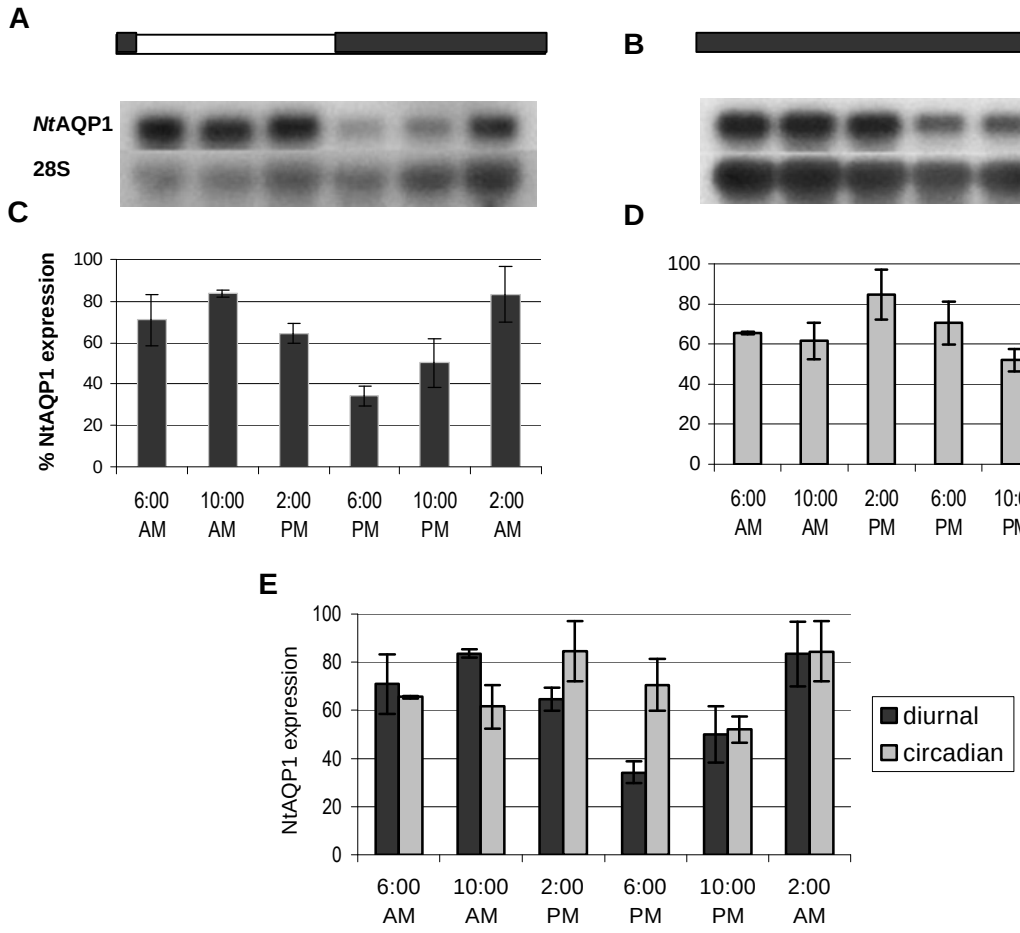

Figure B.11: Typical time course of *Nt*aqp1-expression in roots. Bars above the diagrams and pictures symbolize the photoperiod.
A. Northern blot of root RNA isolated from tobacco subjected to day/night light rhythm. Samples are taken at different times of day and night: upper row shows hybridization with [α-^{32}P]dCTP labeled *Nt*aqp1-, lower row with [α-^{32}P]dCTP labeled 28S-probe. B. Northern blot of root RNA isolated from tobacco subjected to continuous darkness. C. Diagram of evaluations of three independent Northern blots of day/night light rhythm, D. Diagram of evaluations of three independent Northern blots of continuous darkness. E. Summary of the diagrams. Standard errors are given in black bars.

It was shown, that *Nt*aqp1 was expressed in a day/night rhythm and also in a circadian manner. It displayed a pattern similar to the circadian aperture of the stomata. This implicates that also the water permeability may vary due to aquaporin expression and may be correlated with the need of high water supply during the day. Studies of the root hydraulic conductivity in the functional analysis of *Nt*AQP1 should confirm this hypothesis.

1.3.5 LightCycler Analysis

Diurnal and Circadian Expression

A similar pattern for diurnal expression of *Nt*aqp1 could be found in LightCycler experiments (Figure B.12). Root RNA was isolated from plants, subjected to either a continuous day/night (12 h/12 h) rhythm. cDNA was derived from the mRNA (D5.2). Actin was used as internal standard in the PCR amplification step (details are described in section B3.1.4). The highest value of *Nt*aqp1-expression related to the actin standard was set to 100 %.

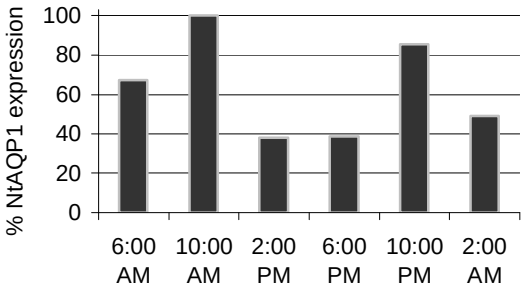

Figure B.12: Diagram of the results of the LightCycler experiments on diurnal expression of *Nt*aqp1. The highest value of relative *Nt*aqp1-expression related to the actin standard was set to 100 %.

The maximum of *Nt*aqp1-expression in the day/night cycle was found at 10:00 AM, like in the Northern studies. The minimum of 38 % was determined at 2:00 PM and 6:00 PM. These studies were supplementary to the Northern blots and should be repeated at least twice to get standard errors and with that reliable results.

1.4 Functional Analysis of *Nt*AQP1 in Tobacco Roots

The molecular function of several aquaporins is well characterized, e.g. by analysis of aquaporin-expressing *Xenopus* oocytes. However, their significance in the physiology of water transport of multicellular organisms is still uncertain in many cases. To elucidate the physiological role of this aquaporin, *Nt*aqp1 -antisense plants were constructed to study the effect of aquaporin deficiency at cellular and whole plant level.

1.4.1 Construction of *Nt*AQP1-Antisense Plants

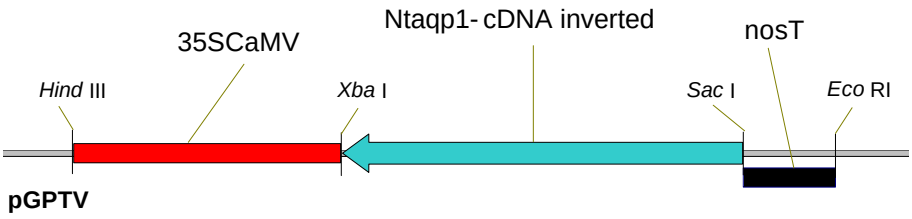

Figure B.13: Schematic representation of the *Nt*aqp1-antisense construct (pNtAQP1AS) with nopaline-synthetase terminus (nosT) in the binary vector pGPTV (only partially shown).

Tobacco plants, impaired in *Nt*aqp1-expression, were generated by leaf disc transformation with an antisense *Nt*AQP1-construct, driven by the strong constitutive 35SCaMV promoter together with a kanamycin resistance marker gene (nptII).

Therefore, the *Nt*aqp1 1.2 kb full-length cDNA (AJ001416.1, GI: 2385377) was cloned in an inverse orientation into the binary vector pGPTV (11kb) 3' to a 35SCaMV promoter and 5' to a nopaline-synthetase terminus. This was achieved by restriction of the cDNA containing plasmid (pGEMHE) with *Sac*I (5' of the cDNA) and *Xba*I (3' to the cDNA) and ligation of the fragment into the 35SCaMV promoter (5' to *Xba*I) and nopaline-synthetase terminus (3' *Sac*I) containing vector pGPTV (with 35SgusnosT-cassette originating from pBI221) which was cut with *Xba*I/*Sac*I. The resulting plant expression vector (p*Nt*AQP1AS, Figure B.13) was transformed into *E.coli* TOP10F'. *Agrobacterium tumefaciens* LBA 4404 was transformed with p*Nt*AQP1AS by Triparental mating (D9.3). Transformation and regeneration of transgenic tobacco was done as described in section D10. Regenerated plants were self-pollinated and the resulting generations were analyzed.

1.4.2 Consequences of *Nt*AQP1-Antisense on Aquaporin Expression

Figure B.14 presents the mechanism of the antisense technique used for the reduction of *Nt*aqp1-expression:

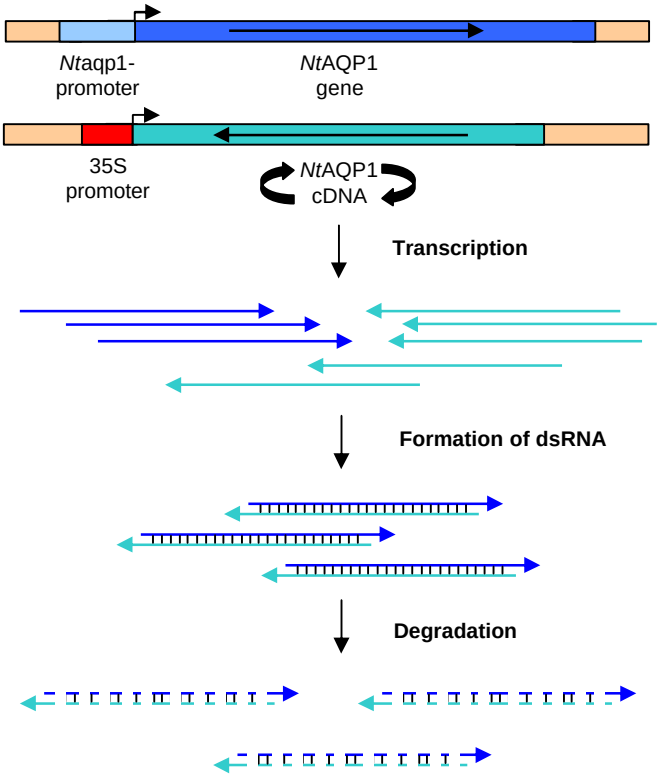

Figure B.14: Scheme of antisense effect:

The transcription of the introduced inverted cDNA is driven by the strong 35SCaMV promoter to produce high amounts of *Nt*aqp1-antisense RNA (AS RNA). This AS RNA hybridizes with the sense *Nt*aqp1-RNA produced from the endogenous aquaporin gene and the corresponding promoter. The formation of double stranded RNA (dsRNA) triggers a specific RNA degradation mechanism in the cell and leads to a reduction of *Nt*aqp1-sense RNA. The lack of translatable *Nt*aqp1-RNA (sense RNA) results in decreased levels of the *Nt*AQP1- protein.

Ten regenerated tobacco lines were tested for reduced *Nt*aqp1-expression. Four independent lines with clearest reductions were used for further investigations. With RT-PCR the presence of AS RNA in the transgenic plants could be demonstrated.

To quantify the antisense effect on *Nt*aqp1 and related aquaporin expression Northern hybridizations of root RNA of control and four independent antisense lines were performed. Northern blot signal intensities clearly revealed a severe reduction of *Nt*aqp1-mRNA steady state levels (Figure B.15, A) in every one of the antisense lines. For analyzing the effect of *Nt*aqp1-antisense expression on RNA-levels of other related genes, gene specific probes against the tobacco *Nt*PIP1a (AF440271), *Nt*PIP2a (AF440272), or *Nt*TIPa (AJ237751) were generated by PCR, based on available sequence information. The nucleic acid sequence identity with *Nt*aqp1 was 78 %, 57 % or 38 %, respectively. The main difference between *Nt*aqp1 and *Nt*PIP1a was found in the region coding for the protein's amino-terminus in front of the first transmembrane helix. Thus, in contrast to *Nt*PIP2a or *Nt*TIPa, the identity for the remaining major part is very high (>95 %). As a representative example, the hybridization signals with RNA obtained from line AS5 is given in Figure B.15, B. Regarding the signal intensities, a reduced expression of the closely related *Nt*PIP1a gene is visible, although the reduction was less

severe than that of *Nt*aqp1-mRNA, the antisense target. In contrast, RNA-levels of other aquaporin genes belonging to other subfamilies were unaffected by *Nt*aqp1-antisense expression. Thus, the results obtained by the subsequent analysis of the antisense plants using plant physiology techniques could be correlated to the function of *Nt*AQP1 and closely related PIP1-genes.

PCR-Hybridization probes:

*Nt*AQP1: *Nt*AQP1 in situ as primer, 673bp, including 5'-UTR, (primers see F3)

*Nt*PIP1a: *Nt*PIP1a antisense primer, 271bp, including 5'-UTR (98 bp) + CDS, 86 % identity to *Nt*AQP1-probe

*Nt*PIP2a: *Nt*PIP2a antisense primer, 226 bp, CDS, 84 % to *Nt*AQP1-probe

*Nt*TIPa: *Nt*TIPa antisense primer, 624 bp, CDS, only similarities to the *Nt*AQP1-probe

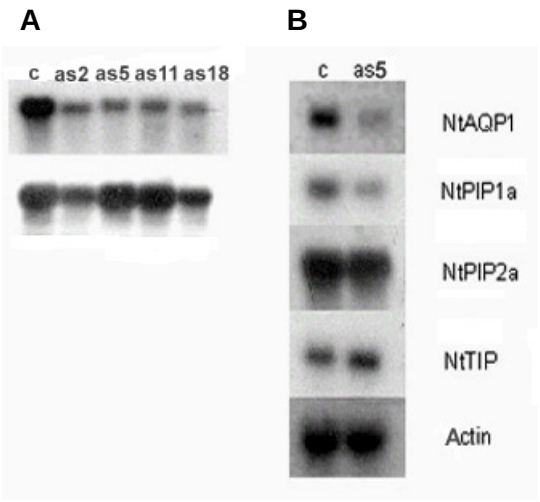

Figure B.15: Northern hybridization signals with RNA from controls or antisense plants.

A. Hybridization with a probe specific to *Nt*aqp1 (upper panel) or to 28S rRNA as a loading control (lower panel). Root RNA was extracted from control plants (c) or four independently transformed antisense *Nt*aqp1-expressing lines (as2, as5, as11, and as18).
B. Hybridization with RNA from antisense line 5 (as5) and control (c). Radioactive probes were synthesized from tobacco aquaporins, named according to their *Arabidopsis* counterparts, *Nt*PIP1a, *Nt*PIP2a, *Nt*TIPa or actin.

1.4.3 Morphology

To determine morphological differences of Ntaqp1- antisense plants compared to control plants, root growth was measured. Therefore, seeds of four independent AS-lines (2, 5, 11, and 18) and control lines (35SGUS) were germinated on horizontal petridishes with solid 1 x M&S medium. The second number specified the seed capsule of the parental plant from which the seedling originated. All lines have strongly reduced Ntaqp1-expression. The root length was measured over a two weeks period. Five to ten seedlings of each "capsule" line were used. Figure B.16 depicts the results: Seedlings of AS line 18 (capsules 2 and 3) clearly exhibited increased root

growth, but e.g. AS line 2 (capsule 1, 2, 7) displayed shorter roots. Repetitions of the experiment showed variations in the results. AS line 5 showed split results: Capsule 2 seedlings displayed increased root system, the ones of capsule 6 decreased growth and capsule 5 was about equivalent with the control increase. Figure B.17 depicts seedlings of AS 5-2 in comparison with a control seedling.

The parameter of root-length is variable; no obvious correlation to growth conditions could be established. Macro- and microscopic inspection of antisense plants revealed no differences in plant organ morphology or in size of cells. For functional analysis root surface was always measured and included in the evaluations.

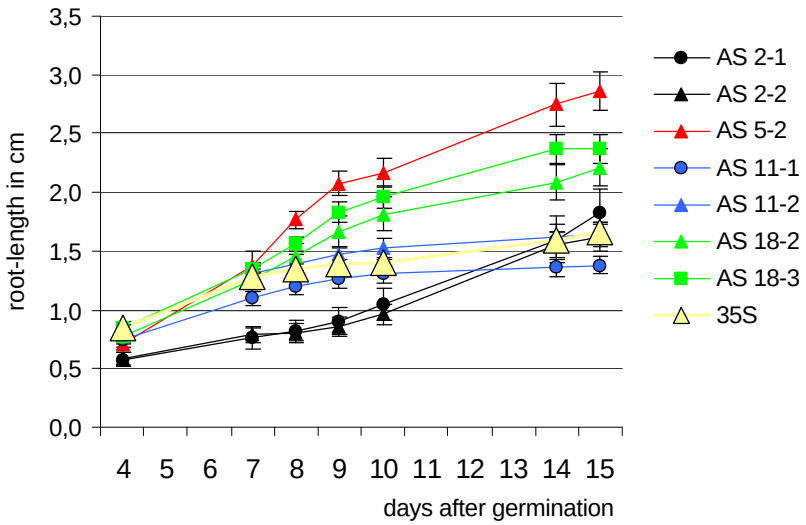

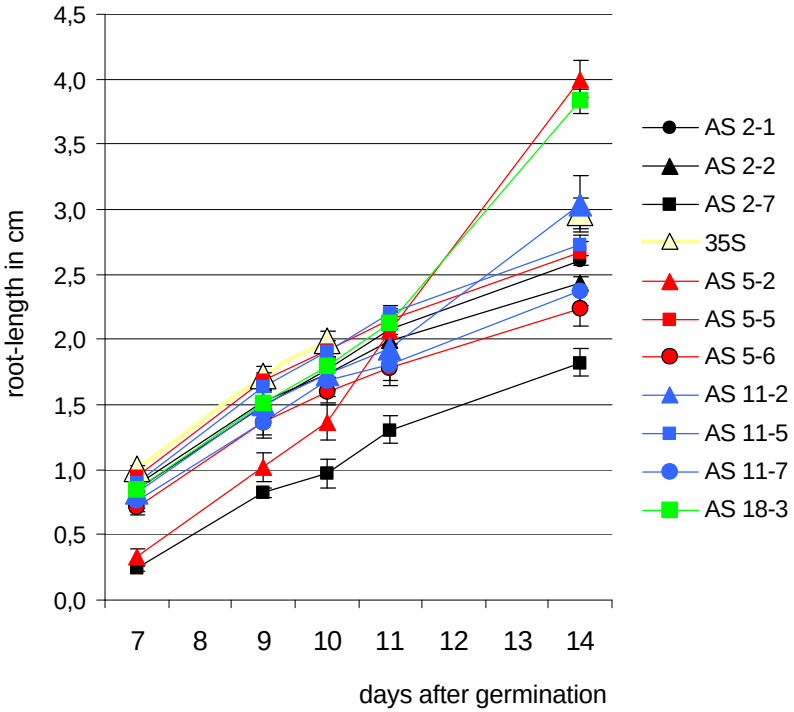

Figure B.16: Diagrams of root length (cm), two independent observations over two weeks period (15 and 14 days). Seedlings of different AS (2, 5, 11, and 18) and control lines (35SGUS) were measured.

Five to ten seedlings of each line were used. The first number describes the independent AS-line (2, 5, 11, and 18); the second number the seed capsule of the parental plant. All lines were shown to have strongly reduced *Nt*aqp1-expression.

Seedlings were grown on vertically-placed petridishes with solidified 1 x MS medium. Roots were measured with a ruler.

Figure B.17: Growth observation on tobacco seedlings: Four *Nt*aqp1-antisense seedlings (AS 5-2) on the left and one representative control on the right side of a vertically-placed petridish with solid 1 x M&S medium.

1.4.4 Chemical Composition

AS and control tobacco plants were compared in their chemical composition after anion, sugar, amino acid and cation analysis of their tissue extracts. Additionally, the osmotic potential of the specimens was determined.

As represented in Table B.1, the osmotic values of AS plants were lower (down to -0.7 MPa) in leaves compared to control plants (-0.65 MPa). In roots of seedlings the values displayed a high variance (-0.3 to 0.44 MPa), but the mean value for AS plants is higher (-0.36 MPa) than for the controls (-0.42 MPa). The sugar concentration in the AS tobacco plants was lower than in controls (Table B.1). In seedlings, this fact is even more pronounced: Here the sugar concentration was less than the half of that of controls (leaves and roots). Anion concentrations are dissimilar: Chloride (Cl^-) and nitrate (NO_3^-) were increased in leaves, while nitrate displayed the strongest differences. In roots only nitrate was increased (chloride is decreased) but these values exhibited a higher variance. Sulfate (SO_4^{2-}) concentration was higher in AS than in control seedlings. Adult AS plants had decreased sulfate concentrations.

The ratio glycine to serine (G/S) is decreased in AS plants because serine contents were higher and glycine contents were lower than in controls. This ratio gives information about the ratio of photorespiration to Calvin cycle. The ratio of glutamine to glutamate (Q/E) was also decreased in AS plants (Table B.2, detailed amino acid analysis results, see F2). Potassium, calcium and sodium were only determined in seedlings; only slight variations can be found (Table B.2). Variations in the chemical composition of AS plants were observed.

Table B.1: Chemical characterization of antisense and control tobacco plants. Osmolality, calculated osmotic potential, and sugar content of tissue extracts from eight-weeks-old plants (leaves, n = 2) and four-weeks-old seedlings (hypocotyl/leaves and roots, n = 15-20) grown on solidified 1 x MS-medium are compared. Sugar content is given in mM per g fresh weight (FW).

Young Tobacco Plants (eight-weeks-old)

leaves	osmolality mosmol/kg	osmotic potential	glucose mM/g FW	fructose mM/g FW	sucrose mM/g FW
control	**288**	**-0.65**	**3.75**	**2.75**	**1.65**
AS 3-4	306	-0.69	1	0.6	0.8
AS 4-3	306	-0.69	3.98	2.4	1.88
AS 5-2	312	-0.71	1.83	1.33	1.22
AS 5-5	288	-0.65	2.85	2.18	1.35
AS 11-7	300	-0.68	0.6	0.4	0.8
AS 18-3	336	-0.76	2.48	1.43	1.58
AS mean	**308**	**-0.7**	**2.1**	**1.4**	**1.3**

Seedlings:

Hypocotyl and Leaves

control	**185**	**-0.42**	**34.4**	**26.8**	**4**
AS 5-2	255	-0.58	12.4	7.2	2.4
AS 11-7	220	-0.5	17.2	12.8	1.6
AS 18-3	200	-0.45	18.4	18.8	1.2
AS mean	**225**	**-0.51**	**16.0**	**12.9**	**1.7**

Roots

control	**185**	**-0.42**	**28.4**	**15.2**	**20**
AS 5-2	195	-0.44	22	9.6	18
AS 11-7	150	-0.34	15.2	7.2	11.2
AS 18-3	130	-0.3	15.6	6.0	10.8
AS mean	**158**	**-0.36**	**17.6**	**7.6**	**13.3**

Table B.2: Chemical characterization of *Nt*aqp1-antisense and control tobacco plants. Anion concentrations (µM/g FW) and amino acid concentration (µM/g FW) of tissue extracts from eight-weeks-old plants (leaves, n = 2) and four-weeks-old seedlings (hypocotyl/leaves and roots, n = 15-20) grown on solidified 1 x MS-medium. Ratios of the amino acids serine (S) to glycine (G), glutamine (Q) to glutamate (E) are designated S/G, Q/E. Cation concentrations are only given for seedling tissues in mM per fresh weight (FW)). Anion concentrations are also given in mM/FW.

Young Tobacco Plants (eight-weeks-old)

leaves	Cl^-	PO_4^{3-}	NO_3^-	SO_4^{2-}	malate	serine	gly-cine	G/S	Q/E
control	**59.7**	**8.2**	**5.9**	**11.7**	**23.7**	**0.51**	**0.11**	**0.21**	**0.77**
AS 3-4	67.3	4.0	7.9	6.3	38.4	0.42	0.03	0.07	0.28
AS 4-3	83.7	7.5	0	14.3	21.8	0.49	0.04	0.08	0.28
AS 5-2	63.3	2.6	12.6	4.2	47.4	0.42	0.09	0.21	0.33
AS 5-5	71.2	6.6	6.0	11.0	27.0	0.52	0.06	0.12	0.77
AS 11-7	73.3	1.3	59.3	5.4	13.4	0.55	0.02	0.03	0.18
AS 18-3	66.3	2.8	33.9	4.8	31.4	0.87	0.18	0.21	1.06
AS mean	**70.9**	**4.1**	**20.0**	**7.7**	**29.9**	**0.55**	**0.07**	**0.12**	**0.48**

Seedlings:

Hypocotyl and Leaves

	Cl^-	PO_4^{3-}	NO_3^-	SO_4^{2-}	malate	S	G	G/S	Q/E	K^+	Ca^+	Na^+
control	**26.5**	**0.7**	**17.6**	**0.5**	**9.1**	**0.44**	**2.12**	**4.82**	**5.56**	**42.43**	**1.72**	**1.74**
AS 5-2	35.4	0.6	91.8	2.7	-	0.74	0.79	1.07	2.10	82.41	5.34	2.35
AS 11-7	36.9	0.75	44.4	1.4	6.75	0.5	0.52	1.04	4.22	57.93	3.90	1.76
AS 18-3	47.5	1.0	15.2	1.8	19.5	0.56	3.97	7.09	7.43	47.01	3.02	2.09
AS mean	**39.93**	**0.78**	**50.47**	**1.95**	**13.13**	**0.60**	**1.70**	**3.07**	**4.58**	**62.45**	**4.09**	**2.07**

Roots

control	**51**	**0.9**	**3.2**	**0.4**	**16.1**	**0.28**	**0.08**	**0.29**	**3.77**	**21.13**	**0.53**	**27.7**
AS 5-2	35.9	0.6	14.1	6.1	8.5	0.26	0.07	0.27	1.87	19.48	1.11	22.9
AS 11-7	45.7	0.7	5.0	4.1	10.9	0.17	0.03	0.18	2.60	14.19	0.72	27.4
AS 18-3	33.9	0.4	1.7	4.9	8.4	0.2	0.06	0.30	3.00	1.28	0.11	0.11
AS mean	**38.5**	**0.57**	**6.93**	**5.03**	**9.27**	**0.21**	**0.05**	**0.24**	**2.49**	**11.65**	**0.65**	**16.8**

1.4.5 Cellular Water Permeability: Protoplast Swelling Assay

Studies on *Nt*AQP1-function started with the scope to determine the cellular membrane water permeability of control and antisense plants. Because *Nt*aqp1-expression was highest in roots and the effect was expected to be most evident in cells with abundant *Nt*aqp1-RNA, root-cells were chosen for these studies. The fact that *Nt*aqp1-expression in the root apex is more or less distributed all over the root cross section with main concentration at the passage of the water fluxes between apoplast and symplast justified the investigation of the whole apex root protoplast population in a protoplast swelling assay.

For these studies an accurate method to monitor intact, globular protoplasts changing their volume in response to rapid osmotic change combined with a fast, standardized analysis procedure for calculation of their osmotic water permeability was developed. A special chamber was used in combination with a Leitz inverse microscope and a digital video camera system which allowed the videotaping of swelling kinetics on the PC (Figure B.18, D12). The recorded films were used for determination of the change in protoplast volume during time.

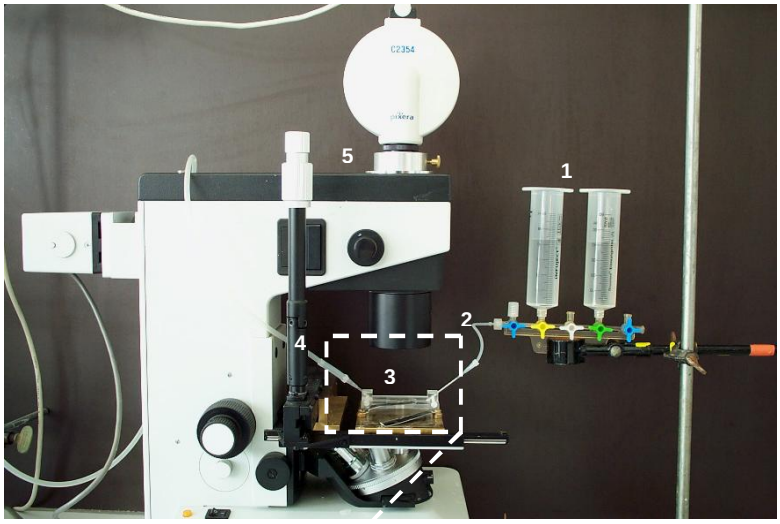

Figure B.18: Approach for measuring protoplast swelling and determination of the osmotic water permeability of their plasma membrane. Numbers in the picture mark components: 1 Two 60 ml syringes (solution containers), 2 tube feeding the solutions in the chamber, 3 experimental chamber magnified in next figure, 4 tubing connected to a pump (removal of solution), 5 CCD-camera connected to the microscope.

1.4.5.1 The Experimental Chamber

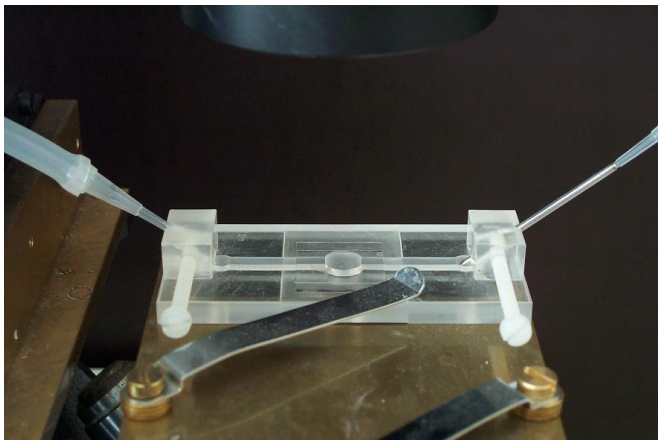

Figure B.19: Experimental chamber for determination of osmotic water permeability of protoplast: A lucite block of Plexiglas with a straight groove 3 mm in width, 4 mm in depth and 50 mm in length and a central hole (∅ 8 mm), connected to reservoirs of osmotic solutions and a pump to remove the solution to the waste. The central hole was covered with cover slides. Scheme see Figure B.20.

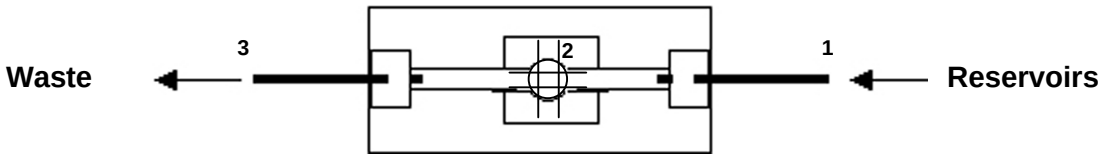

Figure B.20: Scheme of the experimental chamber. The central hole was covered with a cover slide at the bottom, marked with a grid (2) to determine the center of the solution flux in the chamber. The influx of the solutions (1) was regulated by opening and closing of the valves at the reservoirs. The removal of the surplus of solution was achieved by the connection to a pump (3).

The chamber consisted of a lucite block of Plexiglas with a straight groove (4 mm width, 3 mm depth, 50 mm length, Figure B.19) and a central hole. The bottom of the central hole was covered with a cover slide (Figure B.20). For each measurement a cover glass was cleaned with ethanol, marked with a central double cross (grid) and clued to the chamber with a thin rim of silicon grease. One drop of poly-L-lysine (0.1 %) was applied to the central hole of the chamber and left for about 5 min, before rinsing twice with water and once with isotonic solution. The remnants were shaken away and replaced with a drop of cell containing solution. Another cover glass was applied on the top and sealed with silicon grease. The chamber was placed under the microscope and connected to the solution reservoirs (60 ml syringes) with a tube (6 cm length, ∅ 1 mm) to ensure constant flow. Isotonic solution was rinsed into the groove until the central hole was completely filled up. Then the flux was stopped and the protoplasts were left without any manipulations for about 10 min. Cells were selected from the central grid, following a flush with isotonic solution to eliminate less sticky protoplasts. Cells were assayed during a continuous solution flow. The velocity of the flow (4ml/min) minimized solution mixing problems and, in particular, the unstirred layer thickness around the protoplasts.

1.4.5.2 Photomicrography

Recording (1 frame·s^{-1}) started after the manual change from iso-osmotic (300 mosmol) to hypo-osmotic (180 mosmol) conditions. The protoplast volume change (area) was monitored and recorded at RT with the microscope video system (1-2 min, 1 frame·s^{-1}, D12.2.1.1). The protoplasts stayed absolutely round as shown by a side view of a fixed protoplast (Figure B.21, A) which is a necessity for the data assessment. The protoplast volume was extrapolated from the recorded area of the spherical cells. Image processing was done as described in D12.2.1.2. The recorded measurements were copied to MS Excel™.

1.4.5.3 Determination of the Membrane Permeability P_{os}

The relative protoplast volume change (V_x/V_0) was plotted versus time. The membrane permeability coefficient P_{os} was calculated from the slope of the linear range of the graph (Figure B.22, A) using equation 2 (D12.2.2). P_{os} was calculated for Δt of 5 s steps.

In order to monitor the velocity of buffer exchange, buffer aliquots were taken directly from the chamber and the sample osmolarity was determined. Figure B.22, A illustrates an average buffer dilution kinetic of ten experiments and the averaged swelling curves of all investigated protoplasts from *Nt*aqp1-antisense or control plants (n = 36).

The exchange of solution was considerably faster than the volume change. The water flow across the membrane was rate-limiting not the flush. Protoplast volume increase started almost instantaneously after the onset of buffer-solution exchange. Because only some of the cells continued swelling for more than 60 s and many were bursting, only the first minute time interval is presented. In addition, experiments that extended the assay with an additional change from hypo-osmotic back to iso-osmotic conditions, revealed a relaxation of protoplasts to their initial volume, which indicates that the protoplasts behave as true osmometers. Accordingly, the chamber is suitable for calculating osmotic water permeability values (P_{os}) of plant protoplasts, taking the initial swelling rate into account. In addition and most important for the following studies, a difference in volume increase rates between cells from antisense lines and controls is quite obvious.

The average calculated P_{os} for control protoplasts was 27.12 ± 1.8 $\mu m \cdot s^{-1}$ and 12.35 ± 1.1 $\mu m \cdot s^{-1}$ for those from the antisense lines. In order to get a more detailed picture, data from individual protoplasts that relate to a linear volume increase were selected for the water permeability calculations. As expected, individual tobacco root protoplasts from both controls and antisense plants displayed a wide range of water permeability values starting from P_{os} of 2 $\mu m \cdot s^{-1}$ to more than 60 $\mu m \cdot s^{-1}$. A comparison of the cell populations from the different lines revealed obvious dissimilarities.

In Figure B.22, B the data obtained from individual protoplasts were collected into groups according to their osmotic water permeability. While the protoplast population from control lines peaked in the class with a P_{os} of 16 to 32 $\mu m \cdot s^{-1}$, the majority of antisense protoplasts showed P_{os} values between 8 to 16 $\mu m \cdot s^{-1}$. Therefore, the inhibition of *Nt*AQP1 by the antisense expression decreased the overall cellular P_{os}. Conclusively, *Nt*AQP1-function increases membrane water permeability of tobacco root protoplasts.

Figure B.21: Side view of a root protoplast attached to a microscopic slide by poly-L-lysine.

Figure B.22: Protoplast swelling analysis.

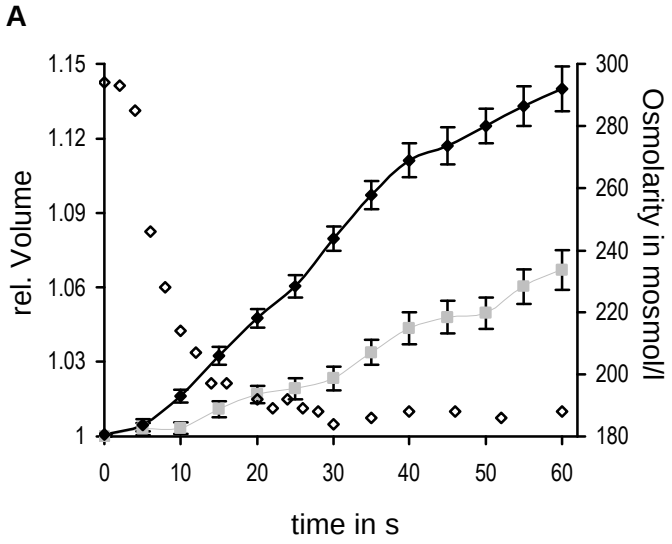

A. Protoplasts were produced from roots of control plants (filled black rhombs) or antisense *Nt*aqp1-expressing lines (filled grey squares) and subjected to hypo-osmotic conditions. The mean volume increase of control (n = 36) or AS protoplasts (n = 36, n = 9 each line) in the first 60 s after osmolarity change is shown. In separate experiments under the same conditions, the osmolarity of aliquots taken from the chamber buffer-solution were determined (open rhombs, n = 10).

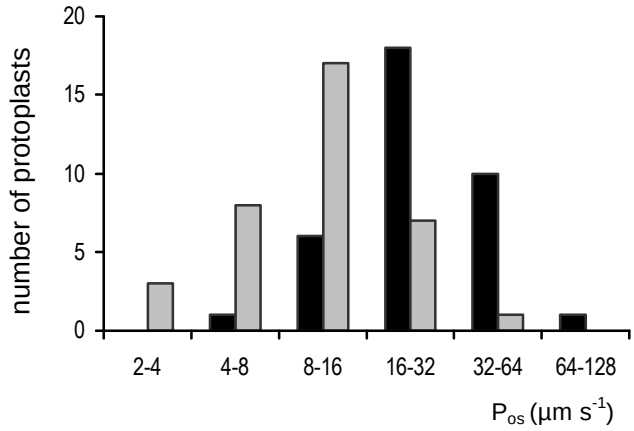

B. P_{os}-value-distribution of the investigated protoplasts obtained from controls (grey bars) or antisense lines (black bars).

1.4.6 Significance of NtAQP1 at the Organ Level

Because *Nt*AQP1 is primarily expressed in roots, it was assumed that a lack of the aquaporin has an effect on the root water permeability. Consequently, root hydraulic conductivity per unit root surface area (K_{RA}) was measured using the high-pressure flow meter method (HPFM, Tyree et al, 1995). The K_{RA} of roots from the antisense lines was 11.9 ± 4.2 mmol·m^{-2}·s^{-1}·MPa^{-1} compared to 26.5 ± 2.0 mmol·s^{-1}·m^{-2}·MPa^{-1} from the controls (Figure B.23, A). This corresponded to a 45 % lower water permeability in the AS plant roots. The flow rates of antisense roots and control roots are shown in Figure B.23, B. The AS plants display a higher resistance to water flux than the controls.

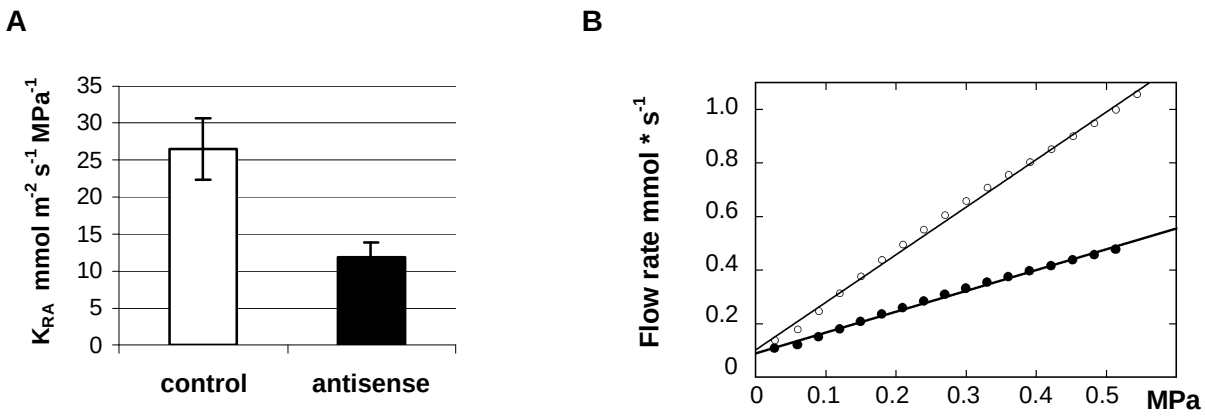

Figure B.23: Determination of root hydraulic conductivity by the high pressure flowmeter method. A. Average specific root hydraulic conductivity of controls and antisense *Nt*AQP1 expressing tobacco plants as measured by the high pressure flowmeter method. B. Representative pressure/flow rate relationship of a control plant (open circles) and a *Nt*aqp1-antisense line (closed circles). Both plants had a similar root surface (control = 0.0605 m^2, antisense = 0.0615 m^2). The applied pressure increased in 2 s time intervals.

This decrease was in the same order of magnitude as the mean cellular water permeability reduction. The results indicate that aquaporin expression is essential in maintaining a natural root hydraulic conductance. Furthermore, this observation may be the first definitive proof that the pathway of water uptake from the root surface to the xylem involves passage across membranes, e.g. the plasma membranes of cells in the *Casparian Bands*. If the pathway of water transport were totally apoplastic via the cell wall space then there would have been no difference between K_{RA} of control and antisense plants.

This notion was supported by determination of root hydraulic conductivity (K_{RA}) before and after two freeze-thaw cycles (Figure B.35), which cause mechanical perforation of the cell membranes by water crystals. As the root hydraulic conductivities were significantly different before the freeze-thaw treatment (45 % difference, Table B.3), they were almost identical afterwards (4 % difference). This finding also confirms that the function and morphology of the vascular system is very similar in controls and antisense. An adaptation at the morphological level due to the constant low cellular water permeability caused by the antisense effect was never observed.

Table B.3: Specific hydraulic conductivities of control and antisense lines before and after two freeze/thaw cycles.

	Specific root hydraulic conductivity (mmol m^{-2} s^{-1} MPa^{-1})	**Specific root hydraulic conductivity freeze-thaw** (mmol m^{-2} s^{-1} MPa^{-1})
control	26.5 ± 4.2 (n = 9)	114.0 ± 8.05 (n = 8)
***Nt*AQP1-antisense**	11.9 ± 2.0 (n = 31)	109.5 ± 15.6 (n = 15)

Nevertheless, tobacco plants appeared to withdraw the effects of a strongly reduced *Nt*AQP1-expression, which might result from optimal growth conditions in the greenhouse with regard to water supply and air-moisture. However, under a water-limiting environment, differences in water permeability could cause a more pronounced effect (see, B2.7).

1.4.7 Diurnal and Circadian Influence on Root Hydraulic Conductivity

The root hydraulic conductivity of tobacco plants displayed a striking diurnal and even circadian rhythm (Figure B.24). The circadian period corresponded to 21.1 h, with its maximum around noon and minimum around midnight. Since *Nt*aqp1-expression exhibited a circadian rhythm, too, this effect can be taken as indication that variations in root resistance to water flow can be regulated by aquaporins.

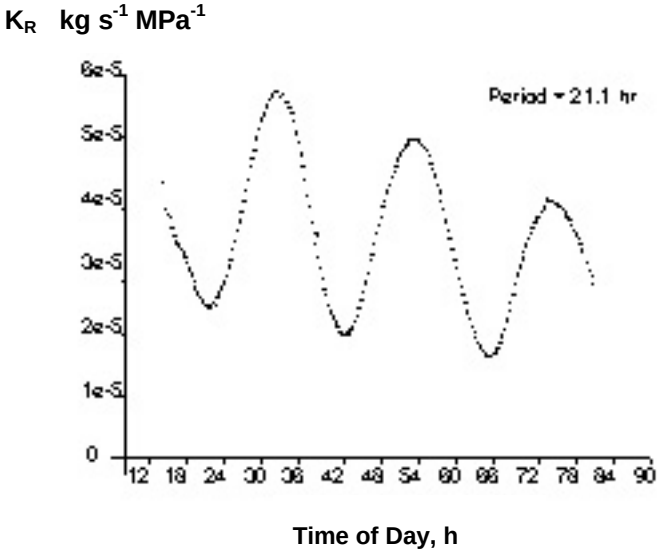

Figure B.24: Circadian rhythm of root hydraulic conductivity (K_R) of a pressurised tobacco wild type plant root in continuous dimmed light. A clear rhythm can be found with a 21.1 h period, with its maximum at noon and minimum around midnight.

2 Expression and Function of *Nt*AQP1 in Stems and Leaves

2.1 *Nt*AQP1-Expression in the Stem

In situ immunological studies indicated that *Nt*AQP1 accumulation in the stem depended on the developmental stage of the stem section. In younger parts, i.e. 5 cm from the apex, the protein was found in the outermost epidermis, in the cortex, in developing xylem vessels and in cells close to the appearing inner phloem. In older parts, at about 30 cm below the shoot apex, the *Nt*AQP1 can mainly be localized in the outer xylem boarder and in cells of the internal phloem. The occurrence close to phloem cells or in phloem companion cells could be explained by a function in balancing osmolyte concentration during phloem loading through an effective water supply. If the presence of the aquaporin in cells of the outer xylem in older shoots indicates high membrane water fluxes, a substantial exchange between xylem and symplast along the whole shoot should occur. The expression in the cortex may have a function in radial water transport to support the fast growing apex, or it can be involved in growth orientation reactions of the apex towards light sources.

Further expression studies of p*Nt*aqp1::gus plants should give new hints, if *Nt*AQP1 is possibly involved in tropism.

2.2 Further Expression Studies

2.2.1 Glucuronidase Assay

Gravity assay

Growth orientation assays with p*Nt*aqp1::gus plants should show, if *Nt*aqp1-expression is involved in gravitropically and light induced orientation of the tobacco shoot. Three ten-weeks-old soil grown tobacco plants were used for this assay. Plant 1 was used as time point 0 control; the other two plants were left in a horizontal orientation for either 6 or 24 h in continuous light.

Figure B.25, shows a time course of a bending reaction of a eight-weeks-old tobacco plant in low light. After 3 h, first bending reactions could be observed below the apex. Curvature increased from internode to internode downstream from the apex until after 23 h the vertical position was reached again.

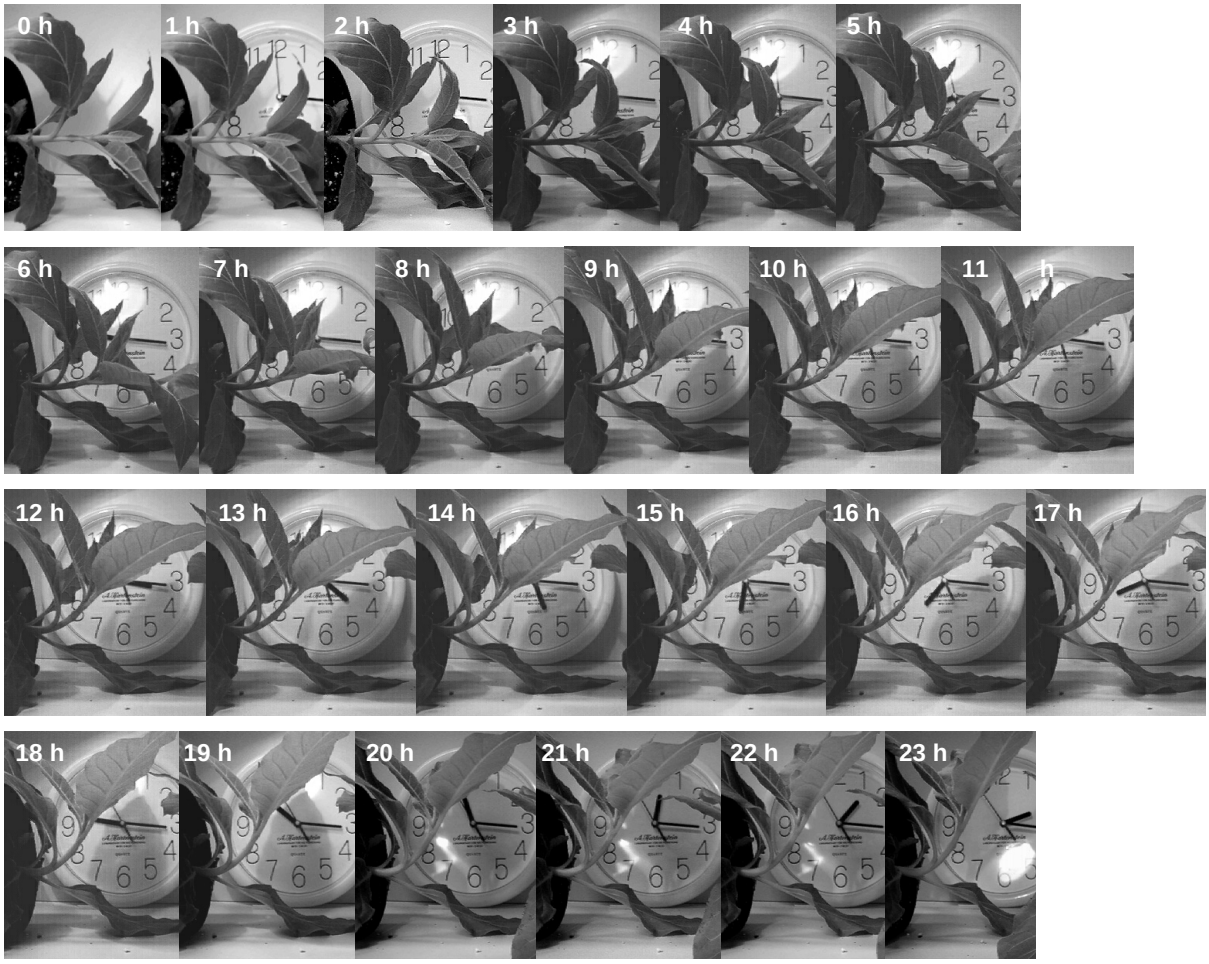

Figure B.25: Bending reaction of a horizontally placed eight-weeks-old control tobacco plant in continuous dimmed light. After 3 h first bending reactions can be observed below the apex. Curvature increase from internode to internode downstream from the apex until after 23 h the vertical position was reached again.

The transgenic plants for the GUS assay were divided in the upper (towards light) and lower half (towards ground) and cut in sections of 3-5 cm. Upper and lower halves were separately stained in β-Glucuronidase enzyme assays (D11.1.1).

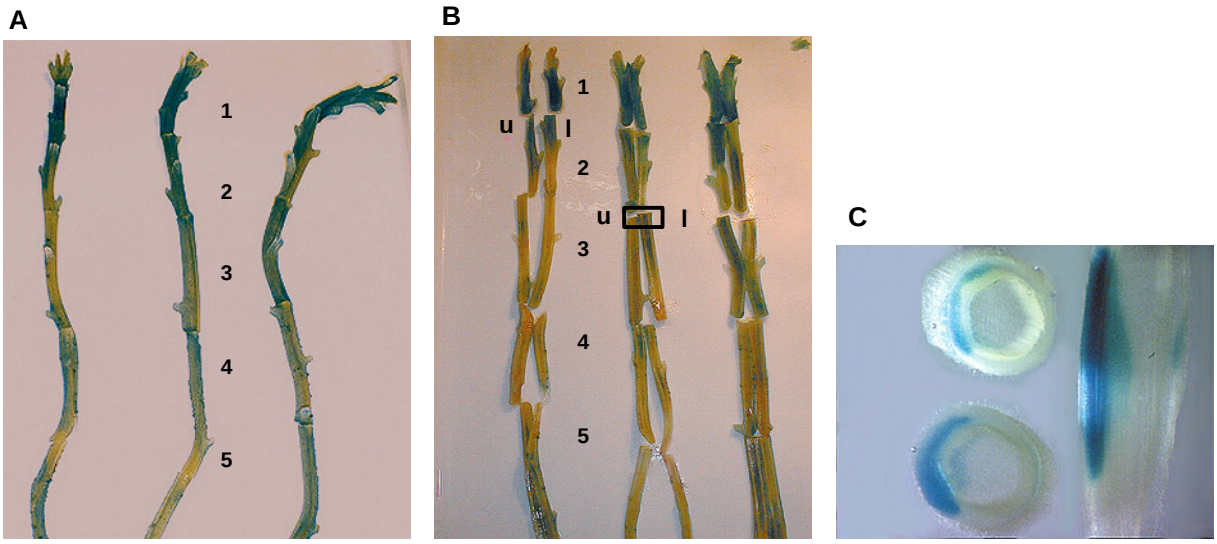

Figure B.26: Results of the GUS assay on three p*Nt*aqp1::gus plants after the photo/gravi-tropic experiment. A. Stems were slightly orientated after their curvature; left: 0 h, middle: 6 h, right: 24 h after horizontal orientation in continuous light. B. Longitudinal sections of the 3-5 cm pieces. C. Cross section of a bent stem. (l) Marks the lower and (u), the upper half of the stem.

As in the immunological studies, this assay showed that in the youngest zone (about 5 cm from the apex) *Nt*aqp1 was expressed in an even distribution all over the cross section in all three plants (Figure B.26, A and B). Obviously this region needed a constitutive high expression of *Nt*aqp1, independently of the orientation of the stem. This subapical region included the elongation zone, where the cells increased their volume 10 to 100 fold in a relatively short time. This increase is generated by uptake of water. A higher expression of *Nt*AQP1 could account for elevated water permeability and water flux.

The plant subjected to horizontal orientation for 24 h showed a completely stained apex compared to the 0 and 6 h time point, where the uppermost tip was not stained. In the 24 h plant this youngest part of the plant was bent compared to the other two (Figure B.26, A). Following the stem further in direction of the older parts the straight part of the control plant was not stained while all the regions of bending displayed the blue signal, even in the control plant. The view of the inner side of longitudinally sections of the stem (Figure B.26, B, C) exhibited a polarized expression of *Nt*aqp1. All positions which showed bending, expressed the blue GUS signal mainly on one side (either upper or lower) depending on the orientation of the curvature (Figure B.26, A). Pictures of cross sections of the bent region demonstrate this polarity even more convincing (Figure B.26, C).

Phototropism and gravitropism both include a differential growth of the stem in response to asymmetrically distributed phytohormones (Iino, 1995; Kaldenhoff and Iino, 1997). The irreversible growth process involves cell wall loosening to yield the wall stress. As consequence of this stress relaxation, the water potential is reduced and water flows into the cell causing a measurable extension of the wall and an increase in cell surface area and volume.

Since *Nt*AQP1 was shown to be influenced by phytohormones, e.g. gibberellic acid, and displayed a differential expression in response to gravi- and photostimulation it could be concluded that *Nt*AQP1 is involved in curvature reaction. It might be necessary to support the increased requirement of water influx.

Treatment with osmoticum

Salt

Soil-grown plants were watered with a 250 mM NaCl solution for 24 h, to induce an osmotic change in the soil. Stems were subjected to GUS staining to monitor the response of the *Nt*aqp1-promoter on this treatment.

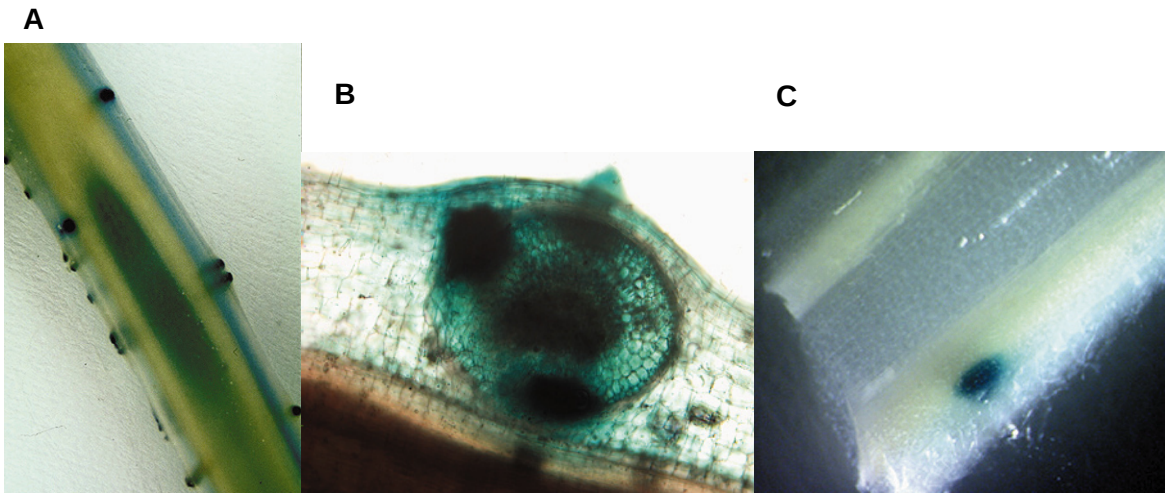

Figure B.27: GUS assay results of the salt experiment with soil grown *Nt*aqp1-promoter::gus plants. A. Shoot section with adventitious root primordia of a salt-treated plant. B. Cross section through an adventitious root primordium of salt treated plant. C. Shoot section with adventitious root primordium of an untreated plant.

Figure B.27, A depicts the stem of a treated plant. The GUS staining could be detected all over the cross section; just the xylem vessels and the epidermis were unstained. This indicated that osmotic treatment also influenced *Nt*aqp1-expression in the stem. The adventitious root primordia were stained dark blue and the vessel connection was clearly stained in the treated plant (Figure B.27, A and B).

Adventitious Root Formation

The adventitious root primordia were also stained in untreated plants. Figure B.27, C depicts a primordium where neither cortex nor vessels to the primordium were stained, but just the clusters of cells that renew their cell division activity. These dividing cells develop into a root apical meristem analogous to the formation of lateral roots. This led to the conclusion that *Nt*AQP1 participated in the establishment of adventitious roots as well as in growth and division processes.

2.3 *Nt*AQP1-Expression in Leaves

Aquaporins of the plasma membrane may be involved in regulating water release into the stomatal cavity. Parameter like transpiration and stomatal conductance may be influenced by the antisense construct in the tobacco plants. In the following studies gas exchange parameters were investigated.

Tobacco leaves displayed a peculiarity, a circadian sleep movement. The petioles were moved from their horizontal orientation to an almost vertical and vice versa. The movement had an about 24 h period under normal light/dark conditions and was extended another 24 h (circadian) under constant light and temperature. For this pronounced and relatively fast movement it was suggested that high and variable water permeability is required.

Protein Expression

The concentration of *Nt*AQP1-protein was much lower in leaves than in other parts of the plant (Otto and Kaldenhoff, 2000). Lowest expression could be observed in the lamina, while in and around the stomatal cavities the concentration was high. The leaf veins and especially the vascular bundles displayed highest concentrations of the *Nt*AQP1-protein. The expression was extended into the petioles of younger leaves. The expression pattern changed in the petioles with increasing distance from the apex. Petioles (5 cm from the apex) showed high concentration of the protein around the xylem. This expression was extended to the phloem and parenchyma cells in the petioles of the middle part of the plant, while the expression around the vessels disappeared in the oldest part of the plant. In those petioles and distinct parenchymatic cells exhibited increased protein levels. Longitudinal sections of the petioles contained vertical rows of 2-20 parenchymatic cells with *Nt*AQP1-expression which might be involved in the leaf movement.

2.4 Further Expression Studies

The expression of *Nt*aqp1 was investigated in more detail and its time dependence was closer examined. Promoter reporter studies were used to focus on circadian rhythms and salt induced expression. Additionally, Northern hybridizations of petiole RNA were performed to focus on the participation of *Nt*AQP1 in the leaf movement.

2.4.1 Glucuronidase Assay

Treatment with Osmoticum

Soil-grown p*Nt*aqp1::gus plants were subjected to an osmotic treatment, where they were watered with 250 mM NaCl and kept with the solution for 24 h. Leaves were subjected to GUS staining in order to monitor the response of the *Nt*aqp1-promoter on this treatment.

The β-Glucuronidase assay confirmed the observation achieved by the protein expression analysis. Leaf cross sections displayed a slight overall expression of *Nt*aqp1 with highest concentration in the veins of the petiole (Figure B.28, A-C). It also exhibited the shift in expression from younger to older petioles (Figure B.28, B and C). This showed that tobacco reacted on osmotic changes with increasing *Nt*aqp1-expression in leaves.

Additional information was obtained by the salt treatment. The hairs and some spots of the leaf surface of salt treated plants displayed the blue stain (Fig. B.28.D,E) which was absent in the control plants (Fig.B28.F). The cells near the base of some secretory structures had suberized or cutinized walls, some of which were equipped with *Casparian Bands*. These bands could limit and direct the flow of secreted substances. They might also be important in limiting water loss through a ruptured cuticle as in preventing the backflow of the secreted substances into the apoplasm (Schnepf 1974).

Maybe *Nt*AQP1 played a role in a related process to increase the permeability of the plasma membrane to water or other small solutes.

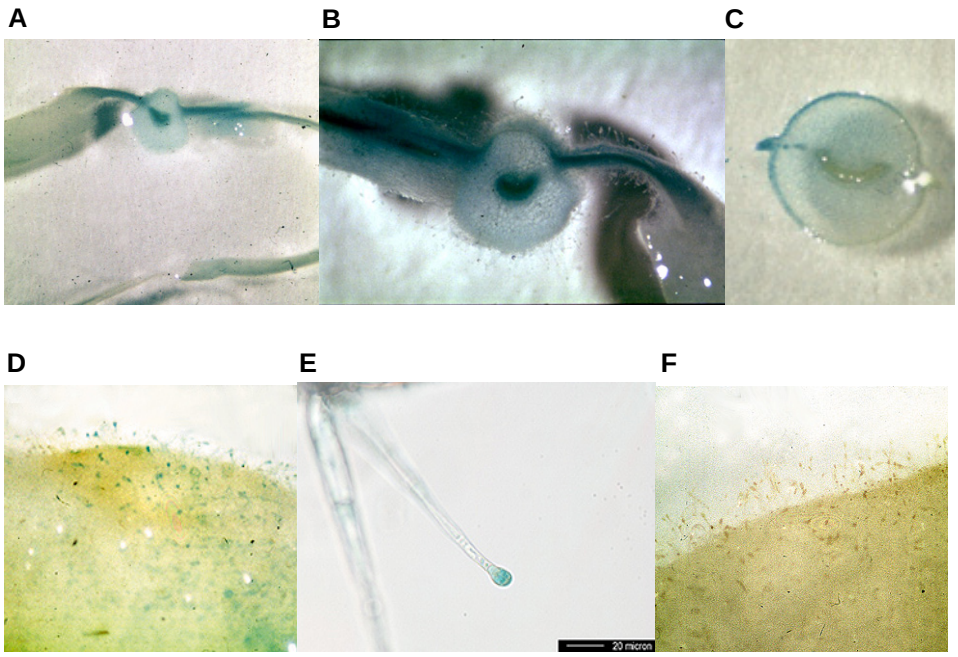

Figure B.28: β-Glucuronidase assay on p*Nt*aqp1::gus plants subjected to salt treatment (250 mM, 24 h). A. and B. Cross section of young leaves. C. Cross section of a petiole of an older leaf. D. Leaf surface with leaf hairs. E. Leaf glandular hair enlarged (100 x). F. Leaf surface with leaf hairs of an untreated plant.

2.5 *Nt*AQP1-Expression in Petioles

2.5.1 Luciferase Assay

p*Nt*aqp1::luc plants were generated to follow the dynamic process of the tobacco leaf movement simultaneously to the *Nt*aqp1-expression. Adult tobacco plants and seedlings were sprayed with luciferin and subsequently subjected to continuous darkness to record the luciferase activity.

An obvious temporal correlation of luciferase expression and the leaf movement was observed (Figure B.29, A). The movement started with the "open" position, with highest expression seen in the petiole. During the upward movement the expression vanish to a minimum at the "closed" position. Luciferase activity increased again with lowering of the leaves to the maximum expression of the enzyme at the open position again.

For *Nt*AQP1, it can be concluded, that its differential expression may be required to regulate the movement. But to elucidate the function of the aquaporin in this process a different approach was necessary. For that *Nt*aqp1-AS plants were tested for their leaf movement capacity (see section B2.8).

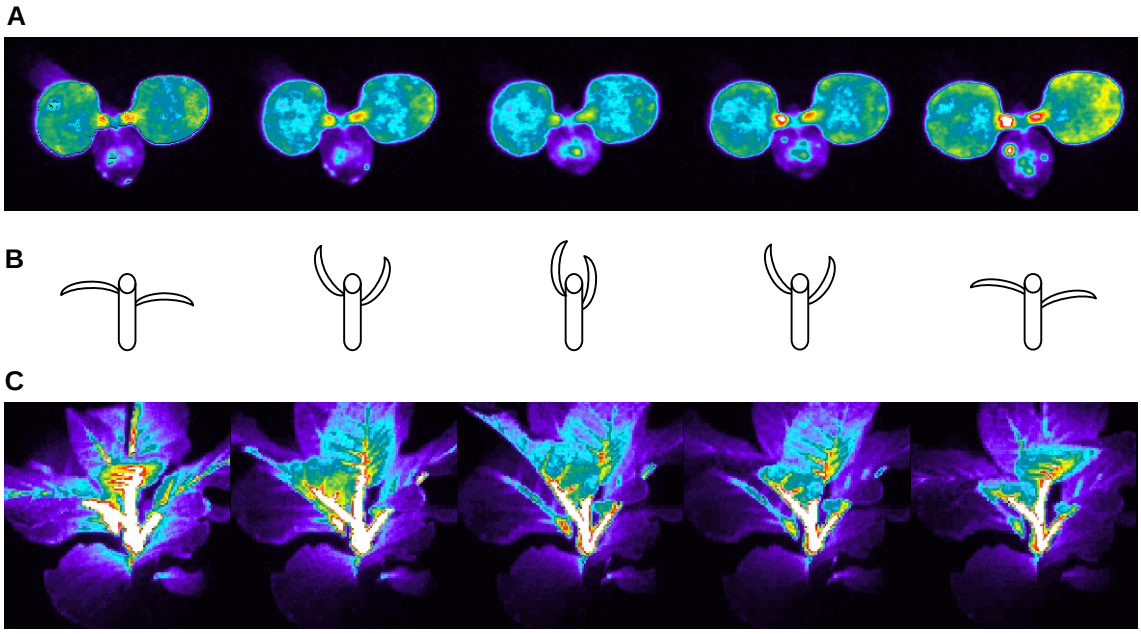

Figure B.29: Results of the luciferase assays with p*Nt*aqp1::luc seedlings and adult plants kept in continuous darkness (24 h) to follow the dynamic process of the tobacco leaf movement. A. Five time points of the continuous movie of a seedling. B. Scheme of the tobacco sleep movement. C. Five time points of the continuous movie of an adult tobacco plant. Images of luciferase activity are depicted with false color scales (blue indicating low activity, red indicating high activity, white shows overload).

2.5.2 Northern Analysis

Diurnal Expression of *Nt*aqp1 in Petioles

The leaf movement was also investigated by Northern blot analysis of the *Nt*aqp1-expression in the petioles. Tobacco plants were subjected to a continuous day/night (12 h/12 h) light rhythm with darkness from 6:00 PM to 6:00 AM. Leaf movement started around 5:00 PM to the "sleeping position" (leaves up, steep angle) and from 2:00 AM to the "open position".

Leaf petiole RNA was isolated every four hours from three plants. Northern blot was performed with [α-^{32}P]dCTP probes against *Nt*aqp1 and 28S RNA. The level of *Nt*aqp1-RNA content, correlated to the highest 28S-hybridization signal, ranged between 28-100 % (Figure B.30). Its maximum was found at 6:00 AM and minimum at 2:00 PM. Like in the luciferase assay the maximum expression could be seen in the "open" position of the leaves. The large time steps of 4 h in the Northern experiments didn't allow precise predictions, but since the results of the promoter luciferase were similar, the luciferase assay would be the assay of choice for more detailed investigations. Another possibility might be that the increase of *Nt*aqp1-expression was due to the higher water supply requirement of the leaves during the day. To elucidate this issue, functional studies were done on AS plants.

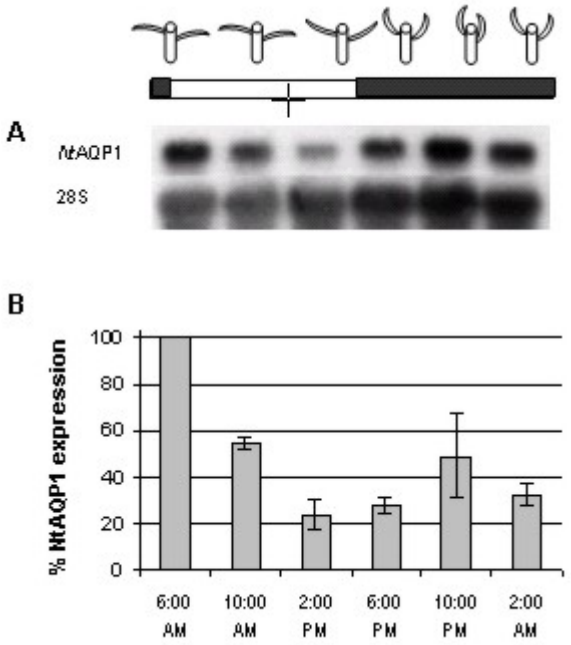

Figure B.30: Typical time course of *Nt*aqp1-expression in petioles. The bare above the picture symbolizes the photoperiod and the scheme presents the leaf movement.

A. Northern blot of leaf petiole RNA: Upper row shows hybridization with [α-^{32}P]dCTP labeled *Nt*aqp1-probe, lower row with [α-^{32}P]dCTP labeled 28S-probe.

B. Diagram of evaluations of three independent Northern blots; standard errors are given in black bars.

2.6 Function of *Nt*AQP1 in Gas Exchange

Net photosynthesis and stomatal conductance (g_s) was assessed by gas exchange measurements on leaves on the plants and on detached leaves. Measurements were taken for several hours.

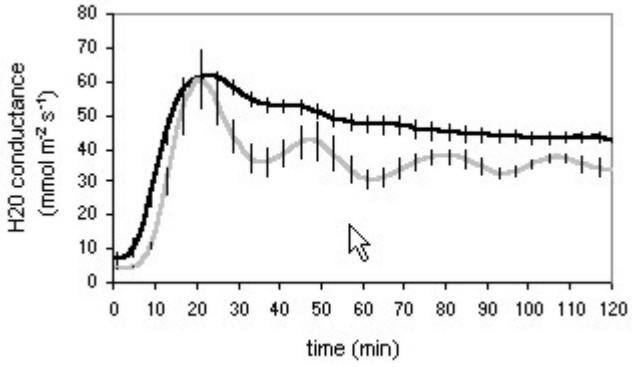

Figure B.31: Stomatal conductance (gs) of leaves on the plants: Black line represents g_s of controls (n = 10), grey line the one of AS plants (n = 10). Black bars describe the standard errors.

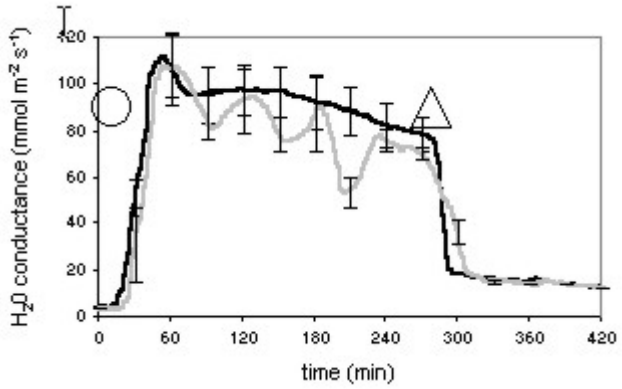

Figure B.32: Stomatal conductance (g_s) of detached leaves: Black line represents g_s of controls (n = 12), grey line of AS plants (n = 12). The circle inserted in the diagram shows onset of light. The triangle represents the application of 100 µM ABA. Black bars describe the standard errors.

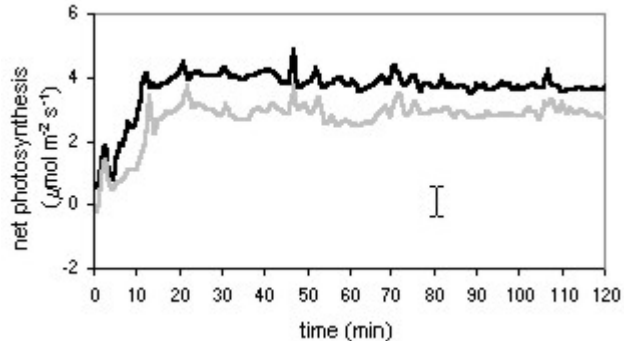

Figure B.33: Net photosynthesis of leaves on the plant: Black line represents net photosynthesis of controls (n = 10), grey line the one of AS plant leaves (n = 10).

Stomatal conductance (g_s) as well as net photosynthesis was influenced by the antisense effect. g_s was significantly lower in AS (Ø 35.6 $mmol \cdot m^{-2} \cdot s^{-1}$) compared to control plants (Ø 45.9 $mmol \cdot m^{-2} \cdot s^{-1}$) as long as the leaves were attached to the stems (Figure B.31). The stomatal conductance displayed a striking continuous oscillation. Detached leaves of AS plants also showed the oscillation but the values of g_s were not significant lower any longer. This fact directed the effect of lowered conductance to hydraulic limitations in roots or stems. Lower

conductance is normally observed under water stress, artificial induction of embolism in xylem and manipulation of roots, shoots and canopies.

The application of 100 µM ABA caused the instantaneous closure of the stomata and the corresponding drop of g_s. In AS plants the response on ABA was delayed (Figure B.32) which was probably due to the reduction of ABA-responsive *Nt*AQP1. The question arose if the stress response may be influenced by *Nt*AQP1-reduction, thus gas exchange measurements were done on AS plants exposed to drought stress. Further investigations were done on osmotic stress.

2.7 Function of *Nt*AQP1 in Stress Response

Tobacco plants appeared to cope with the effects of a strongly reduced *Nt*AQP1-expression, which might result from optimal growth conditions in the greenhouse with regard to water supply and air-moisture. However, under a water-limiting environment, differences in water permeability could cause a more pronounced effect. Desiccation experiment with control and AS plants should show if *Nt*AQP1 influences the reaction on mild drought stress. For that two sets of plants were used for the following treatment:

A moderate water stress was induced in antisense and control plants by cultivation without irrigation for one week. The set for comparison was normally watered. Four control and sixteen AS (four independent AS lines each with four representatives) plants were used for measuring leaf and root area, leaf water potential (Ψ_{leaf}), stem water potential (Ψ_{stem}), transpiration rate (E), plant transpiration (E_{plant}), root hydraulic conductivity (K_{RA}) and plant root hydraulic conductivity (K_{Rplant}).

During this first week of drought the soil water potential fell from -0.01 to -0.07 MPa (Table B.4) and soil-moisture decreased from 62.2 ± 1.63 to 22.1 ± 2.91 % w/w. The most sensitive plant reaction to water stress can be observed by determination of stomatal closure, which is indicated by the transpiration rate (E). E was assessed by gas exchange measurements from all leaves.

The values for transpiration rate E (Table B.5), Ψ_{stem} and Ψ_{leaf} (Table B.6) were lower under well-watered conditions in AS compared to control plants, indicating that the absence of *Nt*AQP1 causes a certain stomatal closure and induces a water stress signal, which was most likely induced by the lower hydraulic conductance of the roots in AS plants. Ψ_{stem} and Ψ_{leaf} decreased under the water stress conditions in both plant lines. However, it became evident that AS plants remained at more negative water potentials than the control plants, even though a further decrease in transpiration of AS plants was detected in comparison to controls (Figure B.34).

The root hydraulic conductivity K_{RA} dropped under drought condition, the decrease was more pronounced in the AS plants (Table B.5, Figure B.35) which can be due to the deficiency of regulation of aquaporin activity in the AS plants.

Table B.4: Measured values of leaf and root area, water potential (Ψ_{soil}) of control and AS lines in drought and watered condition.

	Leaf area watered (m^2)	**Leaf area drought** (m^2)	**Root area watered** (m^2)	**Root area drought** (m^2)	Y_{soil} **watered** (MPa)	Y_{soil} **drought** (MPa)
Control	0.331 ± 0.038 (n = 4)	0.371 ± 0.025 (n = 4)	0.429 ± 0.039 (n = 4)	0.409 ± 0.013 (n = 4)	-0.01 ± 0.005 (n = 12)	-0.07 ± 0.01 (n = 11)
AS	0.227 ± 0.015 (n = 8)	0.236 ± 0.026 (n = 7)	0.338 ± 0.045 (n = 8)	0.277 ± 0.042 (n = 7)	-0.01 ± 0.005 (n = 12)	-0.07 ± 0.01 (n = 11)

Table B.5: Transpiration rates (E), transpiration of the whole plant (E_{plant}), specific hydraulic conductivity K_{RA}, and hydraulic conductivity of the whole plant (K_{plant}) of control (Contr.) and AS lines (AS) in drought and watered condition.

	Transp.rate E watered (mmol m^{-2} s^{-1})	**Transp.rate E drought** (mmol m^{-2} s^{-1})	E_{plant} **watered** (mmol s^{-1})	E_{plant} **drought** (mmol s^{-1})	K_{RA} **watered** (mmol m^{-2} s^{-1} MPa)	K_{RA} **drought** (mmol m^{-2} s^{-1} MPa)	K_{plant} **watered** (mmol s^{-1} MPa)	K_{plant} **drought** (mmol s^{-1} MPa)
Contr.	2.99 ± 0.02 (n = 19)	1.82 ± 0.15 (n = 9)	0.990 (n = 19)	0.674 (n = 9)	34.63 ± 6.11 (n = 4)	23.76 ± 6.01 (n = 4)	14.867 (n = 4)	9.726 (n = 4)
AS	2.77 ± 0.06 (n = 95)	1.23 ± 0.09 (n = 61)	0.629 (n = 95)	0.291 (n = 61)	12.02 ± 2.00 (n = 8)	9.48 ± 1.51(n = 8)	4.060 (n = 8)	2.622 (n = 7)

Table B.6: Measured values of stem (Ψ_{stem}) and leaf (Ψ_{leaf}) water potentials of control and AS lines in drought and watered condition.

	Y_{stem} **watered** (MPa)	Y_{stem} **drought** (MPa)	Y_{leaf} **watered** (MPa)	Y_{leaf} **drought** (MPa)
Control	-0.182 ± 0.04 (n = 8)	-0.231 ± 0.018 (n = 8)	-0.297 ± 0.027 (n = 8)	-0.397 ± 0.03 (n = 8)
AS	-0.202 ± 0.008 (n = 20)	-0.275 ± 0.014 (n = 20)	-0.32 ± 0.02 (n = 20)	-0.437 ± 0.025 (n = 20)

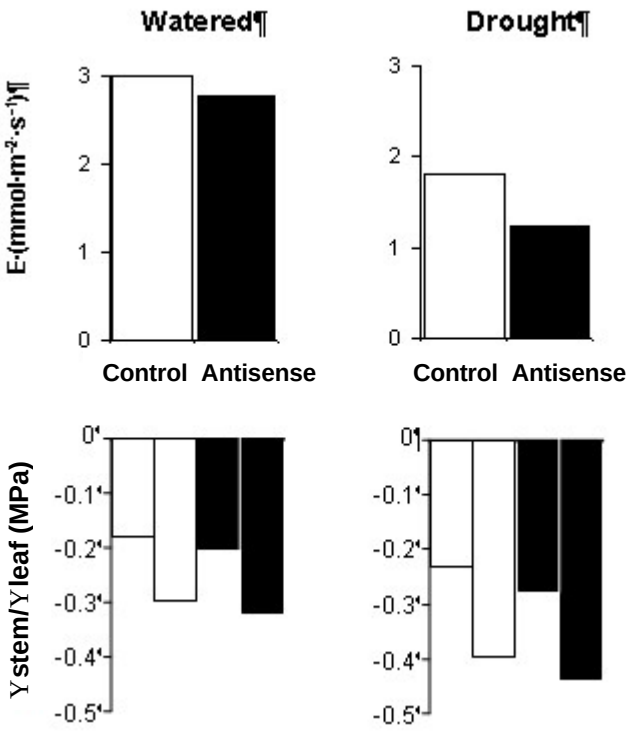

Figure B.34: Data for control and antisense *Nt*AQP1 tobacco.
Transpiration rates (E; top), stem water potential (Ψ_{stem}; bottom left), and leaf water potential (Ψ_{leaf}; bottom right) of control (white bars) and antisense *Nt*AQP1 (black bars) tobacco are shown. Plants were either watered or not watered for 1 week (drought). Complete data are given in Table B.5 and Table B.6.

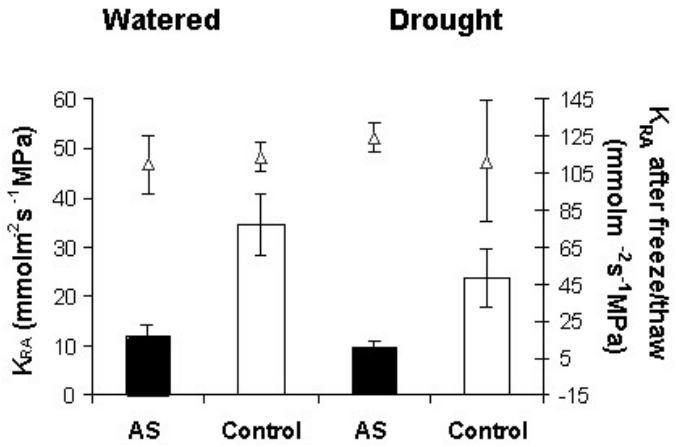

Figure B.35: Root hydraulic conductivity measured before (bars) and after (triangles) two freeze/thaw cycles under watered and drought conditions. Error bars are given for all values.

Regarding the findings described so far, *Nt*AQP1 seemed to contribute to water stress avoidance of tobacco. The treatment employed in the drought experiments was relatively mild, reducing the soil water potential just from -0.01 MPa to -0.07 MPa. These water stress conditions were apparently not strong enough to cause observable plant reactions. Thus, a more stringent water stress was employed by irrigation with a PEG-solution (138.4 g/l PEG6000) with an osmotic potential of -0.35 MPa. PEG6000 does not permeate roots, consequently it imitates soil dehydration. Two hours after PEG-addition, AS plants apparently started wilting, while controls remained visibly unaffected (Figure B.36). The effect of wilting was quantified by measuring the leaf blade angle to the plant axis. Figure B.37 depicts the results of these measurements. The control started about 6 h later to display a similar reaction.

Taken all these observations together, this led to the conclusion that *Nt*AQP1-function is required for the resistance to extreme water depletion effects.

Figure B.36: Water stress symptoms. Plants were watered with a PEG-solution inducing an osmotic pressure of -0.35 MPa and photographed at 0, 1, and 3 h. Left: Control plant, right: *Nt*aqp1-AS-expressing plant.

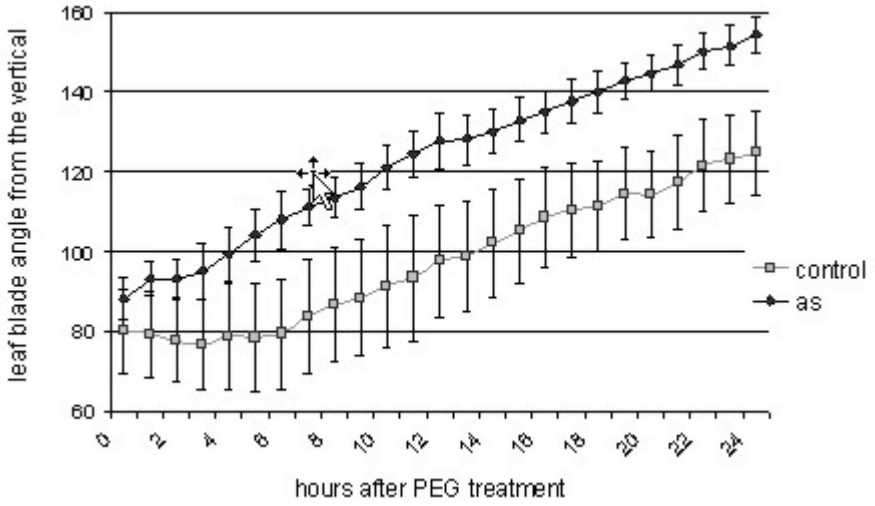

Figure B.37: Average angle of leaves from plants treated with a PEG-solution. The angles were measured in relation to the shoot axis for *Nt*aqp1-AS lines (black rhombs, n = 6) or controls (grey rectangular, n = 8) starting from 2:00 PM in continuous light.

2.8 Function of *Nt*AQP1 in Petioles

To elucidate the function of the aquaporin, *Nt*AQP1-deficient plants were compared in their capacity to move the upper leaves in a diurnal and even circadian way to control plants. The movement was recorded by a digital camera system (Pixera, BDS, Bremen). To evaluate the differences in the moving reaction, the angle between the leaf blade and the axis was measured in the extracted pictures. Figure B.38, A presents the time course of the diurnal leaf movement of

an AS and a control plant. Figure B.38, B depicts a 16 h time course recorded subsequent to 24 h in continuous dimmed light (circadian). The graph of the control plants in Figure B.38, A shows a change in the angle between the leaf and the axis between 58° at 1:00 PM and 18° at 12:00 AM, which means a change of 40°. The graph of the *Nt*aqp1-AS plants displayed a change from the maximum value of 64° at 4:00 PM and the minimum of 45° at 9:00 AM which corresponds to only 19°, thus about half of the angle of the control. Therefore, the leaf movement in AS plants is reduced in velocity and extend of the reaction.

Since *Nt*aqp1 was expressed in a diurnal way in the leaf petioles and the leaf movement was inhibited in *Nt*AQP1 deficient plants, *Nt*AQP1 or at least PIP1b family members are necessary for this process.

After 24 h in dimmed light (after dark period), the control plant continued to display leaf movement (Figure B.38, B). The control plants exhibited a change in the angle from 48° at 9:30 AM to 25° at 2:30AM, which was a difference of 23°. The AS plants had their maximum angle of 56° at 8:30AM and the minimum of 40° at 1:30AM, corresponding to 16°. Thus, the control plants showed a 50 % reduction of leaf-movement after 24 h in dimmed light, while the AS plants didn't react further on the change in light condition. Tobacco plants lose their extensive rhythm after 24 h in dimmed light.

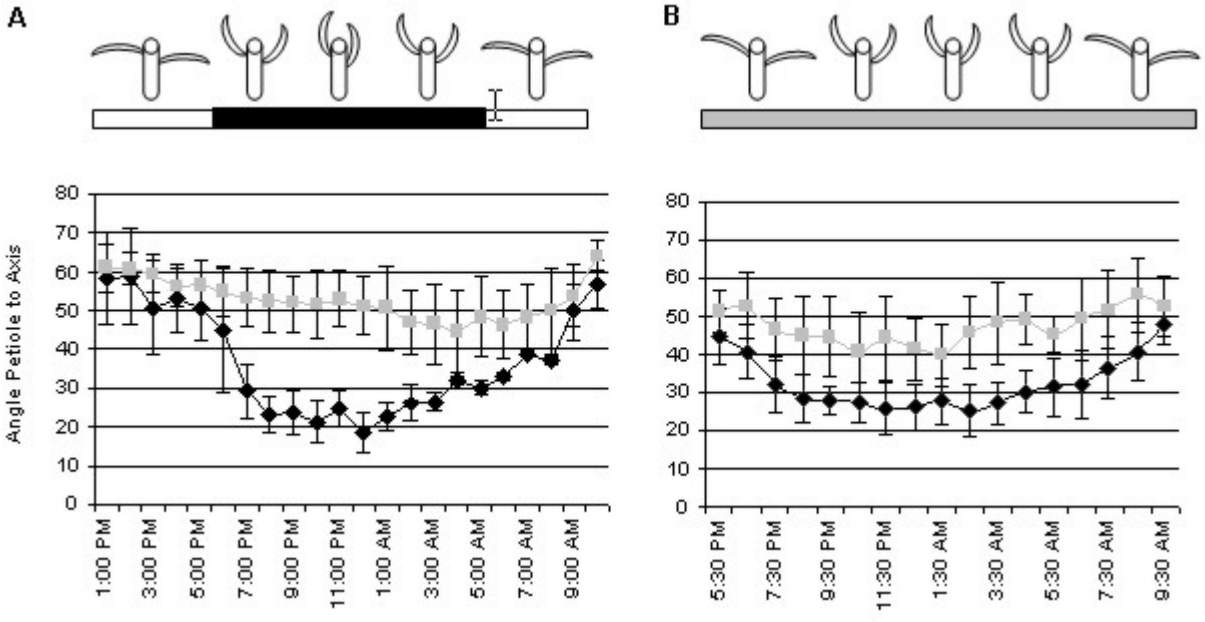

Figure B.38: Diagrams of angles of petioles to the plant axis.
A. 22 h time course of control (black rhombs, n = 4) and AS (grey rectangulars, n = 4) plants.
Plants were kept in a day night rhythm of 12/12 h light/dark. B. 16 h time course of control and AS plants. Plants were kept in continuous dimmed light for 24 h from the beginning of light/day change before measurements were done (after 12 h darkness).

3 Further Attempts to Determine the *Nt*AQP1-Function

3.1 *Nt*AQP1-Overexpression Plants (oe)

*Nt*AQP1-overexpression studies can complete the picture of *Nt*AQP1-function obtained by the AS plants. Antisense protoplasts showed reduced cellular water permeability by about 50 %. The question arises if the induction of *Nt*aqp1-expression in protoplasts can increase the water permeability. Constitutive overexpression of plasma membrane spanning pores often causes serious damage to the cells or even leads to lethal phenotypes. In order to circumvent these problems, plants were constructed in which the aquaporin overexpression can be chemically induced at a defined time point and period.

The system used in this study originates from prokaryotes: Promoter-repression system of tetracycline (tc) - inducible gene expression. The repression principle is based on sterical interference of a repressor protein (TetR) with the transcription initiation complex (Figure B.39). The DNA-binding activity of this protein is abolished by very low amounts of the antibiotic tetracycline. Tetracycline rapidly enters eukaryotic cells and is therefore a favorable inducer for the plant system.

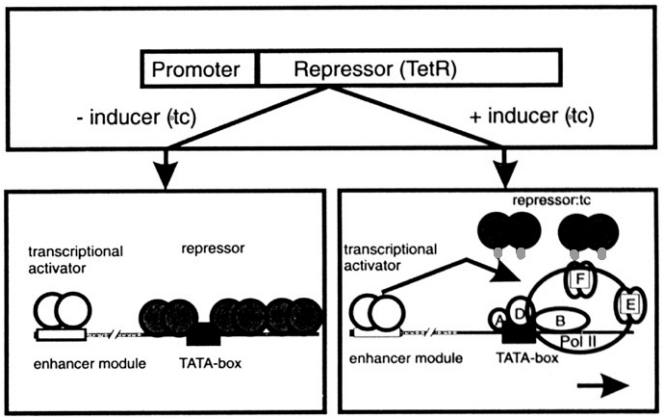

Figure B.39: Schematic representation of a tetracycline (tc) - inducible repression system. The repressor (TetR, black circles) is synthesized under the control of a strong constitutive promoter. The target promoter contains plant enhancer modules upstream of the TATA-box as well as operator sequences (indicated in black) in vicinity of the TATA-box. In absence of the inducer tc (small gray symbols), repressor molecules bind to the operator sequences and interfere with transcription initiation. In presence of tc, the repressor dissociates from the DNA, allowing assembly of the transcription initiation complex that transcription can take place (Figure taken from Gatz, 1997, modified).

3.1.1 Construction of *Nt*AQP1-Overexpression Tobacco Plants

For inducible expression of *Nt*AQP1, the *Nt*aqp1-cDNA was inserted by the restriction sites *Sma*I/*Xba*I into the pBinHyg-Tx vector (see F5). This vector contains three partial 35SCaMV promoters for an effective overexpression of the fused cDNA and an operator region where the tetracycline driven repressor (TetR) binds in the absence of tetracycline to suppress transcription. Competent Agrobacterium was transformed by heat shock with the construct. Tobacco leaf disks

bearing the construct of a constitutively expressed TetR (confirmed by Northern blot) were transformed by means of Agrobacterium. The self fertilized kanamycin resistant plants were tested for tetracycline induced transcription.

3.1.2 Morphology

Whole plant morphology of the uninduced overexpression (oe) plants wasn't obviously different from the controls. But the transformed plants showed a striking phenotype at the flower organs. About 70 % of the flowers and pods abscised prematurely. Surviving flowers were male sterile: The anthers filaments didn't contain fertile pollen. The pistils of the overexpression plants rose up above the petals and anther filaments. They were about 1/3 longer than the pistils of the control plants. Developing seed capsules were 80 % smaller than those of controls but without seeds. It was assumed that this phenotype was due to the "leaking inducible promoter" causing a continuous slight *Nt*aqp1-overexpression.

3.1.3 Northern Blot Analysis

First, confirmation of the overexpression capacity was accomplished by a Northern dot blot of RNA from leaf disks (Figure B.40) incubated for 24 h in 1 mg/ml tetracycline. As a control leaf disks treated with the same solution without antibiotics were used. The control clearly displayed less *Nt*aqp1-expression, than the induced leaf disks from one of the transformed plants.

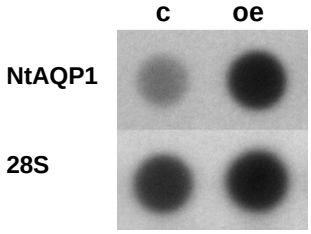

Figure B.40: Northern dot blot of total RNA of leaf disks incubated for 24 h in water (control c, left) or in 1 mg/ml tetracycline (oe, right). Hybridization with [α-^{32}P]dCTP labeled cDNA probes of *Nt*aqp1 (upper row) and 28S (lower row).

3.1.4 LightCycler Experiments

3.1.4.1 Primer Design

3.1.4.1.1 Internal Standard, Actin

Actin was used as internal standard for relative quantification of *Nt*aqp1-expression. For the primer design a homologue region of the tobacco actin fragment Tob103 to ACT2/8 was used. ACT2 and ACT8 are constitutively expressed in all vegetative tissues and determine 80 % of the whole actin expression (An et al, 1996). The melting temperature T_m, determined with the %GC

method was 66.2°C for *Nt*Tob103fwd and 64.4°C *Nt*Tob103rev (see F3). The primer test showed an optimal annealing temperature (T_{an}) from 48 to 54°C with a primer concentration of 0.5 µM. The amplified product was 275 bp in length. For the experiments a T_{an} of 54°C was chosen.

3.1.4.1.2 *Nt*AQP1-Primers

*Nt*aqp1-primers were designed to have comparable T_m to the actin primer pair and to show at least four mismatches to other known tobacco aquaporin sequences. The calculated T_m was 63.5°C for *Nt*aqp1-LCfwd and 64.4°C for *Nt*aqp1-LCrev. The primer tests (see D6.10.1.1) revealed an optimal T_{an} from 48°C to 56°C. The amplified product had a length of 339 bp. For the experiments a T_{an} of 54°C was chosen.

3.1.4.2 Studies of *Nt*AQP1-Expression in Protoplasts

In a first attempt isolated leaf protoplast from overexpression plants treated with tetracycline for 0.5, 1, 2, and 4 h were tested. It was expected that these show an increased *Nt*aqp1-expression compared to control protoplast from plants without the construct.

LightCycler experiments revealed that the protoplasts from both plant types had a similar steady decrease in *Nt*aqp1-expression. Figure B.41 also depicts that the *Nt*aqp1-content in the overexpression plants was slightly higher at the 0.5 and the 1 h time point which was probably due to the "leaking", not very tight repressor system and with that a constitutive increased level of *Nt*AQP1-mRNA.

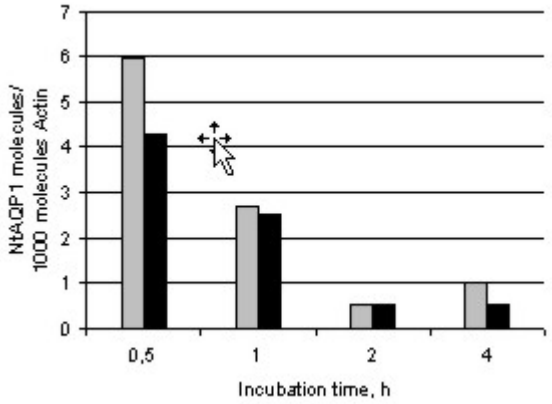

Figure B.41: *Nt*AQP1-mRNA content of protoplasts isolated from control and overexpression plants, incubated in tetracycline medium (1 mg/l) for 0.5, 1, 2, and 4 h. Black bars describe the control and grey the ones from *Nt*aqp1-overexpression leaf disks.

The decrease of mRNA content implied that an increasing incubation of the protoplasts in tetracycline containing solution inhibited the *Nt*AQP1-overexpression in the transformed plants. On the other hand the viability of the protoplasts and activity of cellular metabolism could be influenced followed by a reduction of transcription. A fast turnover rate of *Nt*aqp1-mRNA could explain the decrease of this specific transcript. Actin transcripts might be more stable so that they sustained the inhibition of transcription. Microscopic observation displayed that the incubated protoplasts lost their integrity and didn't show any cytoplasmic streaming any longer.

The decrease could also be explained by a circadian variation of *Nt*aqp1-expression and that the tetracycline induction was not jet observed because of the relative short time of application (4 h). But since Gatz (1997) got a transcriptional activation in minute range, the decrease can probably be traced back to the treatment of the cells which were isolated from the tissue and further incubation in a shaking tube. To rule out the effect of the cell isolation procedure, leaf disks were used in the next experiments. For that disks (Ø 1cm) of *Nt*AQP1-inducible- and control plant leaves were punched out and treated with tetracycline for 0, 2, 4, 8, 16, 32, 48, and 64 h (1 mg/l in H_2O).

3.1.4.3 Studies of *Nt*AQP1-Expression in Leaf Disks

cDNA (see section D5.1.2 and D5.2) obtained from mRNA isolated from these leaves were used in the LightCycler to monitor *Nt*aqp1-transcript content and the isolation of whole protein from the same samples were used in Western blot to monitor *Nt*AQP1-protein content.

LightCycler results displayed an increase in *Nt*aqp1-expression compared to control leaf disks undergone the same treatment (Figure B.42). The expression level was related to the actin expression of both leaf disk populations. Already after 4 h a three fold increase related to the control expression of the *Nt*aqp1 transcript could be observed.

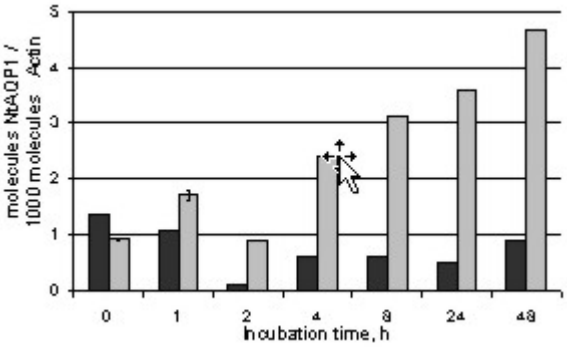

Figure B.42: Result of LightCycler experiments. *Nt*AQP1-cDNA content (molecules *Nt*aqp1/ 1000 molecules actin) of leaf disks from control and overexpression plants, incubated in tetracycline containing medium (1 mg/l). Black bars describe the control and grey bars the overexpression-leaf disks.

For comparison of different cDNAs preparations, consistent control samples (one control cDNA and overexpression cDNA) were always included in LightCycler runs. The ratio of *Nt*aqp1-expression between these two samples remained constant in all experiments. Thus, variations in PCR performance could be observed and considered for the subsequent calculations. The ratio was between 1.8, 2.8, and 2.4 which is a regular range of variation of PCR-reactions.

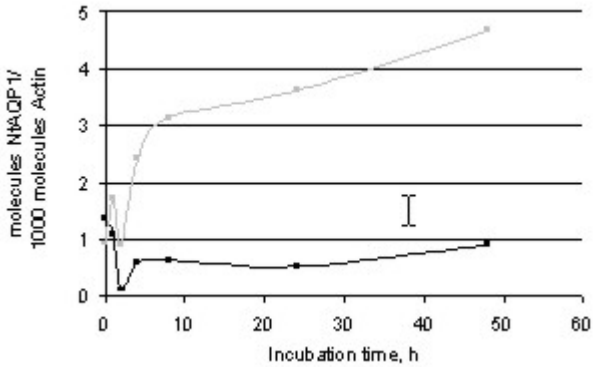

Figure B.43: Result of LightCycler experiments. Time course of *Nt*aqp1-transcript content (molecules *Nt*aqp1/ 1000 molecules actin) from leaf disks of control and overexpression plants, incubated in tetracycline medium (1 mg/l). Black squares describe the control, grey squares the leaf disks of oe.

The control displayed a relatively constant expression of *Nt*aqp1-transcripts (Figure B.43). Only slight variations were visible which were most likely due to circadian rhythm of *Nt*aqp1-expression (see B1.3.4 and B2.5.2).

The constant increase of *Nt*aqp1-mRNA in overexpression leaf disks implicated that its expression was induced by tetracycline. After about 6 h a decline of mRNA content could be observed which reaches almost saturation (Figure B.44).

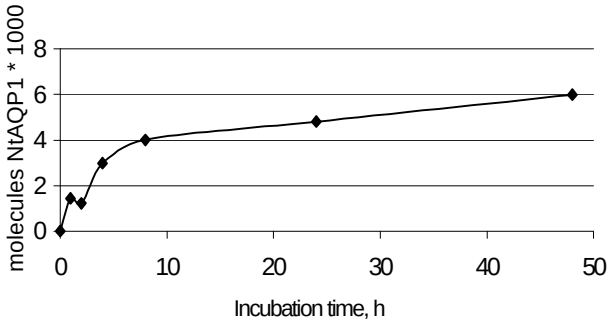

Figure B.44: Result of LightCycler experiments. Difference in *Nt*aqp1-content (molecules *Nt*aqp1/ 1000 molecules actin) of leaf disks from induced and control plants to eliminate circadian variations.

Leaf disks of the same treatment were subjected to protein expression analysis to prove that also the translation machinery passes this increase in expression on.

3.1.5 Protein Analysis

*Nt*AQP1-protein expression was high in roots and low in leaves. An induction of protein expression in leaves was expected to lead to a specific 30.5 kDa protein accumulation. If protein accumulation followed mRNA production the protein was expected to be visible by PAGE and Coomassie and Silver staining or by Western blot/ immuno-detection.

Proteins were extracted from the samples and subjected to a SDS-PAGE. The expression pattern of the overexpression and the control leaf disks was different (Figure B.45, A). In the chemiluminescent Western blot (Figure B.45, B), an elevated expression of a ~30 kDa protein (marked with an arrow) was identified for the overexpression leaf disks. The specific band was already present in the first sample which directs to an "leaky promoter" or with other words to a constitutive overexpression of *Nt*AQP1. This also explains the phenotype of uninduced overexpression plants (B3.1.2). A further increase in chemiluminescence intensity with elongated incubation time in the tetracycline solution could not be detected which points to a posttranscriptional regulation mechanism avoiding the translation of the *Nt*aqp1-mRNA.

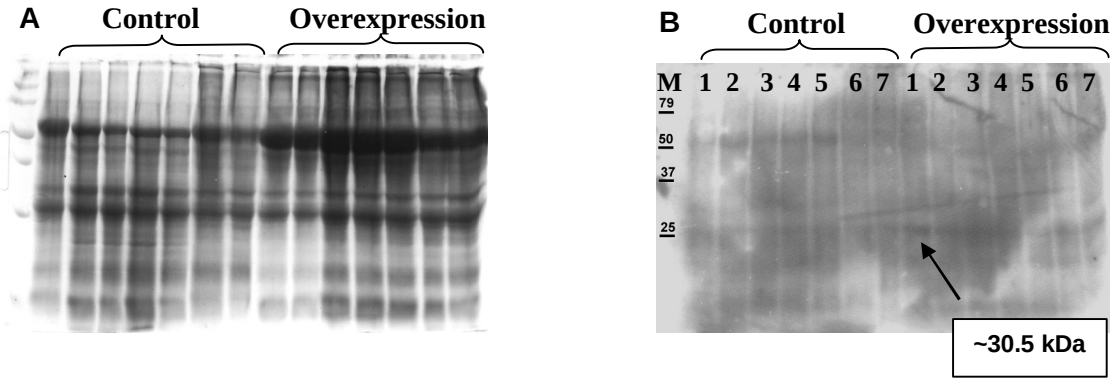

Figure B.45: Results of the protein analysis of tetracycline induced *Nt*aqp1-overexpression in tobacco leaf discs. A. Coomassie stained gel. B. Chemiluminescent Western with a specific PIP1b-antibody. Lanes 1-7 correspond to time points of incubation of 0, 2, 4, 8, 16, 32, 48, and 64 h with tetracycline.

These results indicated that the TetR expression system was not suitable for inducible but only for constitutive *Nt*AQP1-overexpression. Comparable problems also occurred when *Nt*AQP1 was overexpressed in the heterologous expression system of yeast and *E.coli* (B. Otto, personal communication).

3.2 Pollen Tube Growth as a Model System

The extremely fast growth process of pollen tubes requires continuous water uptake. It provides an accessible and well characterized system for studying the role of aquaporins in growth processes.

The *Nt*aqp1-promoter contained the AGAAA activator unit of lat52 at position -1281 (-), 1070 (-), -993 (+), -682 (+), 557 (-), +10 (+) (POLLEN1LELAT52 see appendix F4.1,). The tomato lat52 gene encodes an essential cysteine-rich protein preferentially transcribed in the vegetative cell during pollen maturation. It was shown by Bate and Twell (1998) that this minimal sequence containing the activator unit is responsible for lat52 specific expression in pollen. Additionally, the *Nt*aqp1-promoter contains the GTGANTG10 motif (Rogers et al, 2001) at the positions -1228 (+), -850 (+), -198 (+),-936 (-), +64 (+), +278 (-). The function of the conserved GTGA motif shared between the tobacco g10 and tomato lat56 promoters was demonstrated in g10. The tobacco gene g10 is preferentially and maximally expressed in mature pollen. Is *Nt*AQP1 therefore also expressed in pollen and does it play a role in water uptake processes?

3.2.1 Expression of *Nt*AQP1 in Pollen

p*Nt*aqp1::gus plants were used to detect *Nt*aqp1-expression in pollen grains. For that anthers were harvested from GUS and control plants. The pollen grains were washed off in a solution of calcium, boron and sucrose and were subjected to *in vitro* germination (D3.1). A GUS assay (D11.1.1) was performed at different time points (Figure B.46, Figure B.47). The blue staining could be seen all over in the hydrated pollen grains and slightly in the growing pollen tubes. About 50 % of the pollen grains displayed GUS activity, which is due to the segregation of the genes during meiosis.

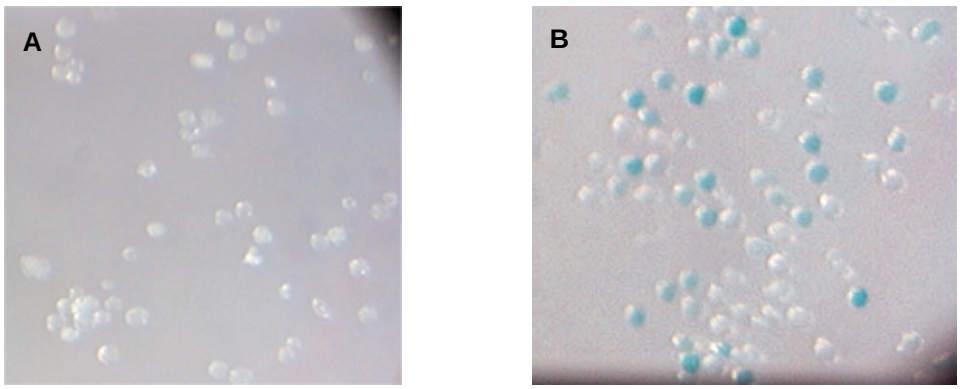

Figure B.46: Results of GUS assay on pollen grains germinated on solid medium, (10 x magnification). A. Control pollen grains of wild type plants. B. Pollen grains of p*Nt*aqp1::gus plants, 30 min after incubation in liquid germination medium (GM).

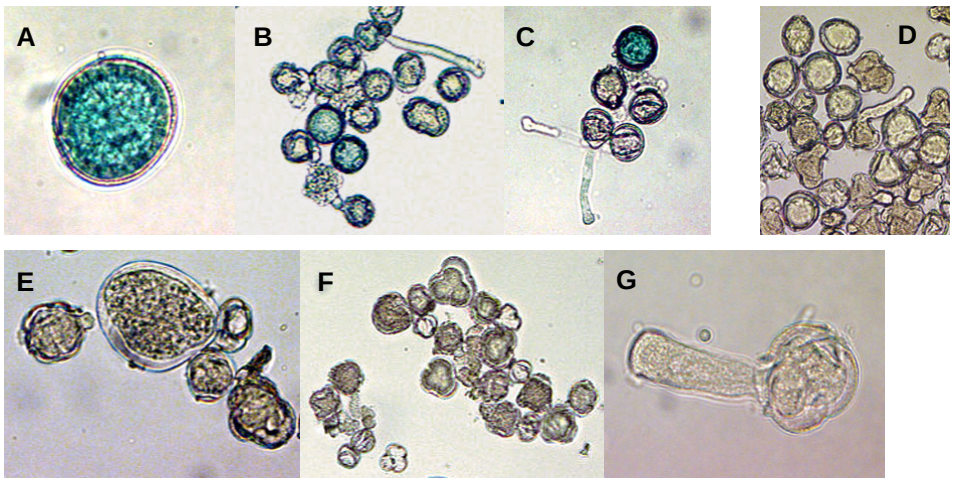

Figure B.47: Results of GUS assay on pollen grains germinated on solid medium; magnification is given in brackets. A. p*Nt*aqp1::gus, 30 min. (100 x) B. p*Nt*aqp1::gus, 2h, overview (16 x). C. p*Nt*aqp1::gus, 2 h (16 x). D. 35SCaMVp::gus, 2 h (16 x). E Control, 30 min (100 x). F Control, 2h, overview (16 x). G. Control, 2 h after incubation in liquid GM (100 x).

*Nt*AQP1, expressed during hydration of pollen, may play a role in the reconstitution of the cellular water uptake.

3.2.2 Function of *Nt*AQP1 during Pollen Germination and Pollen Tube Growth

To analyze the function of *Nt*AQP1 in pollen germination and tube growth, *Nt*AQP1-AS plants were used. Pollen grains were harvested from AS and control plants and subjected to *in vitro* germination (D3.1). After 20 min incubation in liquid germination medium the pollen grains were plated on petridishes containing solidified germination medium. The tube growth was recorded by a digital camera system mounted on a Zeiss microscope. Single pictures were extracted and used to measure the tube length (Figure B.48). The germination time point was recorded and growth rate was determined. Detailed data for one typical growth experiment are summarized in Table B.7. In contrast to the expected delay in hydration, germination and tube growth, AS pollen grains hydrated, germinated and grew as controls or even faster. This is probably due to the 35SCaMV promoter used to drive the expression of the AS construct. It was reported that this promoter is inactive in pollen (Bate and Twell, 1998). Additionally the 35SGUS construct with the same 35SCaMV promoter also didn't display any activity.

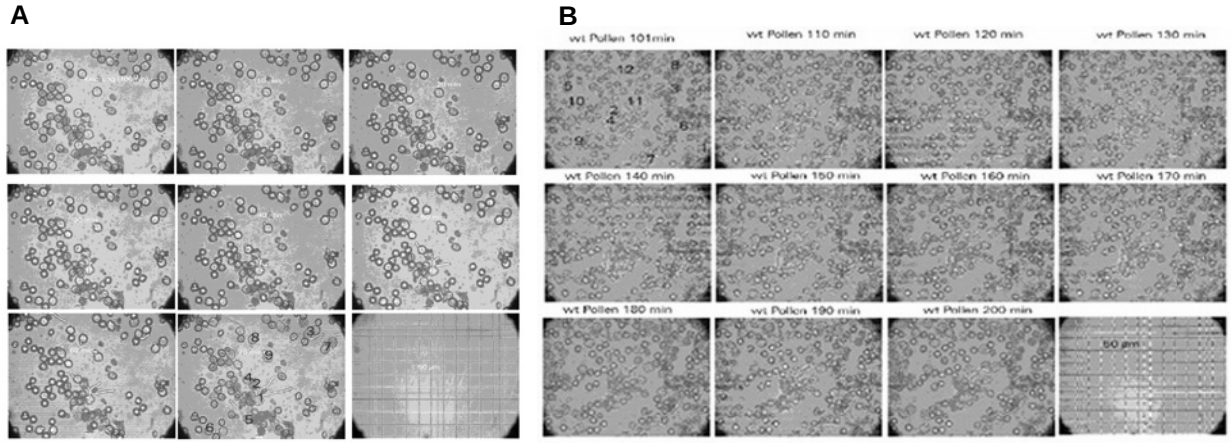

Figure B.48: Microscopic pictures of pollen tube growth of A. AS pollen grains and B. Control pollen grains on germination medium plates at different time points. Pollen grains were numbered and each picture was marked with the capture time point.

Table B.7: Antisense (A) and control (B) pollen germination and tube growth data: Time points of germination after transfer to liquid medium are given for nine AS pollen grains (numbered 1-9) and twelve control pollen grains (numbered 1-12). Due to their orientation three AS pollen tubes and five control tubes could be measured in this assay. The growth rate minimum (GR_{min}) and maximum (GR_{max}) as well as the average growth rate is given in the table.

A

antisense pollen number (PN)	**1**	**2**	**3**	**4**	**5**	**6**	**7**	**8**	**9**
germination (min)	40	40	61	47	61	79	81	75	50
growth rate min. (GR_{min} in µm/min)	1.27	1.02	2.33						
growth rate max.(GR_{max} in µm/min)	2.98	3.69	2.71						
Æ **growth rate (GR in µm/min)**	2.03	2.92	2.05						

B

control PN	**1**	**2**	**3**	**4**	**5**	**6**	**7**	**8**	**9**	**10**	**11**	**12**
germination (min)	44	60	60	60	60	60	68	85	101	101	120	120
GRmin					2.11	1.18	0.25			1.26	0.22	
GRmax					2.54	2.48	1.43			1.80	1.75	
Æ **GR**					2.30	1.66	0.64			2.06	0.94	

C DISCUSSION

1 *NtAQP1*-Expression

The aquaporin *Nt*AQP1 was identified as an intrinsic protein of the plasma membrane and characterized as a heavy metal insensitive aquaporin by analysis of Xenopus oocytes expressing the corresponding cRNA (Biela et al, 1999). Additionally to facilitation of water flux, *Nt*AQP1 also displays permeability to urea and glycerol. If the data obtained by the oocyte experiments reflect the same protein features in the plant, the significance of *Nt*AQP1 for the passage of water and small solutes from plant roots to leaves could be concluded from its location.

To study the expression pattern of *Nt*AQP1 in detail, promoter reporter studies were performed. For these studies the β-glucuronidase system (GUS), which is characterized by its intensive blue stain and its high sensitivity and the non-invasive but less sensitive luciferase (LUC) were applied. Computer based analysis of the *Nt*aqp1-promoter region (Siefritz, 1998, sequence see F4) revealed putative tissue-specific and regulatory sequences which influence the transcription of the aquaporin. Tissue-specificity, developmental and environmental as well as phytohormone regulation of *Nt*AQP1 could be detected in these studies.

1.1 Transcriptional Regulation

1.1.1 Tissue-Specificity

Root specific sequences were highly abundant in the promoter region (ROOTMOTIFTAPOX1, Elmayan and Tepfer (1995)). Elmayan and Tepfer (1995) could show that this motif strongly directs expression to roots, and much less to stems and leaves. The increased concentration of *Nt*AQP1 in roots was shown by Northern blot experiments (Siefritz et al, 2001). Promoter GUS studies revealed an accumulation in the root hair zone, the region of water uptake. The *Nt*AQP1-protein was found to be expressed in virtually all parts of tobacco close to the vascular bundles with highest levels in the root. Therefore it can be predicted that *Nt*AQP1 most likely contributes to water uptake processes (Otto and Kaldenhoff, 2000).

Another putative tissue-specificity was discovered: The *Nt*aqp1-promoter showed similarities to the Lat52 (late anther tomato 52)-promoter. Lat52 encodes an abundant cysteine-rich protein and plays an essential gametophytic role in pollen hydration and tube growth demonstrated by AS down regulation in tomato (Muschietti et al, 1994). Twell showed already in 1994, that the Lat52 5'-UTR acts as tissue-specific translational activator. Taylor and Hepler (1997) suggested that germination and initial tube growth depends on translation of stored mRNAs, produced in the late stages of pollen development. The *Nt*aqp1-promoter GUS studies clearly revealed *Nt*aqp1-expression in the pollen grains, thus this aquaporin is a candidate for a protein required in pollen germination and initial tube growth.

Additionally, the *Nt*aqp1-promoter contained the GTGANTG10 motif at the positions -1228 (+), -850 (+), -198 (+),-936 (-), +64 (+), +278 (-) (Rogers et al, 2001). The function of the conserved GTGA motif shared between the tobacco g10 and tomato lat56 promoters was demonstrated in g10. The tobacco gene g10 is preferentially and maximally expressed in mature pollen. Analysis of transgenic plants showed that 1190 bp of g10 5'-sequence directed preferential expression of GUS in pollen. Transient expression analysis defined the minimal g10 promoter region capable of directing expression in pollen as -86 to +217.

It could also be shown that *Nt*AQP1 was expressed in leaf glandular hairs. This expression could be due to myb-like protein activity (see next section).

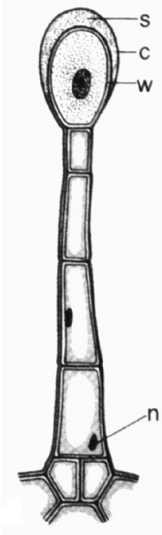

Figure C.1**:** Characteristic glandular hair (magnification about 200 fold). Glandular hairs consist of living cells, which are differentiated into stalk cells and a capitate cell. The secretion is produced in the cytoplasm of the capitate cell and accumulates between the wall and its cuticle. It is liberated when the cuticle ruptures (Fahn, 1979). s = secretion c = cuticle and cuticular layer, w = wall (cellulose), n = nucleus. (Scheme taken from Nultsch, 2001)

Some of the glandular hairs release aqueous solutions of hydrophilic substances, but the majority release lipophilic secondary plant products, including essential and fatty oils, resins, etc. Most of the glandular hairs, have a well-expressed phase of granulocrine (vesicles fuse with plasma membrane) excretion similar to the essential oil production in leaves and resin accumulation. Substances are produced in the cytoplasm of the capitate cell and accumulated between the wall and its cuticle (see Figure C.1). They are liberated when the cuticle ruptures. The cells near the base of some secretory structures possess suberized or cutinized walls; some are equipped with *Casparian Band*s. By separating the cell wall apoplasm of the secretory tissues from the remainder of the cell wall apoplasm, these bands could limit and direct the flow of secreted substances. They may also be important in limiting water loss through a ruptured cuticle as in preventing the backflow of the secreted substances into the apoplasm (Schnepf, 1974). *Nt*AQP1 may be involved in the developmental process of glandular hair formation or in the regulation of water flux, or it may transport other substances than water, since it has been shown to be also permeable to glycerol and urea.

1.1.2 Developmental and Environmental Regulation

The analysis of the *Nt*aqp1-promoter region identified multiple MYB-like protein binding sites: MYB2AT at position -965 (-), MYBATRD22 at position -614 (+), MYBCORE at position -965(+), -968 (-), MYBGAHV at position -1146 (+) MYBPLANT at position-612 (+), -744 (-). Myb-like proteins are sequence-specific DNA-binding proteins that can activate or inactivate promoters containing their binding site (reviewed in Luscher and Eisenman, 1990). Myb-domain proteins are involved in the regulation of a number of plant-specific functions such as phenylpropanoid and flavonoid accumulation (Paz-Ares et al, 1987; Grotewold et al, 1991; Sablowski et al, 1994), hormone and dehydration responses (Gubler et al, 1995; Urao et al, 1993), trichome or hair formation (Oppenheimer et al, 1991), and cell shape determination (Noda et al, 1994). In transient expression studies it was already shown that the *cis*-acting regulatory DNA-elements of the phytohormones gibberellic acid (MYBGAHV) and abscisic acid (MYBATRD22) activate *Nt*aqp1-transcription (Siefritz et al, 2001). Investigation of stable transformed tobacco (p*Nt*aqp1::gus, p*Nt*aqp1::luc) confirmed this activity *in planta*. It was demonstrated that GA strongly induced *Nt*aqp1-expression. With the high time resolution of *Nt*aqp1-promoter driven luciferase expression, a correlation between reporter increase and hypocotyl- as well as root tip growth was detected. But also ABA acted in a dose dependent manner on the transcription of the aquaporin. Therefore *Nt*AQP1 is regulated by GA and ABA.

p*Nt*aqp1::luc plants also revealed that the *Nt*aqp1-expression is highly regulated during the germination process. The tonoplast intrinsic aquaporin α-TIP of *Phaseolus vulgaris* was shown to be a seed-specific aquaporin and to be regulated during germination (Maurel et al, 1997b). It was suggested that TIP aquaporin activity may help to achieve cytoplasm osmoregulation and control of the vacuolar volume. Osmoregulation may also be one of the functions of *Nt*AQP1 during the process of rehydration. But the luciferase studies showed a further differential expression: It was turned on with hydration, increased during breaking of the radicle through the seed coat, decreased afterwards and turned on again in a defined moment in the root tip where highest water uptake is required. *Nt*AQP1 seemed to be involved in seedling expansion and development and in the uptake of water similar to γ-TIP which progressively substitutes α-TIP after seed germination remaining expressed throughout plant development mainly in elongating tissue (Ludevid et al. 1992, Maeshima et al, 1994). Confirmation for *Nt*AQP1-function can only be obtained by further investigation of AS plants.

The *Nt*aqp1-promoter contains cis-acting elements present in light-regulated genes. The *Nt*aqp1-promoter GUS studies revealed an expression during light dependent processes like phototropism. Some of the important cis-acting elements present in light-regulated genes include GT-1 core (GGTTAA) or consensus sites (GRWAAW), I-Boxes (GATAA) and G-Boxes. None of these elements alone is able to confer light-regulation onto a non-light-regulated gene. Light-regulation arises from various combinations of different elements. Combination in pairs is required (Puente et al, 1996). The *Nt*aqp1-promoter contained all of the above mentioned motifs except the G-BOX in multiple copies.

The direction of plant growth is controlled by two main guidance systems: phototropism and gravitropism. Phototropism is a growth orientation of plant organs in response to a light stimulus: mainly of shoots towards a unilateral light source. It ensures that leaves and stems of shoots will receive optimal sunlight for photosynthesis. The bending reaction in response to tropic stimuli often results from the lateral redistribution of hormones (Iino, 1995; Kaldenhoff and Iino, 1997). *Nt*aqp1-expression showed a clear induction in these processes, mainly on the elongating side of the bent stem so that it may be involved, e.g. in the redistribution of water in the bending reactions. Blue- and white light regulation was already shown for AtPIP1b (Kaldenhoff, 1995 and 1996). Smart et al (1998) could demonstrate that MIP transcripts are accumulated during turgor-driven cell expansion with highest levels in the period of peak expansion and a decline with the onset of secondary wall synthesis. Studies of AS plant reaction, in response to stimulation by gravity and/or light could confirm this hypothesis for *Nt*AQP1. Stimulation e.g. by blue light from one side onto AS and control plantscould reveal if *Nt*AQP1 is involved in phototropism. Bending assay in red light can reveal the influence of *Nt*AQP1 in gravitropism.

Another important environmental factor is the water availability. *Nt*aqp1-expression was increased by salt and osmotic stress in the root. Guerrero et al showed already in 1990, that aquaporin expression is induced by turgor variations during wilting of stems. Several other PIPs have already been demonstrated to be up-regulated under salt and drought stress (Yamada et al, 1997; Fray et al, 1994; Yamaguchi-Shinozaki et al, 1992). In opposition Martinez-Ballesta et al (2000) postulate that aquaporin activity is reduced under saline conditions. Wilting experiments with *Nt*AQP1-AS plants revealed, that this aquaporin has to be present to render tobacco plants more resistant to extreme water deficiency. When exposed to high salinity or drought conditions most plants begin to accumulate low molecular weight metabolites such as proline, glycine-betaine, or polyols in cells (Bohnert et al, 1995). It has been proposed that aquaporins play a dual activity in cell osmoregulation in the tonoplast and the plasma membrane (Gerbeau et al, 1999).

1.1.2.1 Circadian Expression

Identification of tomato Lhc promoter motif "CIACADIANLELHC" (see appendix) in the *Nt*aqp1-promoter may explain the results of luciferase and Northern experiments, where diurnal as well as circadian expression of *Nt*aqp1 could be demonstrated. The motif described by Piechulla et al (1998) is necessary for circadian expression of tomato Lhc. A short sequence of 47 nucleotides is necessary for conferring circadian Lhc mRNA oscillations. Sequence alignment of the specified promoter regions revealed a novel motif 'CAANNNNATC'. This motif is conserved in 5'-upstream regions of clock controlled Lhc genes and overlaps with a sequence relevant in phytochrome mediated gene expression. The temporal expression of *Nt*aqp1 in roots could explain the circadian variation of the root hydraulic conductivity. The maxima and minima of the expression anticipate the conductivity rhythm by 2-4 h. To confirm this striking

correlation it is planned to investigate whether AS plants perform a circadian rhythm of the hydraulic conductivity.

The observed diurnal variation of *Nt*aqp1-expression in leaves was coordinated with the tobacco leaf movement. It could be shown by luciferase experiments and AS plant analysis that *Nt*AQP1-prescence is significant for this plant movement (next section). Previous studies (Moshelion et al, 2002; Clarkson et al, 2000) could only show the correlation of a phenomenon and an aquaporin expression. The presented studies can provide evidence that aquaporins are indeed involved regulatively in plant movement.

2 *Nt*AQP1-Function

2.1 Water Uptake and Transport in Roots

In this work it was shown, that the high concentration of *N*tAQP1 in roots accounted for the conductivity of the plasma membrane and the whole root system to water. By comparing *Nt*aqp1-antisense plants inhibited in *Nt*aqp1-expression to control plants, evidence was found for the aquaporin function in cellular- and whole plant water-relations. The *Nt*aqp1-antisense expression affected only the closely related *Nt*PIP1a, other less similar mRNAs like *Nt*PIP2a or *Nt*TIPa accumulated to the same level as in control plants. These results were in agreement with studies on PIP1b-antisense Arabidopsis plants (Grote et al, 1998). Accordingly, the results obtained by the subsequent biophysical and physiological studies can be accounted for the reduced expression of PIP1 family members and specify the function of these proteins.

A significant decrease in cellular water permeability was determined by a new method. Here the swelling kinetics of root protoplasts subjected to a steep osmotic gradient were measured and found to be significantly reduced. Therefore *Nt*AQP1 is important for cellular water transport. Consequences for the whole plant were an about 50 % reduction of root hydraulic conductivity and the lower water stress resistance shown by the wilting experiments under extreme soil water depletion. A similar effect was also observed in leaf protoplasts from PIP1b-antisense Arabidopsis plants (Kaldenhoff et al, 1998). While these plants developed a larger root system, possibly to compensate the consequences of the reduced cellular water permeability, tobacco did not show such morphological changes.

The strong correlation between cellular water permeability and specific root hydraulic conductivity indicates for the significance of the symplastic pathway with regard to vascular and long distance water transport. It shows, and this is the second conclusion, that cellular water transport is indeed important, and thus a pure apoplastic one is of minor impact in roots. Since the exact number of tobacco aquaporin genes and their pattern of expression is still unknown, the evaluation of the precise relation between the apoplastic and symplastic pathway remains difficult. However, it can be concluded from the presented hydraulic conductivity data that the

relation of apoplastic to symplastic transport is at least 1 to 3. It would be shifted in favor to the symplastic pathway if other aquaporins that were not impaired by the AS expression would also contribute to cellular root water permeability.

As a second physiological response, caused directly or indirectly by signals generated through the reduced aquaporin expression, *Nt*aqp1-AS tobacco changed factors that alter the water mobility. The plants decreased water potential and limited further water loss by reduction of transpiration. In line with this interpretation is the observation that *Nt*aqp1-AS lines were less resistant to PEG addition. This treatment strongly decreased the soil water potential and induced a strong water stress. The tobacco lines with a reduced PIP1-aquaporin expression wilted earlier, possibly because a critical tissue water potential and turgor pressure was reached much earlier.

A correlation between water permeability changes of leaf cells, e.g. those in the stomatal cavity, and the early wilting phenomena under water stress were not apparent, because AS lines responded to an appropriate stimulation of stomatal opening with the same transpiration kinetic as controls in detached leaves. Transpiration kinetic depicted the same reaction on the onset of light. The transpiration rate of detached leaves was the same in AS and control plants. Accordingly, the third conclusion is that expression of *Nt*AQP1 or related PIP1 aquaporins contribute to water stress resistance.

In fact, for tobacco plants that were grown under well-watered greenhouse conditions, the PIP1 aquaporins did not seem to be important for water uptake or -management. However, if increased hydraulic resistance due to a lack of *Nt*AQP1-like aquaporins adds up with low soil water potential, AS plants are not able to maintain turgor above the wilting point anymore. They appear less drought-tolerant. Thus, if water uptake becomes limiting, expression of PIP1 aquaporins will enhance cellular water permeability, increase root hydraulic conductivity, relief osmotic pumps and significantly support the overcoming of dry periods. Taken together, the data present the significance of aquaporin-function for plant physiology. In addition, the importance of the symplastic water transport pathway could be evaluated and a new mechanism for water stress resistance in plants is described.

2.2 Other Functions of *Nt*AQP1

Growth Processes

Tobacco showed a fast reaction on gravi- and photostimuli. This reaction requires high water fluxes during the bending reaction where *Nt*AQP1 may be involved. Bending experiments with p*Nt*aqp1::gus plants showed increased expression of *Nt*aqp1 in the region of increased growth. Extension of the experiments to AS plants can verify the assumption that *Nt*AQP1 is essential for the reactions. Other growth processes, like adventitious root formation where *Nt*aqp1-expression was induced too, should further be investigated with the AS plants.

Gas Exchange – Antisense Effect in Leaves

*Nt*AQP1 is required for regulation of water release. Transpiration and stomatal conductance was affected in AS plants. The reduction of the stomatal conductance (g_s) was not due to the loss of *Nt*AQP1 in the leaves, but elsewhere in the plant because detached AS leaves showed the same mean conductance as control leaves. g_s of AS plants displayed a striking oscillation which can be directed to the loss of *Nt*AQP1-function in the leaf because the phenomenon was also observed in detached leaves. The net photosynthesis and g_s varies, therefore the oscillations may result from effects of the *Nt*aqp1-antisense expression on CO_2 gas exchange. The capacity of aquaporins to be permeated by gases was demonstrated for the mammalian AQP1 after expression in Xenopus oocytes (Nakhoul et al, 1998; Cooper and Boron, 1998) and reconstitution of the purified protein in proteo-liposomes (Ramesh Prasad et al, 1998). Wayne et al (1994) could show that the hydraulic conductivity of *Chara* cells is dependent on CO_2-availability and therefore suggested a correlation of water and CO_2 transport in both algea and higher plants. Conclusively, *Nt*AQP1 may affect not only water relation of gas exchange but also carbon supply. On the other hand *Nt*AQP1 may have a signaling function which is disturbed by the AS effect.

What is the Function of *Nt*AQP1 in the Tobacco Petioles?

Tobacco Leaf Movement

The tobacco leaf movement displays a 24 h period under normal light/dark conditions and also about 24 h (circadian) under constant light and temperature. For this pronounced and relatively fast movement it was suggested that high and variable water permeability is required. Moshelion et al (2002) could demonstrate that the osmotic water permeability of *Samanea saman* motor-cell protoplasts was diurnally regulated and the transcript of SsAQP2 was under circadian control in these cells.

It could be documented that *Nt*AQP1 is involved in the tobacco sleep movement. The AS plants exhibited only a very weak movement of the leaves while the control plants displayed an extended movement from the about horizontal to the almost vertical position of the petioles. The rhythm of the control plants was extended for another 24 h in dimmed light but got lost in the following cycle. The fact that the water permeability of the AS tobacco protoplasts was reduced to 50 %, led to the conclusion that *Nt*AQP1 might contribute to the movement by the change of plasma membrane water permeability. But it might also be involved in other processes, e.g. of the signaling cascade. These findings might reveal further insight in the processes and molecular basis required for plant mobility.

Function in Photorespiration

The ratio glycine to serine (G/S) was decreased in AS plants. Serine contents were higher, glycine contents lower in AS plants. This ratio gives information about the ratio of photorespiration and Calvin cycle. Rubisco (Ribulose-1,5-bisphosphate carboylase/oxygenase) catalyzes the carboxylation and oxygenation of Ribulose-1,5-bisphosphate (RuBP) (Ogren et al, 1984). Carboxylation takes place in the Calvin cycle; oxygenation is the primary reaction in photorespiration. Photosynthetic CO_2 fixation and photorespiratory oxygenation are competing reactions. Photorespiration results in a loss of CO_2 from cells that are simultaneously fixing CO_2. Two molecules glycine are converted to a serine and CO_2. Glycine therefore serves as an intermediate source of photorespiratory CO_2. Photorespiration increases when temperature rises (nature of the gases CO_2 and O_2). It is not known why the cycle of photorespiratory carbon oxidation (PCO) exists. A possible explanation is, it may be important under water stress conditions at high light intensities and low intercellular CO_2 concentrations, to dissipate excess ATP and reducing power from the light reactions, thus preventing damage to the photosynthetic apparatus. AS plants may display disturbed CO_2 uptake together with water limitations due to water resistance in the roots, so that they switch metabolic processes. AS plants will be used for further investigations of the *Nt*AQP1-influence on CO_2 uptake processes.

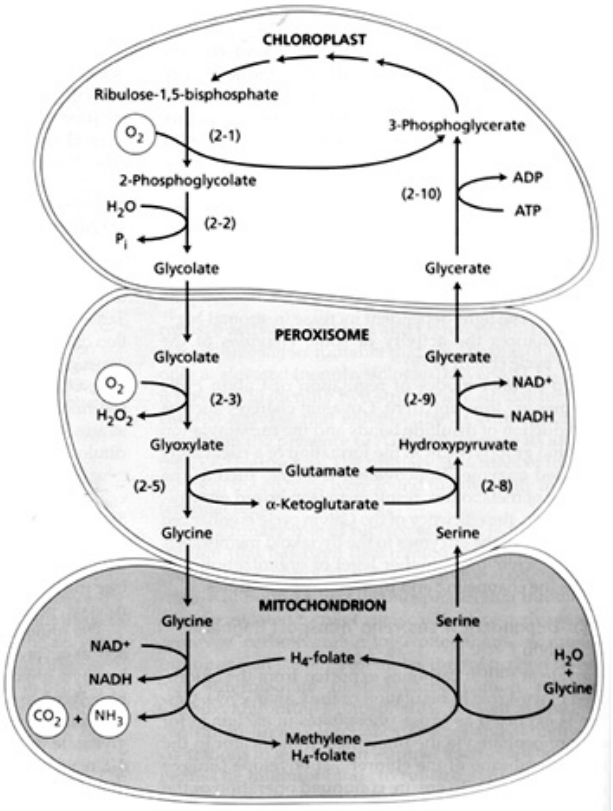

Figure C.2: Schematic representation of photorespiration. The process involves three organelles:
Chloroplasts, peroxisomes, mitochondria. Two glycine molecules are converted to a serine and CO_2 and ammonia.

Pollentube Growth – Fertility

Uninduced *Nt*aqp1-overexpressing plants were male sterile and displayed striking flower abnormalities. Similar results were obtained by Zhang and Roberts (1995) for the expression of a MIP (Soybean Nodulin 26) in transgenic tobacco. Their studies revealed an effect of MIPs on floral and seed development.

Functional analysis of pollen viability of AS plants didn't reveal expected differences to control pollen. In contrast to the expected delay in hydration, germination and tube growth, AS pollen grains hydrated, germinated and grew like the controls or even faster. This was probably due to the 35SCaMV promoter used to drive the expression of the AS-construct. It was reported that this promoter is inactive in pollen (Bate and Twell, 1998). Additionally the 35SGUS construct with the same 35SCaMV promoter also didn't display any activity. The conclusion was that the construct used for these studies should be newly designed with a pollen-specific promoter, e.g. lat52 instead of a 35SCaMV promoter to get a tissue-specific effect.

D MATERIAL AND METHODS

1 Chemicals

If not marked otherwise, all chemicals were received from the companies Sigma, Aldrich, Fluka (all Deisenhofen, Germany) and ICN (Eschwege, Germany).

Gibberellic acid (GA)	GA_3 (Gibberella fujikuroi),	Duchefa, the Netherlands
DL-cis, trans-abscisic acid (ABA)		Merck, Darmstadt, Germany
Antibiotics		Duchefa, the Netherlands
Benzylamylopurine (BAP)		Duchefa, the Netherlands
Naphthalenic acid (NAA)		Duchefa, the Netherlands

2 Enzymes

Cellulase "OnazukaR-10" from *Trichoderma Viridae* (Duchefa, the Netherlands)

Pectolyase from *Aspergillus japonicus* (Sigma, Deisenhofen, Germany)

Restriction Endonucleases:

*Bam*HI, 10 U/µl, 4000 U, (MBI Fermentas, St. Leon-Rot, Germany)
*Eco*RI, 10 U/µl, 4000 U, (MBI Fermentas, St. Leon-Rot, Germany)
*Xho*I, 10 U/µl, 4000 U, (MBI Fermentas, St. Leon-Rot, Germany)
*Hind*III, 10 U/µl, 4000 U, (MBI Fermentas, St. Leon-Rot, Germany)
*Kpn*I, 10 U/µl, 4000 U, (MBI Fermentas, St. Leon-Rot, Germany)
*Xba*I, 10 U/µl, 4000 U, (MBI Fermentas, St. Leon-Rot, Germany)
*Sac*I, 10 U/µl, 4000 U, (MBI Fermentas, St. Leon-Rot, Germany)

T4 DNA Ligase, 1 U/µl (MBI Fermentas, St. Leon-Rot, Germany)

Taq DNA polymerase, Biotherm, 1000U (Diagonal, Münster, Germany)

RNaseA, 100 mg, (Roth, Karlsruhe, Germany)

3 Plant Material

Nicotiana tabacum, cultivar Samsun, grown under different conditions was used for molecular and physiological studies. Plants were grown in soil, hydroponic or aeroponic culture in the greenhouse, or climate chamber.

Greenhouse conditions: 16-25°C, relative humidity (RH) 60-70 %, day/night rhythm16/8 h, if not marked otherwise.

Climate chamber conditions: 16-25°C, relative humidity (RH) 50 %, day/night rhythm12/12 h, if not marked otherwise.

Hydroponic: continuously aerated modified Pirson und Seidel (P&S, 1950) solution.

Aeroponic: Tobacco plants grown in a 90 x 60 x 80 cm (l x d x h) covered container, humidifier (Defensor 550, Aixair, Switzerland) spraying P&S solution at the roots (every 15 min for 10 min).

P&S solution:		
	1.5 mM	KH_2PO_4
	2.0 mM	KNO_3
	1.0 mM	$CaCl_2$
	1.0 mM	$MgSO_4$
	18.0 µm	FeNaEDTA
	8.1 µm	H_3B0_3
	1.5 µm	$MnCl_2$

3.1 Pollen Germination

To germinate pollen, anthers were harvested from tobacco flowers and dried over night under vacuum. The pollen grains were washed off in EASY germination medium and subjected to *in vitro* germination either by plating them on EASY agarose plates or in liquid EASY germination medium.

Germination medium EASY:	
6 %	Sucrose
200 µM	$CaCl_2$
1.6 mM	Boric acid
1.0 mM	KCl
25 µM	MES
	pH to 5.5

4 Analytical Methods

4.1 ICP-Atomic Emission Spectroscopy

Concentrations of the elements potassium, sodium and calcium were determined by ICP-atomic emission spectroscopy (Jobin Yvon 70 Plus, software version 3.34, Jobin Yvon Instruments A. A. GmbH, Gasbrunn, Germany, with sample exchanger Gilson 222, IBM-PC and printer).

4.2 Anion Analysis

Concentrations of chloride (Cl^-), nitrate (NO_3^-), phosphate (PO_4^{3-}) and sulfate (SO_4^{2-}) were determined by High Pressure Liquid Chromatography (HPLC, Inonenchromatograph IC 1000, sample donor BT 7041, conductivity detector BT 0330, Biotronic, Maintal; Integrator Printer-Plotter C-R1B, Chormatopak, Shimadzu, Tokio, Japan).

A mixture of defined anions in a final concentration of 0.1 mM was used as standard. Ground material was diluted with bidest. H_2O and heated to 105°C in a thermo-block. The suspension was centrifuged for 10 min at 4000 rpm. The supernatant was used for analysis.

4.3 Sugar Analysis

Concentrations of water soluble sugars (glucose, fructose, sucrose, maltose, arabinose) were determined by HPLC with pulsed amperometric detection. Sugar solutions of defined concentrations were used as standards. The samples were treated as described in anion analysis.

4.4 Amino Acid Analysis

Amino acids (aa) were separated by HPLC (Biotronic Aminosäureanalysator LC 5001, Eppendorf-Netheler-Hinz GmbH, Hamburg, Germany) with single column method (3.2 mm column, Trennharz BTC 2710, increasing pH 2.7- 3.36 with Citrate/HCl). The aa contents of watery extracts were determined by photometry and derivatisation/detection with Ninhydrin-reagent. Measurements were performed at 570 and 440 nm.

4.5 Osmotic Potential

To determine the osmolality of tissue extracts a cryoskopic osmometer (Osmomat 030, Gonotec GmbH, Berlin) was used. The osmotic potential Ψ was calculated following Van't Hoffs' law:

$\Psi = -R \cdot T \cdot c$

R = Gas constant = 0.0083143 $l \cdot MPa \cdot mol^{-1} \cdot K^{-1}$
T = Temperature in Kelvin (RT = 293°K)
c = Osmolality of the solution

5 RNA Protocols

5.1 Isolation of RNA

5.1.1 Isolation of Total RNA

Tobacco total RNA was isolated using Qiagen RNeasy Plant Mini Kit (Qiagen, Hilden, Germany). The procedure is based on the selective binding properties of a silica-gel-based membrane in a microspin column system. A specialized high-salt buffer system allows the binding of up to 100 µg of total RNA longer then 200 bp to the membrane and its subsequent purification. Bound RNA was eluted with bidest. DEPC-treated water (DEPC-H_2O).

Fresh plant material was ground to a fine powder in a cooled mortar under liquid nitrogen. 100 mg plant material was mixed with 450 µl buffer Lysis buffer. The lysate was transferred to QIAshredder column and centrifuged in two steps for 2 min at max speed. The flow-through was mixed with 450 µl of ethanol and transferred to an RNeasy spin column. After several washing steps the RNA was eluted in 2x 30 µl of DEPC-H_2O. The amount and purity of the RNA was measured in a spectrophotometer (GeneQuant II, Pharmacia Biotech) by determination of the extinction [E] at 260, 230, and 280 nm. A ratio of [E260/E280] with a value of 1.8-2.0 was used as a criterion for pure RNA with low protein contamination. The RNA was stored at -80°C.

5.1.2 Isolation of mRNA via Dynabeads® Oligo (dT)25 (Dynal)

Just a fraction of 1-4 % of the total RNA in the cytoplasm of a typical eukaryotic cell is mature mRNA. As the use of total RNA bears the risk of DNA contamination, isolation of mRNA from total RNA or direct purification out of the tissue was preferred. The use of Dynabeads Oligo (dT)25 relies on base pairing between the poly-A tail of messenger RNA and the oligo dT-sequences bound to the Dynabeads surface. The purification was done by following the producer's protocol with slight variations.

5.1.3 mRNA from Total RNA

The volume of a solution containing 25-40 µg RNA was adjusted to 100 µl with DEPC-H_2O. Optimal hybridization conditions were obtained in Binding buffer added in a 1:1 ratio, heated to 65°C for 2 min to disrupt secondary structures. In the meantime, the Dynabeads Oligo (dT)25 were prepared for use: 50 µl of resuspended beads were removed from the stock suspension into a RNase-free 1.5 ml Eppendorf tube placed in the Dynal Magnetic Particle Concentrator (MPC).

After 30 s the supernatant was removed and the Dynabeads were washed once with 100 µl Binding buffer and resuspended in another 100 µl Binding buffer. The total RNA was added to the Dynabeads solution and mixed thoroughly. Annealing was accomplished by rotating on a rolling shaker for 10 min at room temperature. The tube was placed on the magnet for 30 s and the supernatant was removed. The beads were fixed by means of the magnet and washed twice with 200 µl Washing buffer B. In order to elute the mRNA 50 µl of Elution solution was added and heated to 65°C for 2 min. A second annealing step was performed by adding 50 µl 2 x Binding buffer and incubation on the rolling shaker for 10 min. Two washing steps with Washing buffer B were done before the mRNA was eluted in 8 µl buffer. The eluted mRNA was immediately transferred to a new RNase-free tube.

For reusing, the Dynabeads were regenerated as follows: used Dynabeads were resuspended in 200 µl Reconditioning Solution and transferred to a new RNase-free tube, incubated at 65°C for 2 min. After removing the supernatant they were washed twice in Reconditioning Solution, by repeating steps one and three twice. Then the Dynabeads were resuspended twice in 50 µl Storage buffer Oligo (dT)25.

5.1.4 mRNA Isolation Directly from Plant Tissue

Dynabeads® Oligo (dT)25 were used for isolation of highly purified, intact mRNA from protoplast suspensions.

For the direct isolation of mRNA 70 µl of concentrated material was used. The protoplast suspensions were diluted with the same volume of the 2 x Lysis/Binding buffer and pipetted up and down until complete lysis. The lysate could be frozen and stored at -80°C for later use. The Dynabeads were prepared for use by pre-washing 50 µl from the stock in 150 µl Lysis/Binding buffer. The supernatant was removed and the lysate was combined with the beads and mixed. Annealing was done by rotating on a roller for 15 min at room temperature. The vial was placed on the magnet for 1 min and the supernatant was removed. The beads were thoroughly washed twice with 150 µl Washing buffer A and twice with 150 µl Washing buffer B using the MPC. Elution was performed by adding 50 µl Elution buffer, keeping it at 65°C for 2 min. To get DNA-free mRNA a second annealing step was performed by adding 50 µl 2 x Binding buffer and incubation on the roller for 10 min. Two washing steps with Washing buffer B were done before the mRNA was eluted in 8 µl buffer. 6.7 µl of the mRNA containing supernatant was transferred to a new RNase-free tube for cDNA synthesis (D5.2).

2 x Binding buffer:	40 mM Tris-HCl, pH 7.5/2.0 M LiCl/4 mM EDTA
2 x Lysis/Binding buffer:	200 mM Tris-HCl, pH 7.5/1 M LiCl/20 mM EDTA/2 % LiDS/10 mM Dithiothreitol (DTT)
Washing buffer A:	10 mM Tris-HCl, pH 7.5/0.15 M LiCl/1 mM EDTA/0.1 % LiDS
Washing buffer B:	10 mM Tris-HCl, pH 7.5/0.15 M LiCl/1 mM EDTA
Elution Solution:	10 mM Tris-HCl, pH 7.5

Reconditioning Solution: 0.1 M NaOH

Storage buffer: 250 mM Tris-HCl, pH 7.5/20 mM EDTA/0.1 % Tween-20/0.02 % Sodium azide

5.2 Synthesis of cDNA

In the reverse transcription reaction, oligonucleotide primers are annealed to an RNA population. Reverse transcriptase then extends annealed primers, creating a DNA copy (cDNA) complementary to the RNA sequences. For the production of cDNA the components of two manufacturers were used. One was RETROscript™ (Ambion) and the other was MMLV Reverse Transcriptase (RT), 5 x RT-buffer and oligo-dT from Promega.

Promega reaction was set up with:

6.7 µl mRNA
0.4 µl RT-Primer (oligo-dT, 100 µM)
0.5 µl 10 mM dNTPs
2.0 µl 5 x RT-buffer (Promega)

It was incubated at 70°C for 2 min to destroy secondary structures before 0.4 µl MMLV-RT (100 U/µl) was added. After 1 h at 42°C, the cDNA was ready for further use in LightCycler experiments.

The Ambion reaction:

~1–2 µg total RNA
2 µl gene specific antisense primers (50 µM)
to 12 µl with bidest. H_2O, heated to 70°C before adding
2 µl 10 X RT buffer
4 µl 2.5 mM dNTPs
1 µl RNase Inhibitor (10 U/µl)
1 µl Reverse Transcriptase (MMLV-RT (100 U/µl))
incubated for 1 h at 42°C.

The cDNA then served as template for amplification by PCR. The process of subjecting RNA to reverse transcription followed by PCR is commonly known as RT-PCR. RT-PCR was used to generate inserts for cloning into plasmid vectors, to quantify the relative amounts of mRNA targets.

5.3 Electrophoresis of RNA

10 µg total RNA from different preparations were used for a denaturing electrophoresis in advance to a "Northern blot" (D5.4).

One volume of RNA-Gel Loading buffer were added to 10 µg total RNA and denatured at 65°C for 10 min. After 2 min on ice the individual RNAs were size fractionated in a 1 % denaturing 1 x MEN agarose-formaldehyde gel (80 V), ensuring that all RNA molecules have an unfolded, linear conformation. The typical rRNA pattern could be visualized under UV-light (ImageMaster VDS, Pharmacia Biotech) due to the fluorescence of the intercalating ethidium bromide. Distinct clear bands prove the quality of the preparation.

10 x MEN-buffer:	0.2 M MOPS (Morpholinopropane sulfuric acid) 0.01 M EDTA 0.05 M Sodium acetate
RNA-Gel Loading buffer	0.72 ml Formamide 0.16 ml 10 x MEN 0.26 ml 37 % Formaldehyde 0.18 ml H_2O 0.10 ml 80 % Glycerol 0.08 ml 2 % Bromophenol blue solution 3 µl 1 % Ethidium bromide
MEN-Agarose-Gel (35 ml):	0.35 g Agarose (ICN) 3.5 ml 10 x MEN 30.0 ml bidest. H_2O dissolved in the microwave, cooling to 50°C 2.7 ml 37 % Formaldehyde

5.4 Transfer of RNA

The transfer of RNA from an agarose gel onto a piece of nitrocellulose membrane is named "Northern Blot".

The transfer was achieved by "capillary blotting" after electophoretic separation of the RNA. Large volumes of buffer (10 x SSC) were drawn through the gel and the membrane (Nytran, Schleicher und Schüll or Hybond-N, Amersham Life Science), thus transferring the RNA from the gel to the membrane. The RNA was fixed on the membrane by 120 mJoules of UV-light (UVStratalinker 2400, Stratagene). The membrane could then be subjected to a radioactive hybridization (D6.8).

10 x SSC: 1.5 M NaCl/0.15 M Na_3-Citrate, pH 7,0

6 Manipulation of DNA

6.1 Isolation of Plasmid-DNA from *Escherichia coli*

The procedure of plasmid isolation is based on alkaline lysis of bacterial cells followed by selective precipitation of genomic bacterial DNA and proteins by lowering the pH. The plasmid DNA remains in the supernatant.

1.5 ml of a bacterial culture, grown in LB over night at 300 rpm, was harvested by centrifugation at 13000rpm, RT for 30 s. The bacterial pellet was resuspended completely in 0.3 ml of buffer P1. Addition of 0.3 ml of buffer P2, gentle mixing, and incubation at RT for 2 min led to a clear lysate. 0.3 ml of chilled buffer P3 was added, mixed immediately but gently, and incubated on ice for 10 min. With a centrifugation at maximum speed for 10 min the clear supernatant containing the plasmid DNA could be removed from the precipitated proteins and genomic DNA. Precipitation of the plasmid DNA was performed by adding 600 µl of isopropanol and centrifugation for 15 min. The DNA pellet was washed briefly in 70 % ethanol, and then centrifuged again. The 70 % ethanol helped to remove precipitated salt, as well as to replace isopropanol with the more volatile ethanol. After careful and complete removal of ethanol, the pellet was air-dried briefly (approximately 5 min) before redissolving in an appropriate volume of TE buffer or bidest. water. The plasmid-DNA was stored at -20°C.

DNA concentration was determined quantitatively and qualitatively by UV spectro-photometry or in an agarose gel.

Calculation of the DNA concentration was done by using the following formula:

$$\text{DNA [mg / ml]} = \frac{E_{260} \cdot 50 \cdot \text{dilution factor}}{10^3}$$

LB (Luria - Bertani) nutrient solution: 1 % Tryptone/0,5 % Yeast extract/1 % NaCl, pH 7.0/ 50 µg/ml Ampicillin after autoclaving

P1 (Resuspension buffer): 50 mM Tris/HCl pH8, 10 mM EDTA, 100 µg/ml RNaseA

P2 (Lysis buffer): 200 mM NaOH, 1 % SDS

P3 (Neutralization buffer): 3.0 M KAc ($KHOO^-$), pH 5.5

TE buffer 10 mM Tris/HCl pH8, 1 mM EDTA

6.2 Cleavage of Plasmid-DNA by Restriction Endonucleases

For characterization and further manipulation of the DNA, for example preparation of radioactive probes or cloning into a new vector, it was necessary to separate the cloned DNA from the plasmid carrying it by cleaving with specific restriction enzymes. Reaction conditions were used following the manufacturers protocol (Gibco BRL, MBI Fermentas).

In most cases two units of enzyme were used per µg plasmid DNA during 1 h at 37°C to get complete cleavage. Addition of 1/5 of the volume of loading buffer was used to stop the reaction and to prepare the loading on an agarose gel to check the result by electrophoresis.

6.3 Separation of DNA Fragments by Electrophoresis

Gel electrophoresis was used to separate DNA molecules by their size. Agarose concentration was chosen to suit the size range of the molecules: gels containing 0.3 % agarose separated double stranded DNA molecules between 5 and 60 kb, whereas 2 % gels were used for samples between 0.1 and 3 kb. Routinely 1.0 % gels, suitable for a molecule range of 0.5-12 kb were used. The agarose was melted in 1 x TAE and mixed with 0.5 µg/ml ethidium bromide after cooling to 50°C. The DNA solution was mixed with a suitable amount of loading buffer and subjected to electrophoresis, performed in a 1 x TAE buffer system at a voltage of 5-10 V/cm. As molecular size marker the 1 kb Ladder (Gibco BRL, Eggenstein, Germany) was used. Size fractionation could be checked by the fluorescence of the DNA intercalating dye ethidium bromide under UV-light (ImageMaster, Pharmacia Biotech).

50 x TAE buffer:	2 M Tris/Acetic acid, pH 8,0/50 mM EDTA, pH 8,0
Loading buffer 1 (5 x):	2.0 % Ficoll/0.5 % SDS/50 mM EDTA/0.2 % Orange G/10 % Glycerol
Loading buffer 2 (6 x):	50 %Glycerol/7.5 mM EDTA/0.4 % Xylenxyanol/0.4 % Bromophenol blue

6.4 Elution of DNA from Agarose Gels

Agarose gel electrophoresis separates DNA molecules of different length into distinct bands. They were visualized by the fluorescent dye ethidium bromide under UV-light, cut out of the gel and transferred to a 1.5 ml Eppendorf cup. Isolation of the DNA was performed with the QIAEX II System following the manufactures protocol (QIAGEN, Hilden, Germany). The efficiency of the elution was checked on a gel.

6.5 Cloning of DNA

6.5.1 TOPO TA Cloning®

The TOPO TA Cloning® technology was used to ligate PCR products into the pCR® 2.1-TOPO vector (F5.2) and to transform the recombinant plasmid into competent *E. coli* in one day.

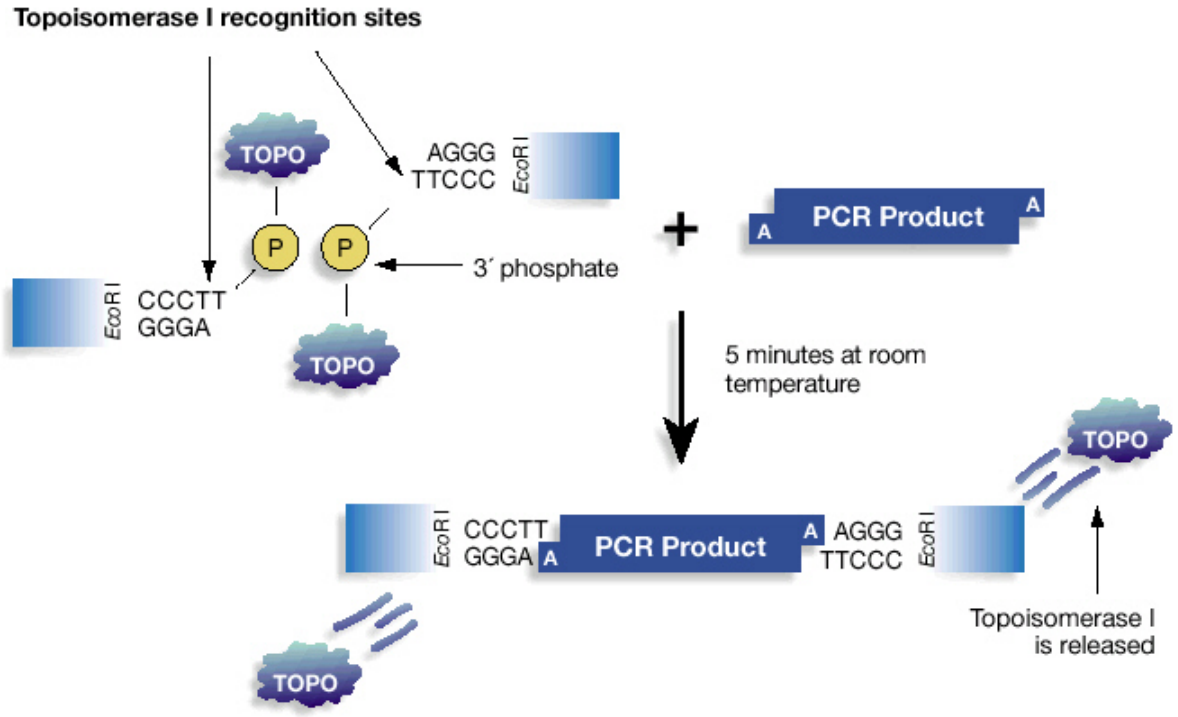

Figure D.1: Schematic representation of the TOPO® Cloning reaction (Invitogen, Groningen, the Netherlands) (Source: www.invitrogen.com).

Taq polymerase has a nontemplate-dependent terminal transferase activity that adds a single deoxyadenosine (A) to the 3'- ends of PCR products. The supplied linearized vector had single, overhanging 3'- deoxythymidine (T) residues allowing an efficient ligation to the PCR inserts. The TOPO® cloning reaction exploits the ability of Topoisomerase I to bind double stranded DNA, cleave a single strand, store the binding energy and transfer it to a new binding reaction (Shuman, 1994). Topoisomerases I covalently bound to the free ends of the pCR2.1 TOPO® vector enabled a highly efficient ligation to the PCR product in 5 min (Shumann, 1994). The principle is shown in Figure D.1.

The pCR 2.1-TOPO® vector has a multiple cloning site with *Eco*RI sites flanking the inserted PCR product on each side and four primer binding sites rendering sequencing possible. The vector also includes an ampicillin and kanamycin resistance gene for antibiotic selection of transformed cells. Since the insertion site is in the middle of a *b-galactosidase* gene fragment, a successful integration of a PCR product can be detected by blue-white screening of transformed cells.

The set up of 6 µl TOPO® Cloning reactions was as follows:
0.5 to 4 µl of the fresh PCR product and 1 µl of Salt solution (final conc. 200 mM NaCl, 10 mM $MgCl_2$) were transferred to a 0.5 ml reaction tube. The volume was adjusted to 5 µl with sterile water before adding 1 µl TOPO® vector to a final volume of 6 µl. The reaction was left at least for 5-10 min at RT. In the presence of salt the number of transformants increased 2-to 3-fold. The inclusion of salt allowed longer incubation times because it prevents topoisomerase from rebinding and potentially nicking the DNA after ligating the PCR product and dissociating from the DNA. Transformation into chemically TOP10F' *E. coli* cells was performed as described in D6.5.3.

Salt solution: 1.2 M NaCl/0.06 M $MgCl_2$

6.5.2 Ligation of Restriction Fragments into Plasmid-Vectors

The molar ratio of linearized vector to the restriction fragment (insert) influences the efficiency of a ligation reaction. A disproportion promotes the religation of the vector and the formation of insert-concatemers. For optimal ligation a ratio (V) of 3:1 of insert to vector-DNA concentration is favorable. The amount of insert-DNA necessary versus the amount of vector employed was calculated with the following formula:

$$\text{x [ng] Insert} = \frac{\text{V} \cdot \text{ng (vector)} \cdot \text{ Insert length [bp]}}{\text{vector length [bp]}}$$

One ligation reaction contained the following components:

2.0 µl 10 x T_4 Ligase buffer
x µl Insert-DNA
0.5 µg Linearized vector
4.0 µl T4 Ligase (1 U/µl)
x µl Bidest. H_2O to 20 µl final volume

The reaction was incubated over night at 16°C, the T4 Ligase was deactivated at 75°C for 5 min. 5 µl of the recombinant plasmids produced in the ligation reaction were used to transform antibiotic-sensitive *E. coli* cells.

6.5.3 Transformation of *Escherichia coli*

Usually the *E. coli* strain TOP10F', which is also included in the TOPO TA®-Cloning system, was used. It had the following genotype F' *{lac*I q T*n10* (Tet R)} *mc*rA.*(mr*r-*hs*dRMS-*mc*rBC) F 8*0lac*Z M15 .*la*c 74 *re*cA1 *de*oR *ar*aD139 *(ar*a-*le*u)7697 *ga*lU *ga*lK *rp*sL (Str R) *en*dA1 *nu*pG.

2 µl of the ligation reaction were mixed with 50 µl of competent cells, put on ice for 10 min, heat-shocked for 30 s at 42°C, and put back on ice. The cells were diluted with 250 µl of SOC

medium, incubated at 37°C for 1 h at 300 rpm, and were subsequently spread on antibiotic containing LB-plates. On the next day, colonies were selected and transferred to over night culture. Preparation of plasmid DNA (D 6.1) and endonuclease restriction (D 6.2) confirmed the presence of the insert. The identification of the sequence was achieved by sequencing (D 6.6).

E.coli transformed with vectors containing the *b-galactosidase* gene-fragment, e.g pCR 2.1TOPO and pBlueskript, were spread on ampicillin (50 µg/ml), IPTG (60 µg/ml) and X-Gal (40 µg/ml) containing LB-plates. On the next day colonies with an insert could be identified by blue/white selection. White colonies had an insert which destroyed the translational reading frame of the *b-galactosidase* gene, thus no enzyme could be synthesized, the substrate X-Gal couldn't be cleaved and the colonies remained white. Those colonies were subjected to plasmid DNA preparation, endonuclease restriction and sequencing like the ones mentioned above.

SOC-Medium: 2.0 % Tryptone/0.5 % Yeast extract/10 mM NaCl/2.5 mM KCl/ 10 mM $MgCl_2$/10 mM $MgSO_4$/20 mM Glucose to pH 7,0

LB-nutrient agar: 1.0 % NaCl/1.0 % Tryptone/0.5 % Yeast extract to pH 7,0/1.5 %Agar

6.6 Sequencing

Sequencing of DNA was done within the framework of the SFB 251 "Ökologie, Physiologie und Biochemie pflanzlicher und tierischer Leistung unter Stress" by Susanne Michel. The sequences were derived by the Sanger-Coulson method using the "Thermo Sequenase fluorescent labeled primer cycle sequencing-kit with 7-deaza-dGTP" (Amersham Pharmacia Biotech, Freiburg, Germany) and the DNA Analyser Gene Readir 4200 (LI-COR, MWG-Biotech GmbH, Ebersberg, Germany). Software for the sequencing was Base Imagir 4.0 (LI-COR, MWG-Biotech GmbH, Ebersberg, Germany). To compare the new sequences with already known ones the BLAST-Algorithms (Altschul et al, 1990) of NCBI (http://www.ncbi.nlm.nih.gov/-BLAST/) were used. To align sequences the ClustalX and DNasis software was utilized.

6.7 Radioactive Labeling of Nucleic Acids

6.7.1 Synthesis of "Random Oligo" Labeled cDNA

The Oligolabelling method by "Ready to Go™"-DNA Labelling Beads (-dCTP) (Amersham Pharmacia Biotech, Freiburg, Germany) is based on a process developed by Feinberg and Vogelstein (1984). It was used for labeling DNA restriction fragments for use as hybridization probes. The procedure was done following the manufacturers protocol.

The DNA (50-100 ng in 45 µl of H_2O) was denatured (5 min, 9°C) and then mixed with the lyophilized sediment of dNTPs (dGTP, dATP, dTTP), Klenow-Polymerase (7-12 U, FPLC*pure*™), buffer salts and oligodeoxyribonucleotides of random sequence. These “random

oligomers" annealed to random sites on the DNA and then served as primers for DNA synthesis by a DNA polymerase. With 50 µCi [α-^{32}P]dCTP present during this synthesis, labeled DNA was generated during a 30 min incubation step at 37°C. Not incorporated nucleotides were removed with Probe Quant G-50 Micro columns (Amersham Pharmacia Biotech, Freiburg, Germany). The specific activity was about 10^7 cpm.

6.7.2 Synthesis of a Single Stranded Probe

(Modified Stürzl and Roth, 1990)

The production of a single stranded probe is based on the principle of a linear PCR-reaction, using a cDNA fragment in combination with a gene specific antisense (AS) primer. The recombinant plasmid containing the cDNA was cleaved at the 5'-end of the cDNA to get a PCR-fragment of defined length and sequence.

Reaction (100 µl):	150 pmol	gene specific AS primer
	10.0 µl	10 x Biotherm Reaction buffer
	5.0 µl	50 mM $MgCl_2$
	200 µM	dATP, dGTP, dTTP
	6.25 µM	dCTP
	50 µCi	[α-^{32}P]dCTP (spec. activity > 3.000 Ci/mmol)
	2.5 U	*Taq* DNA Polymerase
	$10^{9\text{-}10}$	Copies of cDNA to be labeled

The PCR reaction was performed in a thermocycler (Hybaid, Heidelberg, Germany) with the following cycle parameters:

Denaturation	**Annealing**	**Elongation**	**Cycle number**
94°C/5 min			1
94°C/30 s	40-50°C/30 s	72°C/1 min	40
	40-50°C/30 s	72°C/5 min	1

40-50°C (see primers in appendix) corresponds to the range of temperature for optimal annealing of different gene specific primers.

Probe Quant G-50 Micro columns (Amersham Pharmacia Biotech, Freiburg, Germany) were used to remove nucleotides which were not incorporated. The procedure was done following the manufactures protocol. The incorporation rate of [α-^{32}P]dCTP was measured by scintillation counting. The activity of a specific probe for Northern hybridizations was a least 10^7 cpm.

6.8 Hybridization of Nucleic Acids

After UV-fixation of the RNA or DNA on the membrane, the nitrocellulose was washed in about 150 ml 5 x SSC, 0.5 % SDS in a plastic box for 30 min at RT. The pre-hybridization step was performed in 100 ml (68°C, 30 min) of Roti-Hybri-Quick solution (Roth, Karlsruhe, Germany). After addition of the denatured radioactive probe (D 6.7) to a final specific activity of at least 10^6 cpm/ml Roti-Hybri-Quick the hybridization proceeded over night (16 h, 68°C) in a special glass tube for hybridization incubators (Biometra, Göttingen, Germany). The next day, washing of the membrane was done in several steps at 68°C with increasing stringency:

30 min Roti-Hybri-Quick solution
30 min 1 x SSC, 0.1 % SDS
30-90 min 0.1 x SSC, 0.1 % SDS
30 min 0.1 x SSC, 0.1 % SDS

The air-dried membrane was sealed in a plastic wrap and exposed to a x-ray film (X-Ray Retina, Fotochemische Werke, Berlin, Germany) at -80°C or a Imaging plate AS-IP MS 2025 (Fujifilms, Japan) for the Phosphorimaging Unit Fujix BAS2000 (Fuji, Japan) for adequate time. The BAS 2000 substantially shortens experimental time and increases precision. For developing the x-ray film developer and fixative of Kodak was used. Quantification of hybridization signals were evaluated either by Image Master VDS Software (Pharmacia Biotech) or Bas Reader version 2.26 (Raytest Isotopenmeßgeräte GmbH, Germany) to read out image data from the BAS2000 radioluminography scanner.

To prepare the membrane for a subsequent hybridization, bound radioactivity had to be washed off by incubation at 95°C in 0.1 x SSC, 0.1 % SDS (2 x 15 min). Stripped membranes could be kept at -4°C.

6.9 Polymerase Chain Reaction (PCR)

The polymerase chain reaction (PCR) was used as a tool for selective, exponential amplification of rare molecules in cDNA populations, to prove the identity of cloned fragments or to subclone the PCR products. The principle of this exponential amplification is based on the denaturation of the double stranded DNA templates where specially designed oligonucleotide molecules (primers) anneal at the 3'- and 5'- end of the single stranded region of interest. These primers are elongated by a DNA- and Mg^{2+}- dependent DNA polymerase in the presence of free deoxynucleoside-triphosphates (dNTPs). Repetition of denaturation, annealing and amplification cycles leads to an exponentially increasing copy number of the product. Depending on the DNA template, the amount of DNA-template was modified. 10 - 20 ng were included in the reaction when the template was a plasmid and more if genomic or cDNA (100ng) was used. Regarding primer and template parameters suitable cycling parameters were chosen. A 5 min extension at 72°C after the last cycle was included to ensure that all PCR products are full length and 3'

adenylated. The reactions were performed in a thermocycler (Hybaid, Heidelberg) or a RoboCycler Gradient 40 (Stratagene).

50 µl reaction:	10-100 ng	DNA-template
	5.0 µl	10x PCR buffer
	2.0 µl	dNTPs (5 mM)
	5.0 µl	$MgCl_2$ (25 mM)
	2.0 µl	Primer1 (10 µM)
	2.0 µl	Primer2 (10 µM)
	0.2 µl	*Taq* DNA-Polymerase (5 U/µl)
	x µl	H_2O to a total volume of 50 µl

Cycling parameters:

Denaturation	**Annealing**	**Elongation**	**Cycle number**
94°C/5 min			1
94°C/25 s	optimal°C/1min/1kb	72°C/1 min	30-35
	optimal°C/1 min	72°C/5 min	1

The PCR products were visualized by agarose gel electrophoresis and their identity was confirmed by sequencing.

6.10 LightCycler (Roche)

For quantification of a specific cDNA in a cDNA population, the LightCycler System (Roche, Mannheim, Germany) was used. In comparison to conventional thermocyclers, the formation of amplification products could be monitored in real-time and could easily be quantified. The method for the detection of amplification products is based on the DNA-binding fluorescent SYBR Green I dye (Figure D.2). It binds to the minor groove of the DNA double helix. Unbound in solution the dye emitted very little fluorescence which was greatly enhanced upon stable DNA-binding. At the beginning of amplification the reaction mixture contained denatured cDNA, primers, and dye (Figure D.2, A). During the annealing-step a few dye molecules bound to the double stranded DNA (Figure D.2, B). During elongation more dye molecules bound to new DNA causing a dramatic increase of emission upon excitation (Figure D.2, C). At the end of the elongation phase the entire DNA became double stranded, and a maximum amount of dye was bound. Fluorescence (F) was recorded at the end of every elongation step (530 nm) and the increasing amounts of PCR product was monitored from cycle to cycle.

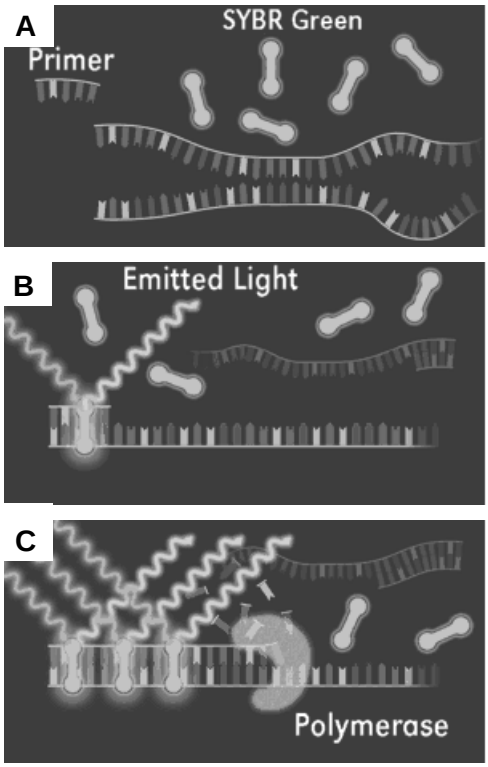

Figure D.2: Monitoring PCR with SYBR Green I (modified http://www.roche.de).

A. The entire DNA becomes single stranded after denaturation. At this stage of the reaction the dye will not bind and the intensity of the fluorescence is low.

B. During the annealing the PCR primers hybridize to the target sequence resulting in small parts of double stranded (ds) DNA to which SYBR Green I binds, thereby increasing fluorescence intensity.

C. In the elongation phase of the PCR, the primers are extended, and more dye can bind. At the end of the elongation phase the entire DNA becomes double stranded, and a maximum amount of dye is bound.

Quantification of the Target Concentration

Quantification of the initial target concentration was done by identifying the first cycle of the PCR run in which the log-linear signal could be distinguished from the background. Figure D.3 depicts the quantification. Serially diluted standards (D6.10.1.2) were used in quantification experiments. Samples with unknown concentration of the target genes (two, in the figure) were included in the PCR-amplification. After completion of the PCR, the LightCycler software calculated the copy number of the target molecules by plotting the logarithm of fluorescence versus the cycle number and setting a baseline x-axis. The baseline (crossing line) identified the cycle in which the log-linear signal could be distinguished from the background for each sample (Figure D.3, A). The x-axis crossing point of each standard was measured and plotted against the logarithm of the concentration to produce a standard curve (Figure D.3, B). The concentration of the target sequence in the samples was extrapolated from the standard curve.

Melting Curve Analysis

Each dsDNA product has its own specific melting temperature (T_m), which is defined as the temperature at which 50 % of the DNA becomes single stranded, and 50 % remains double stranded. The most important factors that determine T_m are the length and the GC content. Checking the T_m of a PCR product can thus confirm the identity and differentiate the specific product from a nonspecific one, like e.g. primer-dimers.

The LightCycler allowed monitoring the melting behavior of the nucleic acids at the end of the PCR run. After the last annealing step the temperature was slowly heated up to 95°C. During the slow heating process fluorescence was measured at 0.2°C increments. As soon as the dsDNA started to denature, the SYBR green was released resulting in a decrease of the fluorescence signal (Figure D.4, A). The T_m of the PCR fragment could be visualized by taking the first negative derivative of the melting curve (F/T).
The turning point of this new plotted curve (-dF/dT) resulted in a peak, which permitted the easy identification of T_m (Figure D.4, B).

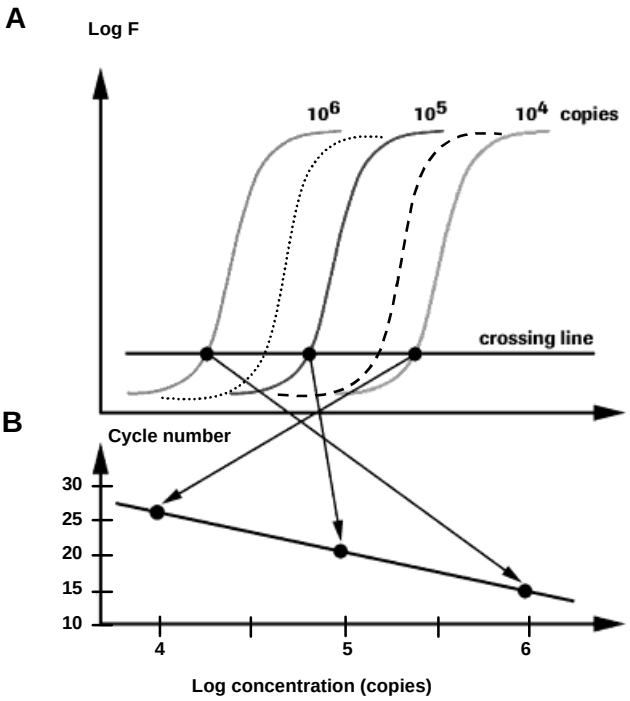

Figure D.3: Exemplified quantification of a target sequence (modified http://www.roche.de). A. Representation of the logarithmic plot of fluorescence versus cycle number. The two dotted graphs represent samples of unknown target sequence concentration; the three continuous ones are standards.

B. Standard curve: Crossing point (cycle number) of the log-linear correlations with the baseline (crossing line), plotted against the logarithmic concentration of the standards.

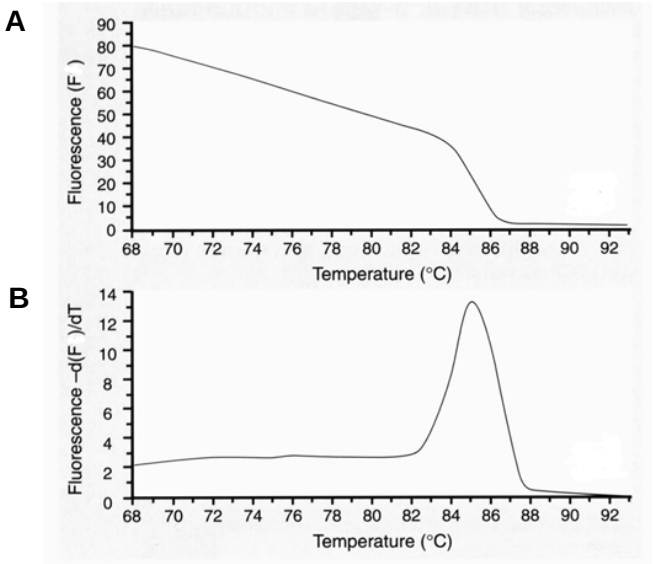

Figure D.4: Exemplified melting curve analysis (modified http://www.roche.de). A. The fluorescence (F1) drops sharply as the fragment is denatured.

B. Visualization of the melting temperature T_m by taking the first negative derivative of the melting curve (-dF/dT). The turning point results in a peak, which permits the easy identification of T_m.

6.10.1.1 Primer-Design and Testing

Primer-design was done using Oligo™5.0 (National Biosciences) with sequence information from NCBI. Several features of the primer were considered to be important: length not more than 15 bp, no dimerization or internal hairpin structures, T_m of above 60 °C. The primer pair of the inner standard and the ones for the gene of interest should have the same T_m and a comparable amplified fragment length of about 300 bp. The PCR primers have to be very accurate. First, they are tested in the RoboCycler (Gradient 40, Stratagene) with a temperature gradient to ensure the optimal annealing temperature and the unique annealing sites in the gene itself. Then they are tested in the LightCycler System by running different primer concentrations and corresponding melting curves of the product which should reveal the amplification of one single product. Additionally the products are separated on a 2 % agarose gel to see if only one single band of expected size is visible.

6.10.1.2 Preparation of Standards

Gel-purified PCR fragments resulting from amplification by the primer pair were used in the LightCycler experiment. Concentration of the DNA was measured and adjusted to 10 ng/µl. It was kept at -20°C for use as stock solution. Dilution series of 20 fg/µl to 20 atg/µl of the internal standard (actin) and of *Nt*aqp1 were used in quantification experiments.

6.10.1.3 PCR-Setup

2 µl of a 1:20 dilution of cDNAs were used as DNA template. The cDNA derived from mRNA purified twice with Dynabeads was subsequently reverse transcribed following the details given in D5.2.

A 20 µl reaction contained:

1.0 µl Primer 1 (5 mM)
1.0 µl Primer 2 (5 mM)
2.4 µl $MgCl_2$ (25 mM)
11.6 µl H_2O
2.0 µl Enzyme mix
2.0 µl 1:20 Dilution of cDNA or of standard dilutions

Cycling parameters:

Denaturation	Annealing	Elongation	Melting curve	Cycle number
95°C/10 min (20°C/s)				1
80°C/25 s	optimal°C/7s	72°C/19s		30-35
95°C/20s			95-0°C (0.2°C/s)	1

7 Protein Protocols

7.1 Preparation of Proteins

Proteins were extracted from leaf disks. For each preparation of whole protein, 1-2 leaf disks (∅ 1 cm) were ground with 60 µl 4 % SDS in an Eppendorf cup and subsequently mixed with 20 µl loading buffer (Roti®-Load 1; Roth, Karlsruhe, Germany). The samples were cocked for 15 min and treated with a pistil again to destroy the remaining particles. A final centrifugation step was done to separate cell debris from the protein solution. Depending on the detection method 1.0-10 µl of the supernatant were subjected to a SDS-PAGE (SDS-Polyacrylamide-Gel-electrophoresis) to size-fractionate the proteins.

7.2 SDS-Polyacrylamide-Gelelectrophoresis (SDS-PAGE)

To quantitatively analyze protein extracts, they are subjected to a SDS-PAGE. The method is based on separation of denatured proteins by their size which can also be used to determine their molecular mass.

Protein samples were initially boiled in sample buffer (see preparation section, D7.1) containing 2-mercaptoethanol to reduce disulfide bridges (destroying tertiary structure) and SDS, an anionic detergent which binds and denatures the proteins.

Usually a 10 % polyacrylamide gel was used, composed as follows (Neville 1971):

Separation gel: 424 mM Tris/HCl (pH 9.18)
10 % Polyacrylamide
0.1 % SDS
0.045 % TEMED (N,N,N’,N’-Tetramethylethylendiamine)
0.06 % APS (Ammoniumpersulfate)

Stacking gel:	54 mM	Tris/H_2SO_4 (pH 6.1)
	6 %	Polyacrylamide
	0.1 %	SDS
	0.1 %	TEMED
	0.1 %	APS

Lower buffer: 424 mM Tris/HCl (pH 9.18)

Upper buffer: 41 mM Tris/Boric acid (pH 8.64), 0.1 % SDS

10 µl of the protein solution (see preparation) were loaded on the polyacrylamide gel and separated at constant 30 mA. As molecular mass marker the Roti®-Mark 10-100 (Roth, Karlsruhe, Germany) or the SDS-Protein-Standard (Sigma) was used.

The detection was performed by Coomassie or Silver staining.

Coomassie staining: The gel was stained for 1 h in solution 1 (120 ml Methanol, 24 ml Acetic acid, 0.33 g Coomassie Brilliant Blue, 120 ml water), rinsed with water (cooked shortly in the microwave) several times and destained in solution 2 (10 % Methanol, 7 % Acetic acid) over night.

Silver staining (Blum et al, 1987): The protein gel was treated according to the scheme:

Process	**Solution**	**Time**
Fixing	50 % Methanol, 12 % Acetic acid, 37 % Formaldehyde (0.5 ml/l)	60 min
Washing	50 % Methanol	3 × 20 min
Pre-treating	$Na_2S_2O_3$•5 H_2O (0.2 g/l)	1 min
Washing	H_2O	3 × 20 s
Impregnating	$AgNO_3$ (2 g/l), 37 % Formaldehyde (0.75 ml/l)	20 min
Washing	H_2O	2 × 20 s
Developing	Na_2CO_3 (60 g/l), 37 % Formaldehyde (0.5 ml/l), $Na_2S_2O_3$•5 H_2O (4 mg/l)	up to 10 min
Washing	H_2O	2 × 2 min
Stopping	50 % Methanol, 12 % Acetic acid,	10 min
Washing	50 % Methanol	20 min

7.3 Transfer of Proteins on Membranes for Immunodetection (Western Blot)

The proteins separated in a SDS-PAGE were transferred to a nitrocellulose membrane (Schleicher und Schüll, Dassel, Germany) by a "semi-dry-electro-blot"-device (Biometra, Göttingen, Germany). Three Watman papers with a similar size as the gel were soaked in cathode buffer and placed on the cathode plate. The gel was mounted on these filter papers. The membrane, soaked in anode buffer 2, was laid on the gel and covered with three other Watman papers, equilibrated in the same buffer. Three further Watman papers were soaked in anode buffer 1 and placed on top of the stack. After installation of the anode plate the transfer of the proteins was performed at 0.8 mA/cm^2 for 1 h.

To check the separation and quality of the proteins, the membrane was subjected to a Ponceau staining and fixing step (Ponceau S in acetic acid, ICN). The stain could be removed by rinsing several times with water to use the membrane for chemiluminescent protein detection (Western-Light™ PE Biosystem, USA).

Cathode buffer: 40 mM 6-Aminocapronic acid/20 % Methanol

Anode buffer 1: 0.3 M Tris pH 8.8/20 % Methanol

Anode buffer 2: 25 mM Tris pH 8.8/20 % Methanol

7.4 Immunodetection

For specific protein detection the Tropix chemiluminescent method, Western-Light™ (PE Biosystem, USA) was used. Employing this system less then 1 pg of protein can be detected.

The membrane with the bound proteins was incubated in Blocking solution. Then the blot was exposed to the primary antibody. An alkaline phosphatase (ALP) labeled secondary antibody was used to attach alkaline phosphatase to the target protein. Chemiluminescence was initiated by incubating the membrane with the 1, 2-dioxetane-based chemiluminescent alkaline phosphatase substrate CDP-Star®. CDP-Star® reacts with ALP (Figure D.5) to generate an intermediate compound that spontaneously splits into adamantanone and a fluorophor. The fluorophor is in a chemically excited state and emits light on return to its ground state.

This emission of light enabled detection of the protein on an x-ray film.

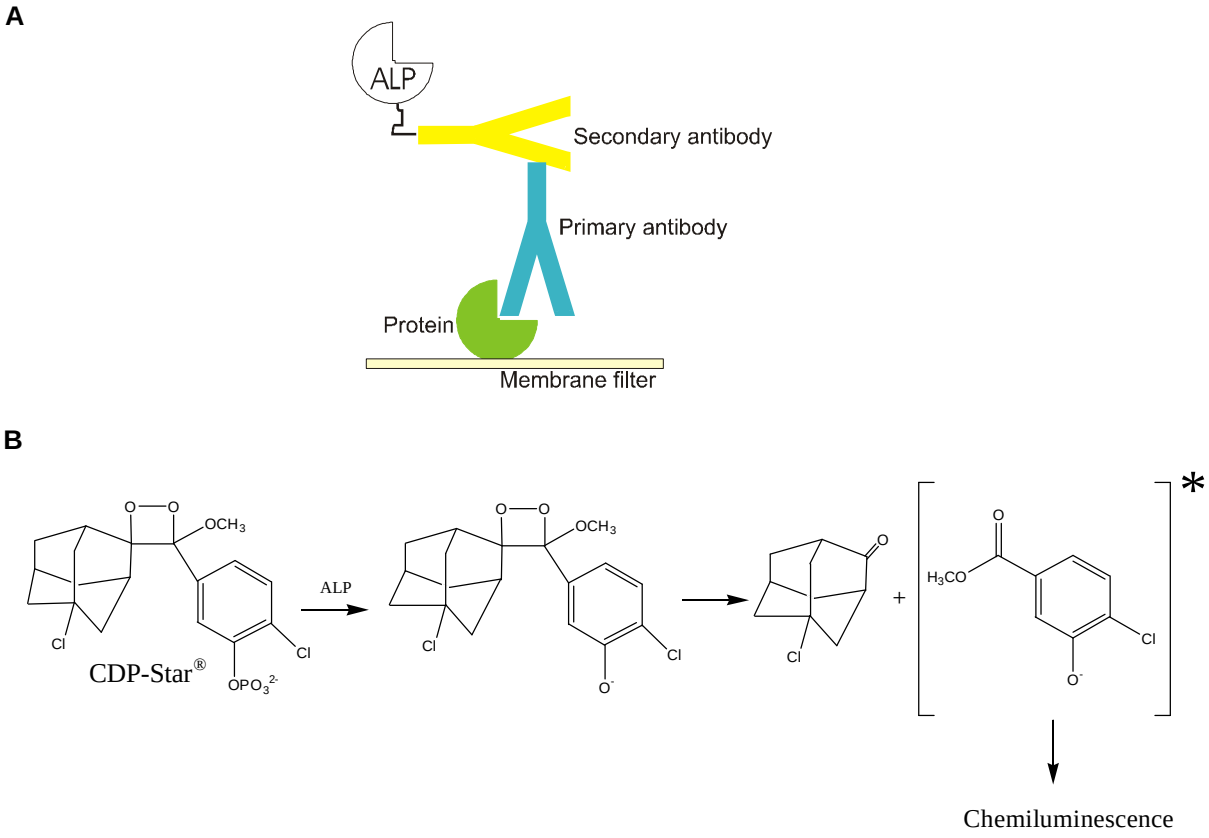

Figure D.5: A. Scheme of the coupling of the alkaline phosphatase (ALP) to the immobilized protein, hybridization of the primary and secondary antibody. B. Reaction of CDP-Star® with ALP, generation of an intermediate compound that spontaneously splits into adamantanone and a fluorophor. The fluorophor is in a chemically excited state and emits light on return to its ground state. (Modified http://www.roche-applied-science.com/pack-insert/).

The procedure included the following details:

The nitrocellulose membrane was shortly rinsed in Wash B, put for 1 h in Blocking solution and was then sealed in a plastic bag with 1 ml of primary antibody. After 1 h of incubation with stroking from time to time, the membrane was removed from the bag and washed 3 x 50 ml for 10 min of Wash B. 1 h of incubation with the secondary antibody was followed by the same washing procedure. Afterwards a 2 x 5 min wash with Assay B was included. Then the membrane was placed in Nitroblock solution for 5 min and washed 2 x 5 min with Assay B. 1 ml of CDP-substrate solution was distributed over the membrane and kept there for 5 min. The chemiluminescent reaction was made visible by exposure to an x-ray film (DuPont) and subsequent developing of the film.

Primary antibody:	1 µl in 500 µl Blocking solution and 500 µl Wash B (1:1000)
Secondary antibody:	0.5 µl added to 2.5 ml Blocking solution and 2.5 ml Wash B (1:10000), anti-rabbit or anti-chicken, depending on primary antibody
10 x PBS (pH 7.3-7.4):	82.3 g Na_2HPO_4/23.5 g NaH_2PO_4/40 g NaCl per liter
Wash B:	1 x PBS/0.1 % Tween20

Assay B:	624 µl DEA (Diethanolamine), pH 10/HCl/70 µl 1 M $MgCl_2$ to 70 ml with water
Blocking solution:	0.1 g I-Block warmed up and dissolved in 20 ml 1 x PBS, filled up to 50 ml with 1 x PBS, 50 µl Tween20 added
Nitroblock solution:	1:20 dilution of Nitroblock in Assay B
CDP-substrate-solution:	10 µl CDP/ml Assay B

8 Tissue Cross Sections and Staining

8.1 Berberine-Aniline Blue

Berberine-Aniline Blue is a fluorescent stain to detect suberin, lignin and callose in fresh or fixed tissue sections (Brundett et al, 1988). It may also be useful in whole tissue pieces to view surface suberinization.

Freehand sections were transferred to section holders (Eppendorf tube: narrow end cut off, covered with a mesh permeable for water and dye) placed in a petridish filled with water. They were transferred to the next petridish containing the Berberine solution for at least 1 h. The tissue and the holders were rinsed by bathing and blotting in several changes of fresh water of by flushing and blotting several times. The next transfer step was 30 min to Aniline Blue followed by another rinsing. Tissue and holders were placed in Mounting medium to allow equilibration of the tissue with the medium. Then the tissue was mounted on a slide in Mounting medium. The preparations could be viewed under blue, violet or ultraviolet fluorescence excitation.

Structures containing the *Casparian Band*, suberin or lignin were stained bright yellow to golden depending upon excitation wavelengths. Lamellar suberin staining is typically partially quenched by the Aniline Blue (bluish), as is cellulosic wall and some phenolic staining. Callose in the phloem would stain yellowish.

Berberine:	0.1 % Berberine hemi-sulfate (Sigma) in bidest. water
Aniline blue:	0.5 % Aniline Blue water-soluble (Fluka) in bidest. water
Mounting medium:	0.1 % $FeCl_3$ in 50 % glycerin by adding glycerin to filtered aqueous $FeCl_3$

8.2 Toluidine Blue O (TBO)

Toluidine Blue O is a metachromatic stain for plant material, e.g. for the negatively charged pectin (O'Brien et al, 1964). The change in color depends on density of surface charge.

Fresh hand-sections were transferred to section holders and stained in a petridish of TBO for 1 min. After rinsing several times with bidest. water, the sections were mounted in bidest. water and observed with transmitted white light.

Cell walls impregnated with lignin or other phenols and tannin-rich vacuoles stain green, turquoise or light blue. Polysaccharides rich in carboxyl groups (e.g. pectic acid, alginic acid) or sulfate groups stain pink or reddish purple, DNA stains green or purplish blue, and RNA stains purple or purplish blue though these materials are usually lost from hand sections of fresh material (O'Brien and Mc Cully 1981, p627).

Benzoate buffer (0.02M, 200ml):	0.25 g Benzoic acid/0.29 g Sodium benzoate dissolved in 200 ml bidest. water to pH to 4.4
TBO (Staining solution)	0.05 % Toluidine Blue O in Benzoate buffer

8.3 Sudan Red 7B

Sudan Red 7B was used to stain suberin lamellae (but not *Casparian Band*s) and lipid deposits in plant tissue (Brundrett et al, 1991). It is similar to other Sudan stains but usually more intense.

Fresh sections were placed in section holders and immersed in Staining solution for about 1 h at RT. Sections were mounted on slides, gently warmed up to hasten the process. Lamellar suberin and lipid deposits stained bright red.

Staining solution	0.1 % (w/v) Sudan Red 7b in polyethylene glycol 400, heated at 90°C for 1h, an equal volume of 90 % glycerol was added to the polyethylene glycol stain

9 Transformation of Agrobacterium

To stable transform tobacco plants the *Agrobacterium* LBA 4404 was used as a vector. The sheer size and the complexity of the T_i-plasmid precluded its direct manipulation. Thus, insertion was performed into a comparatively small binary vector, which was then propagated in *E.coli*, before being introduced into *Agrobacterium tumefaciens.*

Two methods were used to introduce the plasmids into the Agrobacterium strain: Heat shock transformation and triparental mating. Transformation was verified by plasmid isolation and subsequent determination of specific restriction patterns.

9.1 Production of Competent Agrobacterium Cells

To transfer the binary vector into the Agrobacterium they were made competent before heatshock transformation.

3 ml LB were inoculated with LBA 4404 and grown over night. 1 ml of this culture was used to inoculate 50 ml LB (in 300 ml flask). The inoculum was grown for another 3-5 h until OD_{600} reached a value of 0.5-0.8. The flask was put on ice for 15 min and the cells were kept cold from this step on. The cells were spun down (4000 rpm) in a 50 ml tube for 10 min at 4°C. The supernatant was removed and the pellet was washed gently in 10 ml pre-cooled 20 mM $CaCl_2$. After 5 min centrifugation at 4°C the pellet was resuspended in 1 ml $CaCl_2$ and directly frozen in portions of 100 µl in liquid nitrogen. The cells were stored at –80°C.

9.2 Heat Shock Transformation of Agrobacterium

For transformation custom made competent LBA 4404 cells were thawed on ice. 50 ng DNA was added, mixed carefully with the cells and frozen in liquid nitrogen. A heat shock at 37°C for 5 min was done before adding 1 ml LB. To recover the cells, they were incubated for 2-4 hours at 28°C. For selection of transformed cells, 100 µl were plated on LB-plates containing 100 mg/l kanamycin and 50 µg/l streptomycin. The rest of the cells was spun down for 30 s, resuspended in the remaining $CaCl_2$ solution and also distributed on a selective plate. The plates were incubated over night or up to 2 d at 28°C.

9.3 Triparental Mating

Triparental mating is the gene transfer from a donor bacterium strain (*E. coli* TOP 10F', kanamycin resistant) into an Agrobacterium strain (recipient, *Agrobacterium* LBA 4404, streptomycin resistant) in the presence of a helper strain (*E.coli,* HB 101, kanamycin resistant) by conjugation.

5 ml of the *E. coli* donor strain (TOP 10F', carrying the binary vector), the helper strain (*E.coli*, HB 101), and the recipient *Agrobacterium* LBA 4404 were grown to exponential phase. 100 µl of the donor, 100 µl of the helper strain, and 300 µl of the recipient strain were mixed together in a Eppendorf cup. 100 µl of this mixture were plated on a nitrocellulose disk, placed in the center of a LB-agar plate and incubated over night at 28°C. The bacteria were washed off the disk with 10 mM $MgSO_4$. 100 µl samples of the suspension were spread on selective media (kanamycin/streptomycin) and incubated at 28°C for 48 h to allow the growth of transconjugate colonies.

10 Stable Transformation of *Nicotiana tabacum*

10.1 Leaf Disk Transformation Using *Agrobacterium tumefaciens*

(Gallois and Marinho, 1995, modified)

Transformed *Agrobacterium* LBA 4404 (D9) were used to stable transform tobacco by infecting leaf disks and recovering genetically modified plants.

Agrobacterium was pre-cultured in 4ml 2YT (+antibiotics) over night at 28-30 °C and 200 rpm. 1 ml of this culture was used to inoculate 50 ml 2YT (+antibiotics) medium. After growing for 24-36 h the OD_{600} was adjusted to 1.0 with 2YT without antibiotics and filled in a sterile box (Magenta box, about 200ml).

Five to seven leaves of six-weeks-old tobacco plants were surface sterilized with 2 % sodium hypochloride (Roth, Karlsruhe, Germany) and rinsed 4 x with sterile water (4 x 400ml) under a sterile flow-hood. Leaf disks were punched with sterile cork-borer (∅ 1cm). About 80 were used per transformation construct. 20 disks were transferred to the magenta containing the LBA 4404 culture. The samples were mixed by shaking and left for 1 min to secure contact of the bacteria with the wounded surfaces of the leaf tissue. The inoculated leaf disks were recovered from the suspension with sterile forceps. The excess of liquid was eliminated by blotting them on sterile Watman paper. About eight disks were pressed upper leaf surface uppermost in solidified co-cultivation medium in a Petridish which was sealed with Parafilm afterwards. To facilitate the infection the leaf disks were incubated for 2 d at 25°C and 16 h daylight. After co-cultivation, the disks were transferred to Selection medium. The petridishes were left unsealed to lower the humidity which aided to eliminate Agrobacterium. After two days they were sealed again to prevent desiccation of the leaf tissue. About one week later, leaf disks started to expand and the center was lifted away from the medium. In this stage the disks were cut in four pieces and pressed into the new Selection medium. Three weeks after inoculation, shoots started to appear. For plant recovery shoots of 5-10 mm length were excised at the base and put into Magenta boxes filled with Rooting medium. To ensure that the transformants were independent, only one shoot per leaf disk or independent calli of one leaf disk were taken. Fully recovered plants were transferred to soil and put in the greenhouse.

Culture medium (2YT):	16 g Tryptone/10 g Yeast extract/5.0 g NaCl after autoclaving, addition of 50 mg/l kanamycin and 200 mg/l streptomycin
Co-cultivation medium:	1 x MS (Murashige&Skoge) micro- and macroelements/ 3 % Sucrose (ICN)/1 mg/l 6-Benzylaminopurin (BAP) to pH 5,8 (KOH) 8 g/l Bactoagar after autoclaving, addition of MS-vitamins

Selection medium:	Like Co-cultivation medium with 500 mg/l carbenicillin and 300 mg/l kanamycin added
Rooting medium:	1 x MS (Murashige&Skoge, 1962) micro- and macroelements/ 3 % Sucrose (ICN)/0.1 mg/l NAA pH 5,8 (KOH), 8 g/l Bactoagar after autoclaving, addition of MS-vitamins, 250 mg/l carbenicillin, and 100 mg/l kanamycin, 60-80 ml per Magenta box.

11 Reporter Gene Systems and Assays

The regulation and localization of gene expression was investigated by the use of reporter genes. They encode products which can be quantified using bioassays. Transgenic plants had to be generated by transformation with a chimeric gene consisting of the promoter of the gene of interest and the coding sequence of the reporter gene.

11.1 Glucuronidase (GUS) System

The *b-glucuronidase* gene, originating from *E. coli*, is a reliable system to monitor plant promoter activity (Jefferson et al, 1986). The *in situ* enzyme histochemical method was used to localize cells expressing the reporter gene within the cellular context of the tissue. The qualitative assay to measure GUS activity is based on the hydrolysis of the substrate 5-bromo-4-chloro-3-indolyl-β-D-glucuronide (X-Gluc) (Jefferson et al, 1987). The product is a water-soluble intermediate (5-bromo-4-chloro-indoxyl) which is further dimerized by oxidation into the dichloro-dibromo-indigo blue precipitate. The indoxyl dimerization is enhanced by the presence of the oxidant potassium ferri (III) cyanide (Jefferson 1987b).

To produce transgenic plants with a construct of the *Nt*aqp1-promoter and the functional gus gene, several subcloning vectors were used. The vector pBI221 (Clontech-ITC, see appendix) carried a functional reporter gene construct consisting of the 35SCaMV (Cauliflower Mosaic Virus) promoter, the gus gene (Jefferson et al, 1986) and the polyadenylation signal of the nopaline-synthetase gene (nos) from *Agrobacterium tumefaciens*. pCR® 2.1-TOPO contributed the promoter and pUC 18 was used to fuse the components and transfer the complete construct to the binary vector pGPTV.

11.1.1 GUS Assay

Parts of the generated plants or the seedlings were subjected to GUS staining. The material was fixed for 5 min in Fixation solution and rinsed with 1 x Phosphate buffer. The X-Gluc solution was vacuum-infiltrated at -1000 mbar for at least 5 min, depending on the tissue, and incubated for 12 h in the dark at 37°C. The tissue was destained in 70 % ethanol.

10 x Phosphate buffer: 0.5 M NaH_2PO_4/0.5 M Na_2HPO_4, pH 7.0

Fixation solution: Warm up 1 x Phosphate buffer to 60°C, add 2 % Paraformaldehyde, add solid NaOH until solution gets clear, add 0.2 % Glutaraldehyde and set pH to 7.0 with conc. H_2SO_4

X-Gluc solution :

1 mM	5-Bromo-4-chloro-3-indolyl-β-D-glucuronide (X-Gluc)
1 x	Phosphate buffer
500 µM	($K_4[Fe(CN)_6$ x $3H_2O$]
500 µM	($K_3[Fe(CN)_6$]
10 mM	EDTA
0.1 %	Triton X-100

11.2 Luciferase System (LUC)

The luciferase gene (luc) from the North American firefly *Photinus pyralis* has emerged as a powerful tool for *in vitro* and *in vivo* reporting of transcriptional activity in eukaryotic cells. Since DeWet et al, (1985) cloned the cDNA encoding luciferase, the gene has been expressed in plants (Ow et al, 1986), mammalian cells (DeWet et al, 1987) and other organisms like zebrafish (Mayerhofer et al, 1995) and Drosphila (Brandes et al, 1996).

Luciferase catalyses the oxidative decarboxylation of the substrate (firefly) luciferin (Figure D.6). The reaction causes the release of a photon at 562 nm in the catalytic cycles with the substrates luciferin, ATP and oxygen (DeLuca et al, 1974; Aflalo, 1991). The short half-life of the luc mRNA and protein, and the very limited regeneration of the LUC protein after reacting with luciferin, enables monitoring of changes in gene activity with a high time resolution with a 2D-luminometer. The luminometer consisted of an intensified CCD-camera (C2400-77, Hamamatsu Photonics, Japan) or a nitrogen cooled slow-scan CCD camera (512-TBK, Princton Instruments, Trenton, NJ, USA). The photon emission by luc-expressing plants was quantified by *metaphor* software. Images of luciferase activity are depicted with false color or false grey scale.

For enhanced expression in mammalian cells and plants, the luciferase coding sequence was modified and the peroxisomal import sequence (luc $^+$, Promega) was removed (Sherf and Wood, 1994).

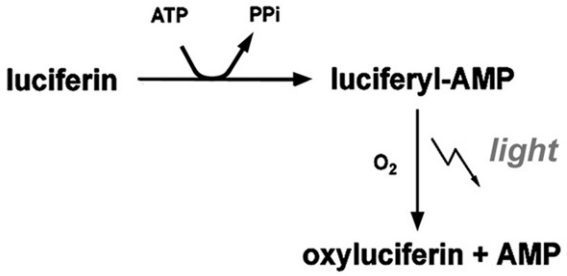

Figure D.6: Simplified model of the oxidative decarboxylation of luciferin. The enzyme requires ATP, molecular oxygen and the heterocyclic compound firefly luciferin to generate light in a two-step process.

To produce transgenic plants containing the *Nt*aqp1-promoter and the functional luc^+- cDNA several subcloning vectors were used. The vector pBluescript SK (F5.1) carried a functional reporter gene construct consisting of the 35SCaMV (Cauliflower Mosaic Virus) promoter, the luciferase cDNA (De Wet et al, 1985) and the CaMV polyadenylation signal (Eckert, 2000). pCR 2.1-TOPO® contributed the *Nt*aqp1-promoter. To transfer the complete construct to the binary vector pGPTV, pUC 18 was used.

11.2.1 LUC Protein Extraction

Leaf parts up to 100 mg were ground in 200 µl GUS-extraction buffer (0.1 M KH_2PO_4/K_2HPO_4, 2 mM EDTA, 5 % Glycerol, 2 mM DTT, pH 7.8). Cell fragments were removed by 4 min centrifugation at 13000 rpm. The supernatant was used in an *in vitro* luciferase activity assay.

11.2.2 *In Vitro* Luciferase Assay

For *in vitro* measurement of luciferase activity, a 5 µl aliquot of luciferase extract was pipetted in a luminometer tube (Sarstedt, 55.476) and measured in a luminometer (Lumat lB9501 Berthold, Wildbau, Germany) by addition of 50 µl CoA-assay buffer (Promega) containing Coenzyme A (CoA) which prolonged the light production (Ford et al, 1995). The steady state light production could then be quantified for 5 s after a 10 s interval directly after addition of the CoA-assay buffer and is shown as relative light units (rlu).

12 Protoplast swelling assay

12.1 Preparation of Protoplasts

To get a reasonable amount of root protoplasts from adult plants, tobacco grown in aeroponic culture was chosen. About 1 cm long pieces (starting from the apex) of the roots, including the *Nt*AQP1-expressing zone, were harvested. The tip was removed and the remaining tissue was transferred into a small petridish (Ø 2cm) with about 2 ml enzyme solution 1, containing pectolyase for faster release of the protoplasts. The specimens were kept in a dark, 30°C rotary shaker for about 2 h at 100 rpm. Then the protoplasts were filtered through a 70 µm mesh, rinsed with isotonic solution into a 15 ml Falcon tube. After a 12 min centrifugation step at 20°C, 800 rpm, deceleration 0, the supernatant was discarded and the protoplasts resuspended in the remaining solution. The protoplasts were kept at about 10°C for the measurements.

Enzyme solution (40 ml): 0.8 %w/v Cellulase/0.1 %w/v Pectolyase/0.5 % BSA/ 0.5 % PVP/1 mM $CaCl_2$/10 mM KCl/8 mM MES (Duchefa, the Netherlands), Sorbitol to 300 mosmol, pH to 5.5 with KOH

Isotonic solution (300 mosmol): 1 mM $CaCl_2$/10 mM KCl, Sorbitol to 300 mosmol, pH to 5.5 with KOH

12.2 Determination of the Protoplasts' Osmotic Water Permeability

The osmotic water permeability of protoplasts was measured with a newly developed experimental setup to follow the volume change after fast exchange of the osmoticum. A special chamber (B1.4.5.1) was used in combination with a Leitz inverse microscope and a digital video camera system (Pixera PVC100C, Pixera Corporation, USA) which allowed the videotaping on the PC. The recorded films were used for determination of protoplast volume change during time.

12.2.1 Measurements

12.2.1.1 Photomicrography

The analysis procedure bases on the cell contour. For this purpose a Leitz inverse microscope with a 50 x LD objective (Zeiss, Jena) was used. The protoplast volume was monitored at RT with the microscope Pixera video system (1-2 min, 1 frame·s^{-1}) directly after switching to hypo-osmotic solution. The buffer containers consisted of two syringes (60 ml) mounted on a 5 valve bench connected to a tube (6 cm long, ∅ 1 mm) feeding into the experimental chamber groove,

to ensure constant flow. The Pixera Imaging software "Pixera Visual Communication Suite" and the corresponding RGB CCD camera (DBS, Bremen, Germany) were used for recording.

12.2.1.2 Image Processing

The first step was to extract the single pictures of the recorded film with Irfan View software and to create a "poster" of a full-time series (consecutive sequence) of images of a single cell within the period of interest. For this a combination of Scion-Image 0.94b3 (Scion Corporation, USA; http://www.scioncorp.com) and Adobe PhotoShop 4.0 software was used. Figure D.7 shows such a poster with images recorded every second for 1 min. The second step was, to turn the cell pictures to uniformly black shapes, to enable measurements of their cross-sectional areas by the Scion Image program. This was achieved with the Adobe PhotoShop 4.0, with the following series of commands:

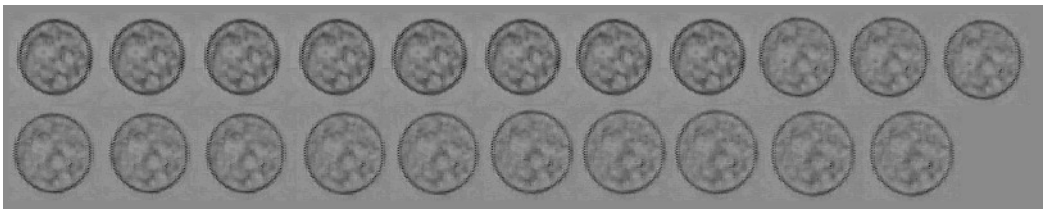

Figure D.7: Poster cut cells in one second-steps.

A. Emphasizing the cells over the background: *Option Filter Stylize Find Edges*. This resulted in edge sharpened cells (Figure D.8).

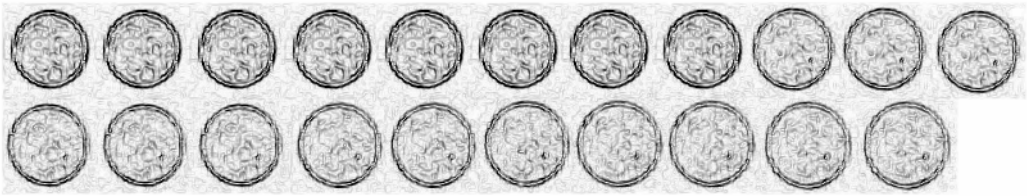

Figure D.8: Poster after *Option Filter Stylize Find Edges*.

B. Whitening the background, using the eye-dropper tool touching a white spot, paint bucket tool (tolerance = 40; adjust the tolerance level to keep the cells unchanged while the background is turning white) touching the background, which became uniformly white (Figure D.9).

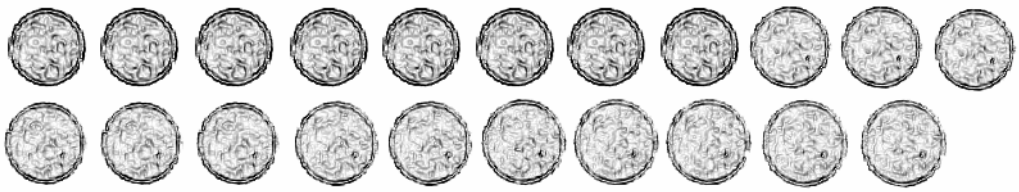

Figure D.9: Poster after whitening the background.

C. Turning the cells to black surface, using *Image Adjust Brightness/Contrast* (-100/+3), whitening the background, as in step B, but with tolerance = 10 (Figure D.10), repeated to get black shadows.

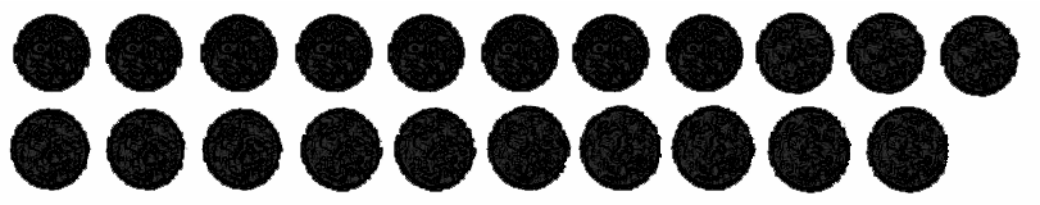

Figure D.10: Poster after darkening the protoplasts and whitening of the background.

D. Because *Scion Image* treats the cells in the poster as a matrix, numbering them from left top to right bottom, the poster had to be tilted to ensure correct numbering: Image Rotate 5° clockwise (Figure D.11). The poster was saved as a TIF-file.

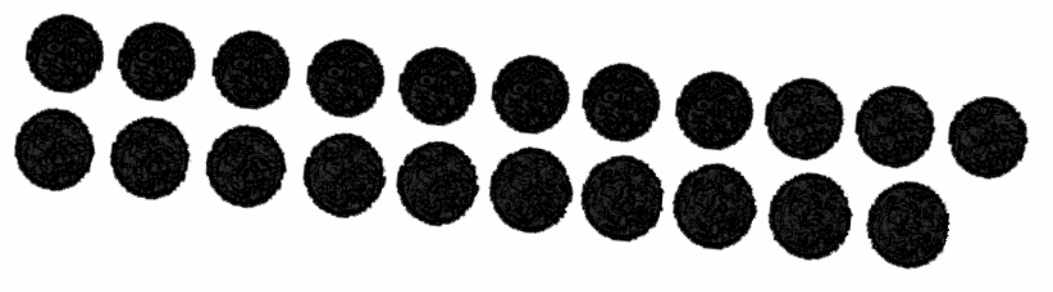

Figure D.11: Rotation of the end-version of the poster.

The measurement of the protoplast area was performed with Scion Image. Analyzing the protoplast requires the adjustment of some parameters:

A. Images were calibrated to spatial standards using the *Set Scale and Calibrate* commands respectively.

B. The *Analyze Particles* command automatically counted and measured features of interest.

C. This required thresholding to discriminate the protoplasts from the surrounding background based on their gray values. This mode was checked in *Option menu Threshold* and was adjusted to comparable levels.

D. In the *Analyse Options menu* the feature of interest was set to *Area*. The program scaned across the image until it found the boundary of a cell, outlined the object, measured the cell.

E. The recorded measurements were displayed in a tabulated list with *Show Results* and could be copied to Microsoft Excel™.

12.2.2 Calculation of the Membrane Permeability Coefficients P_f and P_{os}

The membrane permeability coefficient P_f was determined using Equation 1a (Zhang and Verkman, 1991).

$$P_f = V_0 \cdot \frac{[d(V_x / V_0) / dt]}{S_0 \cdot V_W \cdot (c_i - c_e)} \qquad \text{Equation 1}$$

P_f [µm·s^{-1}]	Permeability coefficient
V_0 [µm^3]	Volume (start)
V_x [µm^3]	Volume (time point x)
V_W [µm^3·mmol^{-1}]	Molar volume of water = 18 cm^3·mol^{-1}
t [s]	Time
S_0 [µm^2]	Protoplast surface (start)
c_i [mosmol·10^{-15}·µm^{-3}]	Solute concentration in the cell (equilibrium with the incubation medium)
c_e [mosmol·10^{-15}·µm^{-3}]	Solute concentration outside the cell

The volume and surface values were derived from the recorded protoplast area with the following equations:

$$A_0 = p \cdot r^2$$

$$S_0 = 4 \cdot p \cdot r^2 = 4 \cdot A_0$$

$$\Rightarrow \quad P_f = V_0 \cdot \frac{[d(V_x / V_0) / dt]}{4 \cdot A_0 \cdot V_W * (c_i - c_e)} \qquad \text{Equation 1a}$$

A_0 [µm^2]	Cross section area of the protoplast
S_0 [µm^2]	Protoplast surface

The osmotic membrane permeability P_{os} was determined using Equation 2 (Ramahaleo et al, 1999). It contains the variable z, to eliminate the effect of protoplast size and solute concentration. Delta c describes the concentration of impermeable solute in the medium.

$$P_{os} = [d(V_x / V_0) / dz)] \qquad \text{Equation 2}$$

$$z = \frac{S_0}{V_0} \cdot V_w \cdot |\Delta c| \cdot t$$

P_{os} [µm·s^{-1}]	Osmotic membrane permeability coefficient

The relative volume change (V_x/V_0) was plotted versus time. The $\Delta V/\Delta t$ value was obtained from the slope of the linear phase (first 15-40 s). P_f and P_{os} was calculated for Δt of 5 s steps. All permeability values are given as P_{os}.

13 Physiological Methods

13.1 Root Hydraulic Conductivity Measurements

Root hydraulic conductivity (K_{RA}) was determined as described by Tyree et al (1995). Shoots were excised from the roots and water was perfused from the rootstalk to soil. The perfusion pressure was increased linearly from 0 to 500 kPa at about 8 kPa per second while taking flow readings every two seconds. The slope of flow versus pressure was divided by root surface area to compute K_{RA}.

13.2 Gas Exchange Measurements

Net Photosynthesis and Stomatal Conductance

Net photosynthesis and stomatal conductance (g_s) was assessed by gas exchange measurements on leaves on the plants and on detached leaves. ABA experiments were performed on detached leaves by application of 100 µM ABA in water (n = 10). Measurements were taken simultaneously on control and antisense plants for several hours (air temperature 23.4 ± 0.01°C, 20.0 ± 0.07 %, 239.3 ± 0.29 $\mu mol \cdot m^{-2} \cdot s^{-1}$) in artificial light. The cuvettes were connected to the open-flow gas circuit photosynthesis system HCM-1000 (Walz, Effeltrich, Germany). The air flow was adjusted to 600 $ml \cdot min^{-1}$. H_2O and CO_2 concentrations at the inlet and outlet of the cuvettes were measured using a differential infrared gas analyzer (BINOS-100/4PS, Walz, Effeltrich, Germany). Data were autorecorded at 1 minute intervals using DATA-1000 software (Walz, Effeltrich, Germany). Data processing and calculations were done with Microsoft Excel™.

Transpiration of Water Stress Experiment

Transpiration rate (E) was assessed by gas exchange measurements from all leaves except two of four control and sixteen antisense plants (4 plants each line, seven weeks old). Measurements were taken from 10:30 AM to 05:00 PM (air temperature 34.7 ± 0.09°C, RH 35.0 ± 0.24 %, PPFD 1462 ± 9.9 $\mu molm^{-2}s^{-1}$) using an open system ADC-LCA3 infrared gas analyzer equipped with a Parkinson Leaf Chamber (Analytical Development Company, Hoddesdon, UK). Processing of the data was done with Microsoft Excel™.

13.3 Water Stress Experiments

A moderate water stress was induced by cultivation without irrigation for one week. Water content in the substrate was determined gravimetrically and related to soil water potential,

previously assessed with the substrate pressure plate method (Richards et al, 1956).

Water Potential Measurements

Leaf water potential (Ψ_{leaf}) and stem water potential (Ψ_{stem}) were measured by the pressure chamber technique (Steudle, 2001) in leaves of four control and sixteen *Nt*aqp1-antisense (AS) plants using a Scholander-Hammel bomb (Soil-moisture Equipment Corp., Santa Barbara, CA, USA). Measurement of Ψ_{stem} was performed according to (Shackel and Turner, 2000). Two leaves per plant were wrapped four hours in advance to the measurement for equilibration of leaf and stem water potential.

Root Hydraulic conductivity K_R

K_R was assessed on isolated roots excised from the stems leaving only a small portion of the stem. A controlled pressure setup at the root system was used according to Schubert et al 1995. After 2 min at 0.3 MPa m^{-1} to eliminated embolism, and after 5 min at 0.1 MPa m^{-1} to allow stabilization, two subsequent flow measurements for 2 min were made at constant pressure gradient (0.1 MPa). Root hydraulic conductivity was calculated from the pressure gradient and the flow measurements. Root specific conductivity (K_{RA}) was calculated by relating hydraulic conductivity to root area.

Calculations

K_R

K_R was calculated according to the water flux equation, as the ratio of transpirational flux (F, $kg \cdot s^{-1}$) through the root to the water potential gradient from the soil to the leaves ($\Delta\Psi$) causing the flow.

Root Area

Root length and weight was measured correlated to root area.

Leaf Area

Length and width of the leaves were measured and correlated to leaf area.

E LITERATURE

Abe, H., Yamaguchi-Shinozaki, K., Urao, T., Iwasaki, T., Hosokawa, D., Shinozaki, K. (1997). Role of *Arabidopsis* MYC and MYB homologs in drought- and abscisic acid - regulated gene expression. *The Plant Cell.* **9**, 1859-1868.

Aflalo C. (1991). Biologically localized firefly luciferase: A tool to study cellular processes. *Int. Rev. Cytol.* **130**, 267-323.

Altschul, S.F., Gish, W., Miller, W., Myers, E.W., Lipman, D.J. (1990). "Basic local alignment search tool." *J. Mol. Biol.* **215**, 403-410.

An, Y.Q., McDowell, J.M., Huang, S., McKinney, E.C., Chambliss, S., and Meagher, R.B. (1996). Strong, constitutive expression of the Arabidopsis ACT2/ACT8 actin subclass in vegetative tissues. *The Plant Journal.* **10,** 107-121.

Bate, N. and Twell, D., (1998). Functional architecture of a late pollen promoter: pollen specific transcription is developmentally regulated by multiple stage-specific and co-dependent activator elements. *Plant Mol. Biol.* **37** (5), 859-869.

Biela, A., Grote, K., Otto, B., Hoth, S., Hedrich, R., and Kaldenhoff, R. (1999). The *Nicotiana tabacum* plasma membrane aquaporin *Nt*AQP1 is mercury-insensitive and permeable for glycerol. *Plant J.* **18**, 565-570.

Blum, H., Beier, H., and Gross, H.J. (1987). Improved silver staining of plant proteins, RNA and DNA in polyacrylamide gels. *Electrophoresis* **8**, 93-99.

Bohnert, H.J., Nelson, D.E., Jensen, R.G. (1995). Adaptations to environmental stresses. *Plant Cell.* **7**, 1099-1111.

Brandes, P.N., Plautz, J.D., Stanewsky R., Jamison, C.F., Straume, M., Wood, K.V., Kay S.A., Hall, J.C. (1996). Novel features of Drosophila period transcription revealed by real-time luciferase reporting. *Neuron.* **16** (4), 687-692.

Brundrett, M.C., Enstone, D.E., and Peterson, C.A. (1988). A berberine-aniline blue fluorescent staining procedure for suberin, lignin and callose in plant tissue. *Protoplasma* **146**,13-142.

Brundrett, M.D., Kendrick, B., and Peterson, C.A. (1991). Efficient lipid staining in plant material with Sudan Red 7B or Fluorol yellow 088 in polyethylene glycol-glycerol. *Biotech. and Histochem.* **66**, 111-116.

Cheng, A., van Hoek, A.N., Yeager, M., Verkman, A.S. and Mitra, A.K. (1997). Structural Organization in a Human Water Channel. *Nature.* **387**, 627-630.

Clarkson, D.T., Carvajala, M., Henzler, T., Waterhouse, R.N., Smyth, A.J., Cooke, D.T., Steudle, E. (2000). Root hydraulic conductance: diurnal aquaporin expression and the effects of nutrient stress. *J. Ex.Bot.* **51** (342), 61-70.

Cooper, G.J. and Boron, W.F. (1998). Effect of PCMBS on CO_2 permeability of *Xenopus* oocytes expressing aquaporin 1 or its C189S mutant. *Am. J. Physiol.* **275** *(Cell Physiol.* **44**), C1481-C1486.

Daniels, M.J., Chaumont, F., Mirkov, T.E., Chrispeels, M.J. (1996). Characterization of a new vacuolar membrane aquaporin sensitive to mercury at a unique site. *Plant Cell.* **8**, 587-599.

Daniels, M.J., Mirkov, T.E., Chrispeels, M.J. (1994). The plasma membrane of *Arabidopsis thaliana* contains a mercury-insensitive aquaporin that is a homolog of the tonoplast water channel protein TIP. *Plant Physiol.* **106**, 1325-1333.

DeLuca, M. and McElroy, W.D. (1974). Kinetics of the firefly luciferase catalyzed reactions. *Biochemistry.* **13**, 921-925.

DeWet, J.R., Wood, K.V., DeLuca, M., Helinski, D.R., Subrami, S. (1987). Firefly luciferase gene: structure and the expression in mammalian cells. *Mol. Cell Biol.**7 (2)***, 725-737.

DeWet, J.R., Wood, K.V., Helinski, D.R., and DeLuca, M. (1985). Cloning of firefly luciferase cDNA and the expression of active luciferase in *Escherichia coli. Proc. Natl. Acad. Sci.* **82**, 7870-7873.

Eckert, M. (2000). Zur Regulation und Expression von Aquaporinen unter Berücksichtigung des pflanzlichen Wasserhaushaltes. Dissertation, J.-v.-S.-Institut, Universität Würzburg.

Eckert, M., Biela, A., Siefritz, F., Kaldenhoff, R. (1999). New aspects of plant aquaporin regulation and specificity, review article. *J. Exp. Bot.* **50** (339), 1541-1545.

Elmayan, T. and Tepfer, M. (1995). Evaluation in tobacco of the organ specificity and strength of the rol D promoter, domain A of the 35S promoter and the 35S2 promoter. *Transgenic Res.* **4**, 388-396.

Fahn, A. (1979). Secretory tissues in plants. Academic Press, London.

Feinberg, A.P. and Vogelstein, B. (1983). A technique for radiolabelling DNA restrictionendo-nuclease fragments to high specific activity. *Anal. Biochem.* **132**, 6-13.

Feinberg, A.P. and Vogelstein, B. (1984). A technique for radiolabeling DNA restriction endonuclease fragments to high specific activity.Addendum. *Anal. Biochem.* **137**, 266-267.

Fleurat-Lessard, P., Frangne, N., Maeshima, M., Ratajczak, B.J.-L., Martinoia, E. (1997). Increased expression of vacuolar aquaporin and H^+-ATPase related to motor cell function in *Mimosa pudica* L. *Plant Physiol.* **114**, 827-834.

Ford, S.R., Buck, L.M., and Leach, F.R. (1995). Does the sulfhydryl or the adenine moiety of CoA enhance firefly luciferase activity*? Biochim. Biophys. Acta.* **1252,** 180-184.

Fray, R.G., Wallace, A., Grierson, D. and Lycett, G.W. (1994). Nucleotide sequence and expression of a ripening and water stress-related cDNA from tomato with homology to the MIP class of membrane channel proteins. *Plant Mol. Biol*. **24**, 539-543.

Gallois, P. and Marinho, P. (1995). Leaf disk transformation using *Agrobacterium tumefaciens*-expression of heterologous genes in tobacco. *Methods in Molecular Biology: In Plant Gene Transfer and Expression Protocols*, H. Jones, ed (Totowa, NJ :Humana Press Inc.). **49**, 39-48.

Gatz, C. (1997). Chemical control of gene expression. *Annu. Rev. Plant Physiol. Plant Mol. Biol.* **48**, 89-108.

Gerbeau, P., Gülüc, J., Ripoche, P., Maurel, C. (1999). Aquaporin *Nt*-TIPa can account for high permeability of the tobacco vacuolar membrane to small solutes. *Plant J.* **18**, 577-587.

Gorin, M.B., Yancey, S.B., Cline, J., Revel, J.P., Horwitz, J. (1984). The major intrinsic protein (MIP) of the bovine lens fiber membrane: Characterization and structure based on cDNA cloning. *The Cell.* **39**, 49-59.

Grote, K., von Trzebiatovski, P., and Kaldenhoff, R. (1998). RNA levels of plasma membrane aquaporins in Arabidopsis thaliana. *Protoplasma* **204**, 139-144.

Grotewold, E., Athma, P., and Peterson, T. (1991). Alternatively spliced products of the maize P gene encode proteins with homology to the DNA binding domain of Myb-like transcription factors. *Proc. Natl. Acad. Sci.* USA. **88**, 4587-4591.

Gubler, F., Kalla, R., Roberts, J.K., Jacobsen, J.V. (1995). Gibberellin-regulated expression of a myb gene in barley aleurone cells: Evidence for Myb transactivation of a high-pl a-amylase gene promoter. *The Plant Cell.* **7**, 1879-1891.

Guerrero, F.D., Jones, J.T., Mullet, J.E. (1990). Turgor-responsive gene transcription and RNA levels increase when pea shoots are wilted. Sequence and expression of three inducible genes. *Plant Mol. Biol.* **15**, 11-26.

Heymann, J.B., Agre, P., Engel, A. (1998). Progress on the structure and function of aquaporin 1. *Journal of Structural Biology.* **121** (2), 191-206.

Heymann, J.B. and Engel, A. (1999). Aquaporins: Phylogeny, structure and physiology of water channels. *NIPS.* **14**,187-194.

Iino, M. (1995). Gravitropism and phototropism of maize coleoptiles: Evaluation of the Cholodny-Went theory through effects of auxin application and decapitation. *Plant Cell Physiol.* **36**, 361-367.

Jefferson, R. A. (1987). Assaying chimeric genes in plants: the GUS gene fusion system. *Plant Mol. Biol. Rep.* **5**, 387-405.

Jefferson, R.A., Burgess, S. M., Hirsh, D. (1986). β-Glucuronidase from *Escherichia coli* as a gene-fusion marker. *Proc. Natl. Acad. Sci., USA.* **83**, 8447-8451.

Jefferson, R.A., Kavanagh, T. A., Bevan, M. W. (1987b). *Gus* fusions: β-glucuronidase as a sensitive and versatile gene fusion marker in higher plants. *EMBO J.* **6**, 3901-3907.

Johansson, I., Karlson, M., Shukla, V.K., Chrispeels, M.J., Larson, C., Kjellbom, P. (1998). Water transport activity of the plasma membrane aquaporin PM28A is regulated by phosphorylation. *The Plant Cell.* **10**, 451-459.

Johnson, K.D., Chrispeels, M.J. (1992). Tonoplast-bound protein kinase phosphorylates tonoplast intrinsic protein. *Plant Physiol*. **100**, 1787-1795.

Kaldenhoff, R., Eckert, M. (1999). Features and function of plant aquaporins. *J. Photochem. Photobiol. B: Biol.* **52**, 1-6.

Kaldenhoff, R., Grote, K., Zhu, J, Zimmermann, U. (1998). Significance of plasmalemma aquaporins for water transport in *Arabidopsis thaliana*. *The Plant Journal.* **14** (1), 121-128.

Kaldenhoff, R., Kölling, A., Meyers, A., Karman, U., Ruppel, G., Richter, G. (1995). The blue light-responsive AthH2 gene of *Arabidopsis thaliana* is primarily expressed in expanding as well as in differentiating cells and encodes a putative channel protein. *Plant Journal.* **7**, 87-95.

Kaldenhoff, R., Kölling, A., Richter, G. (1993). A novel blue light- and abscisic acid-induciblegene of *Arabidopsis thaliana* encoding an intrinsic membrane protein. *Plant.Mol. Biol.* **23**, 1187-1198.

Kaldenhoff, R., Kölling, A., Richter, G. (1996). Regulation of the *Arabidopsis thaliana* aquaporin gene AthH2 (PIP1b). *J. Photochem. Photobiol.* **36** (3), 351-354.

Kaldenhoff, R., and Iino, M. (1997). Restoration of phototropic responsiveness in decapitated maize coleoptiles. *Plant Physiol.* **114**, 1267-1272.

Kammerloher, W., Fischer, U., Piechottka, G.P., Schäffner, A.R. (1994). Water channels in the plant plasma membrane cloned by immunoselection from a mammalian expression system. *Plant J.* **6**, 187-199.

Knepper, M.A., Wade, J.B., Terris, J., Ecelbarger, C.A., Marples, D., Mandon, B., Chou, C.L., Kishore, B.K., Nielsen, S. (1996). Renal aquaporins. *Kidney Int.* **49** (6), 1712-7.

Kushmerick, C., Varadaraj, K., Mathias, R. (1998). Effects of lens major intrinsic protein on glycerol permeability and metabolism. *J. Membrane Biol.* **161**, 9-19.

Ludevid, D., Höfte, H., Himmelblau, E., Chrispeels, M.J. (1992). The expression pattern of thetonoplast intrinsic protein γTIP in *Arabidopsis thaliana* is correlated with cell enlargement. *Plant Physiology.* **100**, 1633-1639.

Luscher, B., Eiseman, R.N. (1990). New light on myb and myc. PartII. Myb. *Gene Dev.* **4**, 2235-2241.

Maeshima, M., Hara-Nishimura, I., Takeuchi, Y., Nishimura, M. (1994). Accumulation of vacuolar H^+-pyrophosphatases and H+-ATPases during reformation of the central vacuole in germinating pumpkin seeds. *Plant Physiol.* **106**, 61-69.

Mariaux, J.B., Bockel, C., Salamini, F., Bartels, D. (1998). Desiccation- and abscisic acid-responsive genes encoding major intrinsic proteins (MIPs) from the resurrection plant *Craterostigma plantagineum*. *Plant Mol. Biol.* **38**, 1089-1099.

Martínez-Ballesta, M.C., Martínez, V., Carvajal, M. (2000). Regulation of water channel activity in whole roots and protoplasts from roots of melon plants grown under saline conditions. *Australian Journal of Plant Physiology*. **27**, 685-691.

Maurel, C., Kado, R.T., Guern, J., Chrispeels, M.J. (1995). Phosphorylation regulates the water channel activity of the seed-specific aquaporin a-TIP. *EMBO J.* **1**4, 3028-3035.

Maurel, C. (1997). Aquaporins and water permeability of plant membranes. *Annu. Rev. Plant Physiol. Plant Mol. Biol.* **48**, 399-429.

Maurel, C., Chrispeels, M.J., Lurin, C., Tacnet, F., Geelen, D., Ripoche, P., Guern, J. (1997b). Function and regulation of seed aquaporins. *J. Exp. Bot.* **48**, 421-430.

Maurel, C., Reizer, J., Schroeder, J.I., and Chrispeels, M.J. (1993). The vacuolar membrane protein γ-TIP creates water specific channels in *Xenopus* oocytes. *EMBO Journal*. **12**, 2241-2247.

Mayerhofer, R., Araki, K., Szalay, A.A. (1995). Monitoring of spatial expression of firefly luciferase in transformed zebrafish. *J. Biolum. Chemilum*. **10** (5), 271-275.

Moshelion, M., Becker, D., Biela, A., Uehlein, N., Hedrich, R., Otto, B., Levi, H., Moran, N., and Kaldenhoff, R. (2002). Plasma membrane aquaporins in the motor cells of *Samanea saman*: Diurnal and circadian regulation. *Plant Cell*. **14** (3), 727-739.

Murashige, T., and Skoog, F. (1962). A revised medium for rapid growth and bioassays with tobacco tissue cultures. *Physiol. Plant.* **15**, 473-479.

Murata, K., Mitsuoka, K., Hirai, T., Walz, T., Agre, P., Heymann, J.B., Engel, A., and Fujiyoshi, Y. (2000). Structural determinants of water permeation through aquaporin-1. *Nature.* **407**, 599-605.

Muschietti, J., Dircks, L., Vancanneyt, G., McComick, S. (1994). LAT52 protein is essential for tomato pollen development: pollen expressing AS LAT52 RNA hydrates and germinates abnormally and cannot achieve fertilization. *Plant J*. **6**, 321-338.

Nakhoul, N.L., Davis, A.D., Romero, M.F., and Boron, W.F. (1998). Effect of expressing the water channel aquaporin-1 on the CO_2 permeability of *Xenopus* oocytes. *Am. J. Physiol.* **274** *(Cell Physiol. 43*), C543-C548.

Neville, D.M. (1971). Molecular weight determination of protein-dodecyl sulfate complexes by gel electrophoresis in a discontinuous buffer system. *J. Biol. Chem.* **246**, 6328-6334.

Noda, K., Glover, B.J., Linstead, P., Martin, C. (1994). Flower colour intensity depends on specialized cell shape controlled by a Myb-related transcription factor. *Nature.* **23,** 369 (6482), 661-664.

Nultsch, W. (2001). Allgemeine Botanik, 11. edition, *Thieme,* Stuttgart.

O'Brien, T. P., Feder, N., and Mc Cully, M. E. (1964). Polychromatic staining of plant cell walls by Toluidine blue O. *Protoplasma.* **59**,369-373.

O'Brien, T.P. and McCully, M.E. (1981). The study of plant structure: Principles and selected methods. Termarcarphi Pty Ltd., Melbourne, Australia. 357 pp.

Ogren, W.L, (1984). Photorespiration: Pathways, regulation, and modification. *Annu. Rev. Plant Physiol. Plant Mol. Biol.* **35**, 415-442.

Oppenheimer, D.G., Herman, P.L., Sivakumaran, S., Esch, J., Marks, M.D. (1991). A myb gene required for leaf trichome differentiation in Arabidopsis is expressed in stipules. *Cell*. **67**, 483-493.

Otto, B. and Kaldenhoff, R. (2000). Cell-specific expression of the mercury-insensitive plasma-membrane aquaporin *Nt*AQP1 from Nicotiana tabacum. *Planta*. **211**, 167-172.

Ow, D.W., Wood, K.V., DeLuca, M., DeWet, J.R., Helsinki, D.R., Howell, S.H. (1986). Transient and stable expression of the firefly luciferase gene in plant cells and transgenic plants. *Proc. Natl. Acad. Sci.* **84,** 4870-4874.

Paz-Ares, J., Ghosal, D., Wienand, U., Peterson, P.A., Saedler, H. (1987). The regulatory c1 locus of Zea mays encodes a protein with homology to myb proto-oncogene products and with structural similarities to transcriptional activators. *EMBO J.* **6**, 3553-3558.

Phillips, A.L., Huttly, A. K. (1994). Cloning of two gibberellin-regulated cDNAs from *Arabidopsis thaliana* by substractive hybridisation: expression of the tonoplast water channel ?-TIP is increased by GA_3 . *Plant Mol. Biol.* **24**, 603-615.

Piechulla, B., Merforth, N., Rudolph, B. (1998). Identification of tomato Lhc promoter regions necessary for circadian expression. *Plant Mol. Biol.* **38**, 655-662

Preston, G.M., Carrol, T.P., Guggino, W.B., and Agre, P. (1992). Appearence of water channels in *Xenopus* oocytes expressing red cell CHIP28 protein. *Science.* **256**, 385-87.

Preston, G.M., Jung, G.S., Guggino, W.B., Agre, P. (1994). Membrane topology of aquaporin CHIP. Analysis of functional epitope-scanning mutants by vectorial proteolysis. *J. Biol. Chem.* **269**, 1668-1673.

Puente, P., Wie, N., and Deng, X-W. (1996). Combinatorial interplay of promoter elements constitutes the minimal determinants for light and developmental control of gene expression in Arabidopsis. *EMBO J.* **15**, 3732-3743.

Ramahaleo, T., Morillon, R., Alexandre, J., and Lassalles, J.P. (1999). Osmotic water permeability of isolated protoplasts. Modifications during development. *Plant Physiol.* **119**, 885-896.

Ramesh Prasad, G.V., Coury, L.A., Finn, F., Zeidel, M.L. (1998). Reconstituted aquaporin 1 water channels transport CO_2 across membranes. *J. Biol. Chem.* **273**, 33121-33126.

Reizer, J., Reizer, A., Saier, M.H.J. (1993). The MIP family of integral proteins: Sequence comparisons, evolutionary relationships, reconstructed pathway of evolution and proposed functional differentiation of the two repeated halves of the proteins. *Crit. Rev. Biochem. Mol. Biol.* **28**, 235-257.

Ren, G., Reddy, V. S., Cheng, A., Melnyk, P., Mitra, A. K. (2001). Visualization of a water-selective pore by electron crystallography in vitreous ice. *Proc. Natl. Acad. Sci. USA.* **98**, 1398-1403.

Richards, L.A., Gardner, W.R., and Ogata, G. (1956). Physical process determining water loss from soil. *Soil Soc. Am. Proc.* **20**, 310-314.

Rogers, H.J., Bate, N., Combe, J., Sullivan, J., Sweetman, J., Swan, C., Lonsdale, D.M., Twell, D. (2001). Functional analysis of cis-regulatory elements within the promoter of the tobacco late pollen gene g10. *Plant Mol. Biol.* **45**, 577-585.

Sablowski, R.W.M, Moyano, E., Culianez-Macia, F.A,. Schuch, W., Martin, C., Bevan, M. (1994). A flower-specific Myb protein activates transcription of phenylpropanoid biosynthetic genes. *EMBO J.* **13**, 128-137.

Santoni, V., Gerbeau, P., Javot, H., Maurel, C. (2000). The high diversity of aquaporins reveals novel facets of plant membrane functions. *Curr Opin Plant Biol*. **3** (6), 476-81.

Sarda, X., Tousch, D., Ferrare, K., Cellier, F., Alcon, C., Dupuis, J.M., Casse, F., Lamaze, T. (1999). Characterization of closely related delta-TIP genes encoding aquaporins which are differentially expressed in sunflower roots upon water deprivation through exposure to air. *Plant. Mol. Biol.* **40** (1), 179-91.

Schnepf, E. (1974). Gland cells. In: Robards AW (ed) Dynamic aspects of plant ultrastructure. McGraw-Hill, London, pp 331-351.

Schubert, A., Restagno, M., Novello, V., and Peterlunger, E. (1995). Effects of shoot orientation on growth, net photosynthesis, and hydraulic conductivity of *Vitis vinifera* L. cv. Cortese. *Am. J. Enol. Vitic.* **46** (3), 324-328.

Shackel, K.A., and Turner, N.C. (2000). Seed coat cell turgor in chickpea is independent of changes in plant and pod water potential. *J. Exp. Bot.* **51**, 895-900.

Sherf, B.A., and Wood, K.V. (1994). Firefly luciferase engineered for improved genetic reporting. *Promega notes.* **49**, 14-21.

Shuman, S. (1994). Novel approach to molecular cloning and polynucleotide synthesis using *Vaccinia* DNA Topoisomerase. *J. Biol. Chem.* **269**, 32678-32684.

Siefritz F. (1998). Identifikation und Analyse des *Nt*AQP1-Aquaporingen-Promotors aus *Nicotiana tabacu*m. Diplomarbeit, J.-v.-S.-Institut f. Biowissenschaften, Universität Würzburg.

Siefritz, F., Biela, A., Eckert, M., Otto, B., Uehlein, N., Kaldenhoff, R. (2001). The tobacco plasma membrane aquaporin *Nt*AQP1. *Journal of Experimental Botany*. **52** (363), 1953-1957.

Siefritz, F., Tyree, M.T., Lovisolo, C., Schubert, A., Kaldenhoff, R. (2002). PIP1 plasma membrane aquaporins in Nicotiana tabacum: From cellular effects to the function in plants. *The Plant Cell*. **14**, 869-876.

Skiver, K., Olsen, F.L., Rogers, J.C., Mundy, J. (1991). Cis-acting DNA elements responsive to gibberellin and its antagonist abscisic acid. *Proc. Natl. Acad. Sci.* **88**, 7266-7270.

Smart, L.B., Vojdani, F., Maeshima, M., Wilkins T.A. (1998). Genes involved in osmoregulation during turgor-driven cell expansion of developing cotton fibers are differentially expressed. *Plant Physiol*. **116**, 1539-1549.

Steudle, E. (1997) Review: Water transport across plant tissue: role of water channels. *Biol. Cell.* **89**, 259-273.

Steudle, E., Frensch, J. (1996). Review Article: Water transport in plants: role of the apoplast. *Plant and Soil*. **187**, 67-79.

Stürzl, M., Roth, W. K. (1990). "Run off" synthesis and application of definied single-stranded DNA-hybridization probes. *Anal. Biochem.* **185**, 164-169.

Sui, H., Han B.G., Lee, J.K., Walian, P., Jap, G.K. (2001) Structural basis of water-specific transport through the AQP1 water channel. *Nature.* **414**, 872-878.

Taiz, L., and Zeiger, E. (1998). Plant Physiology. 2. edition, Sinauer Associates, Inc., Publishers, Sunderland, Massachusetts, USA.

Taylor, L. P., and Hepler, P.,K. (1997). Pollen Tube Germination and Growth. *Annual Reviews in Plant Physiology and Plant Molecular Biology*. **48**, 461-491.

Twell, D. (1994). The diversity and regulation of a gene expression in the pathway of male gametophyte development. In Molecular and Cellular aspects of Plant reproduction, ed. Scott, R.J., Stead, A.D., Cambridge University Press, Cambridge, pp.83-135.

Tyree, M.T., Patino, S., Bennink, J., and Alexander, J. (1995). Dynamic measurements of root hydraulic conductance using a high-pressure flowmeter in the laboratory and field. *J. Exp. Bot.* **46**, 83-94.

Urao, T., Yamaguchi-Shinozaki, K., Urao, S., Shinozaki, K. (1993). An Arabidopsis myb homolog is induced by dehydration stress and its gene product binds to the conserved MYB recognition sequence. *The Plant Cell* **5**, 1529-1539.

Van Os, C.H., Deen, P.M.T., Dempster, J.A. (1994). Aquaporins: Water selective channels in biological membranes. Molecular structure and tissue distribution. *Biochem. Biophys. Acta.* **1197,** 291-309.

Verkman, A.S., van Hoeck, A.N., Ma, T., Frigeri, A., Skach, W.R. (1996). Water transport across mammalian cell membranes. *Am. J. Physiol.* **270**, 12-30.

Walz, T., Hirai, T., Murata, K., Smith, B.L., Heymann, J.B., Mitsuoka, K., Fujiyoshi, Y., Agre, P. and Engel, A. (1997). Three-dimensional structure of aquaporin 1 at 6 Å. *Nature.* **387**, 624-627.

Wayne, R., Mimura, T., Shimmen, T. (1994). The relation between carbon and water transport in single cells of *Chara corallina*. *Protoplasma*. **180**, 118-135.

Yamada, S., Nelson, D.E., Ley, E., Marquez, S., Bohnert, H.J. (1997). The expression of anaquaporin promoter from *Mesembryanthemum crystallinum* in tobacco. *Plant Cell Physiology.* **38**, 1326-1332.

Yamaguchi-Shinozaki, K., Koizumi, M., Urao, S., Shinozaki, K. (1992). Molecular cloning and characterization of 9 cDNAs for genes that are responsive to desiccation in *Arabidopsis thalian*a: Sequence analysis of one cDNA clone that encodes a putative transmembrane channel protein. *Plant Cell Physiol.* **33**, 217-224.

Yamamoto, Y.T, Taylor, C.G., Acedo, G.N., Cheng, C.L., Conkling, M.A. (1991). Characterization of cis-acting sequences regulating root-specific gene expression intobacco. *The Plant Cell.* **3**, 371-382.

Zhang, R. and Verkman, A.S. (1991). Water and urea permeability properties of Xenopus oocytes: expression of mRNA from toad urinary bladder. *Am. J. Physiol*. **260**, C26-C34.

Zhang, Y., and Roberts, D. (1995). Expression of soybean nodulin 26 in transgenic tobacco. targeting to the vacuolar membrane and effects on floral and seed development. *Molecular Biology of the Cell.* **6**, 109-117.

F APPENDIX

1 Abbreviations

%	percent
°C	degree Celsius
35Ster	35S Cauliflower mosaic virus terminus
A	adenine
ABA	abscisic acid
ag	attogram = 10^{-18} g
AQP	aquaporin
ATP	adenosine-5'-triphosphate
*At*PIP1b	*Arabidopsis thaliana* PIP1b
bp	base pair
BSA	bovine serum albumin
C	cytosine
cDNA	copy DNA
cm	centimeter
cm^2	square centimeter
cm^3	cubic centimeter
dATP	deoxyadenosine-5'-triphosphate
DNA	deoxyribonucleic acid
dNTP	2'-desoxyribonucleosid-5'-triphosphate
DTT	dithiotreitol
EDTA	ethylenediamine-tetraacetate
d	day
fg	femto gram = 10^{-15} g
FW	fresh weight
g	gram
G	guanine
GA	gibberellic acid
GARE	GA-response-element
GFP	green fluorescence protein
GUS	ß-glucuronidase
h	hour
IAA	3-indole-acetic acid
IPTG	isopropyl-1-thio-b-D-galactoside
kb	kilo base
kDa	kilo Dalton
l	liter
LB	Luria-Bertani
LUC	luciferase
m	meter

M	molar
m^2	square meter
M&S	Murashige and Skog
mA	milli Ampere
MES	4-morpholinic-ethanesulfonic acid
mg	milligram
min	minutes
MIP	major intrinsic protein
ml	milliliter
mM	millimolar
MOPS	4-morpholinic-propansulfonic acid
mosm	milliosmolar
MPa	mega Pascal
mRNA	messenger RNA
ng	nanogram = 10^{-9} g
nl	nanoliter = 10^{-9} l
nm	nanometer = 10^{-9} m
nosT	nopaline synthetase terminus
nptII	neomycin transferase II, resistance gene
Nt	*Nicotiana tabacum*
*Nt*AQP1	*Nicotiana tabacum* Aquaporin 1 protein
*Nt*aqp1	*Nicotiana tabacum* Aquaporin 1 gene
OD	optical density
P&S	Pirson and Seidel
PAGE	polyacrylamid-gelelectrophoresis
PAR	photosynthetic active radiation
PBS	phosphate buffered salt solution
PCR	polymerase chain reaction
PEG	polyethylene-glycol
PIP	plasmalemma intrinsic protein
pmol	picomol = 10^{-12} mol
prom	promoter
RNA	ribonucleic acid
RNase	ribonuclease
rpm	rounds per minute
RT	room temperature
SD	standard deviation
SDS	sodium dodecyl sulfate
SE	standard error
s	second
SSC buffer	sodium citrate buffer
T	thymidine
TAE	tris-acetate-EDTA
TAE-buffer	Tris/Acetate/EDTA-buffer

T_{an}	annealing temperature
Taq	*Thermus aquaticus*
TEMED	N,N,N,N-tetramethylaminomethane
TIP	tonoplast intrinsic protein
T_m	melting temperature
Tris	Tris-(hydroxymethyl)-aminomethane
U	unit
UV	ultraviolet
V	Volt
Vol	volume
W	Watt
w/v	weight/volume
wt	wild type
X-Gal	5-bromo-4-chloro-3-indoyl-b-D-galactoside

2 Amino Acid Analysis

Values are given in µM/g FW:

Leaves of eight-weeks-old tobacco plants

	control	**AS 3-4**	**AS 4-3**	**AS 5-2**	**AS 5-5**	**AS 11-7**	**AS 18-3**
phosphoserine	0.12	0.08	0.11	0.09	0.14	0.08	0.17
aspartic acid	0.97	0.95	0.64	1.01	1.10	0.72	1.25
threonin	0.20	0.14	0.13	0.15	0.16	0.13	0.26
serine	0.51	0.42	0.49	0.42	0.52	0.55	0.87
asparagine	0.08	0.08	0.05	0.06	0.09	0.04	0.25
glutamic acid	1.04	1.20	0.93	1.22	1.03	1.26	1.49
glutamine	0.79	0.33	0.26	0.40	0.80	0.22	1.58
glycine	0.11	0.03	0.04	0.09	0.06	0.02	1.38
alanine	0.49	0.26	0.24	0.26	0.22	0.27	0.57
valine	0.03	0.03	0.03	0.03	0.03	0.02	0.04
methionine	0.02	0.02	0.02	0.02	0.03	0.02	0.03
isoleucine	0.09	0.04	0.06	0.04	0.07	0.04	0.08
leucine	0.02	0.05	0.04	0.04	0.03	0.00	0.02
phenylalanine	0.04	0.05	0.05	0.04	0.06	0.02	0.05
GABA	0.56	0.63	0.66	0.71	0.75	0.33	1.34
ammonium	0.23	0.11	0.06	0.13	0.12	0.12	0.26
lysine	0.04	0.03	0.04	0.03	0.04	0.02	0.04
arginine	0.09	0.02	0.02	0.02	0.08	0.00	0.11

Tobacco seedlings (L+H: leaves and hypocotyl, R: roots)

	control L+H	**AS 5-2** L+H	**AS 11-7** L+H	**AS 18-3** L+H	**control R**	**AS 5-2 R**	**AS 11-7 R**	**AS 18-3 R**
phosphoserine	0.05	0.09	0.08	0.07	0.03	0.03	0.03	0.02
aspartic acid	0.27	0.41	0.35	0.39	0.09	0.08	0.05	0.05
threonin	0.17	0.16	0.19	0.28	0.1	0.07	0.06	0.06
serine	0.44	0.74	0.5	0.56	0.28	0.26	0.17	0.2
asparagine	0.22	0.53	0.34	0.39	0.13	0.03	0.03	0.07
glutamic acid	0.16	0.58	0.32	0.23	0.13	0.15	0.1	0.11
glutamine	0.89	1.22	1.35	1.71	0.49	0.28	0.26	0.33
glycine	2.12	0.79	0.52	3.97	0.08	0.07	0.03	0.06
alanine	0.16	0.18	0.13	0.14	0.05	0.04	0.03	0.03
valine	0.06	0.07	0.06	0.07	0.03	0.02	0.01	0.02
isoleucine	0.07	0.05	0.08	0.08	0.02	0.01	0.01	0.01
leucine	0.11	0.12	0.14	0.13	0.08	0.07	0.06	0.05
phenylalanine	0.08	0.06	0.09	0.11	0.04	0.03	0.03	0.03
GABA	0.21	0.1	0.23	0.36	0.14	0.11	0.1	0.09
ammonium	0.71	2.3	0.97	0.43	0.51	0.64	0.31	0.23
lysine	0.06	0	0.05	0.08	0.13	0.07	0.12	0.09
arginine	0.34	0.09	0.27	0.44	0.03	0.02	0	0.02

3 Oligo Nucleotide Primers

Name	Nucleotide sequence	T_m	use
M13 Universal	5'-TGTAAAACGACGGCCAGT-3'	53.7	S
M13 Reverse	5'-CAGGAAACAGCTATGAC-3'	53.7	S
T3	5'-AATTAACCCTCACTAAAGGG-3'	53.2	S
T7	5'-TAATACGACTCACTATAGGG-3'	53.2	S
***Nt*AQP1-LCfwd**	5'-ACACAGCCATTAGGA-3'	45.1	LC
***Nt*AQP1-LCrev**	5'-GGTTAAGGACAGTTTC-3'	46.6	LC
***Nt*Tob103fwd**	5'-CCCAGAAGTCCTCTT-3'	66.2	LC
***Nt*Tob103rev**	5'-GGGATGCGAGGAT-3'	64.4	LC
AP2 (Adapter Primer 2)	5'-ACTATAGGGCACGCGTGGT-3'	71.0	C
***Nt*AQP1prom as Xho I**	5'-CTCGAG TTGAACACTCACTAAACTTACCTT-3'	65.5	C
***Nt*AQP1prom s Kpn I**	5'-GGTACCTAAAATATATGGAGCCTTTTTCTGAGG-3'	65.8	C
***Nt*AQP1 in situ as**	5'-CTGGCATTTCTCTTAGCATC-3'	55.3	P
***Nt*PIP1a antisense**	5'-CCAAGATGATAATTCACCAG-3'	53.2	P
***Nt*PIP2a sense**	5'-AGAAACAATGTCAAAGGACG-3'	53.2	P
***Nt*PIP2a antisense**	5'-CCATCACATTTATCAGCAC-3'	52.4	P
***Nt*TIPa antisense**	5'-GAAAGATTCATCACTAGGAAG-3'	54.0	P

Abbreviations: LC: LightCycler, C: Cloning, P: Probe, S: Sequencing

4 *Nt*AQP1-Promoter Sequence

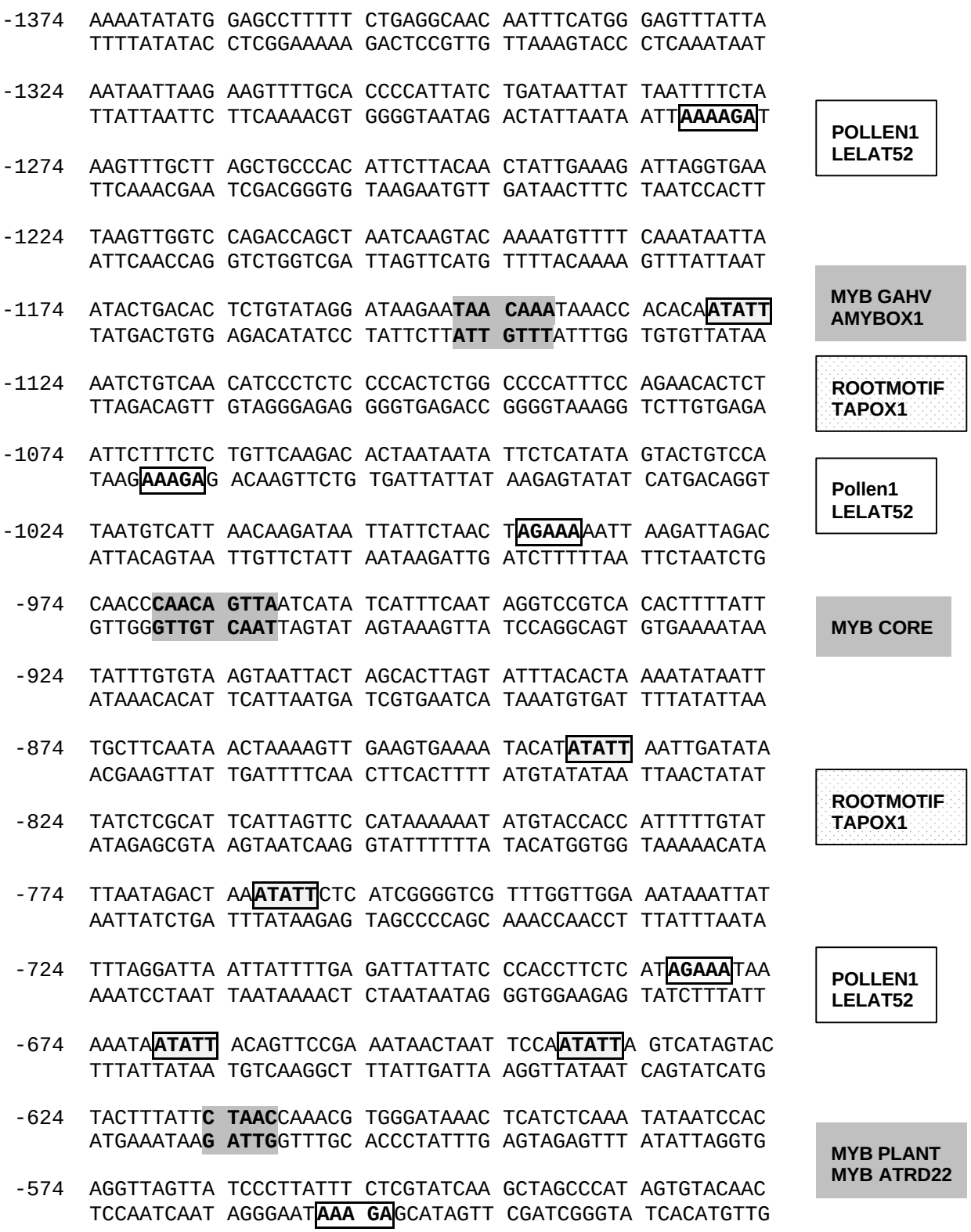

```
-524   ACATAATATG TTAATGACAG ATTAAAGGAC AGTCTGGTAC ACTAAGCTCT
       TGTATTATAC AATTACTGTC TAATTTCCTG TCAGACCATG TGATTCGAGA

 -474  CGCTATGCGG TATTCATAGA GGTGCCAGAC CCTAAAGGTC TATTGTATGC
       GCGATACGCC ATAAGTATCT CCACGGTCTG GGATTTCCAG ATAACATACG

 -424  AGTCTTACCT TATATTTTGT AAGCGGGATT CGGAAAGGGT CGAACTCTAA
       TCAGAATGGA ATATAAAACA TTCGCCCTAA GCCTTTCCCA GCTTGAGATT

 -374  GGTCTATATA TGCAGTCTTA CCCTTCATTT ATGCAAGAGA TTGTTTTCAT
       CCAGATATAT ACGTCAGAAT GGGAAGTAAA TACGTTCTCT AACAAAAGTA

 -324  GGCTCAAATT CATAACCTTC TGACATCAAC TTTACCGATT AAGCCTGGAC
       CCGAGTTTAA GTATTGGAAG ACTGTAGTTG AAATGGCTAA TTCGGACCTG

 -274  AGAATGTTTA TGCTAATTAG GAAAAAAATA TAGACCGACC AACTCAATAA
       TCTTACAAAT ACGATTAATC CTTTTTTTAT ATCTGGCTGG TTGAGTTATT

 -224  TTAACCAGAC CAATTTAATA AGAATGTGAC ACTTTAATGG CTCAAATTCA
       AATTGGTCTG GTTAAATTAT TCTTACACTG TGAAATTACC GAGTTTAAGT

 -174  TAACTTTACC GATTAAGTCA GGACAGAATG TTTATGCTAA TTAGGAAAAA
       ATTGAAATGG CTAATTCAGT CCTGTCTTAC AAATACGATT AATCCTTTTT

 -124  AATATAGACC GACCAACTCA ATAATTAACC AGACCAATTT AATAAGAATG
       TTATATCTGG CTGGTTGAGT TATTAATTGG TCTGGTTAAA TTATTCTTAC

  -74  TAACACTTTA ATTAATTTGT CTTCATAAAT GAGTTCTCCA CTATAAAACA
       ATTGTGAAAT TAATTAAACA GAAGTATTTA CTCAAGAGGT GATATTTTGT
                                  +1
  -24  ACCACAACTC TATCTTTCCT CAACACCAAA CTTGGTTTTT GTACTATCCA
       TGGTGTTGAG ATAGAAAGGA GTTGTGGTTT GAACCAAAAA CATGATAGGT
                                                        +76
  +27  CTTAGCACAA TAAAGAGAGA AAAACAAGGT AAGTTTAGTG AGTGTTCAAA
       GAATCGTGTT ATTTCTCTCT TTTTGTTCCA TTCAAATCAC TCACAAGTTT

   77  TGGCAGAAAA CAAAGAAGAA GATGTTAAGC TTGGAGCTAA CAAATTCAGA
       ACCGTCTTTT GTTTCTTCTT CTACAATTCG AACCTCGATT GTTTAAGTCT
```

ROOTMOTIF TAPOX1

Transcription start (+1)

Translation start (+76)

POLLEN1 LELAT52

*Nt*AQP1-promoter nucleotide sequence with specific DNA-binding motifs: pollen-specific, root-specific and MYB-like protein binding sites are marked by different boxes. Transcription and translation start is marked in bold letters.

4.1 Binding Sites and Motifs

Binding sites and motifs in the *Nt*aqp1-promoter: Names, location, signal sequence and references are given. The location corresponds to the nucleotide numbers also used in the sequence of the *Nt*aqp1-promoter sequence (F4). "-" illustrates location upstream of the transcription start (+1) and "+" the one downstream. (-) and (+) describes the orientation on the nucleotide sequence.

Factor or Site Name	Location (*Nt*aqp1-promoter sequence, see appendix)	Signal Sequence	References
AMYBOX1	-1119 (+)	TAACARA	**Huang, N. et al,** 1990**.** Plant Mol. Biol. 14:655-668.
CCA1ATLHCB1	-336 (-)	AAMAATCT	**Wang, Z.-Y. et al,** 1997. Plant Cell. 9:491-507.
CIACADIANLELHC	-19 (+)	CAANNNNATC	**Piechulla, B. et al,** 1998. Plant Mol. Biol. 38 (4):655-62.
DOFCOREZM-	-1274 (+), -1237 (+), -859 (+), -500 (+), -440 (+), -390 (+), -1337 (-), -1070 (-), -931 (-), -621 (-), -294 (-), -192 (-), -170 (-), -68 (-), -10 (-),	AAAG	**Yanagisawa, S. et al,** 1999. Plant J. 17:209-214. **Yanagisawa, S.** 2000. Plant J. 21:281-288.
GT1CONSENSUS	-1292 (+), -1008 (+), -991 (+), -848 (+), -736 (+), -600 (+), -254 (+), -253 (+), -1130 (+), -129 (+), -1299 (-), -1281 (-), -1089 (-), -699 (-), -1358 (-), -293 (-), -169 (-),	GRWAAW	**Buchel, A.S. et al,** 1999. Plant Mol. Biol. 40:387-396.
GT1CORE	-223 (-), -99 (-)	GGTTAA	**Green, P.J. et al,** 1988. EMBO J. 7:4035-4044.
GTGANTG10	-1228 (+), -850 (+), -198 (+), -936 (-), +64 (+), +278(-)	GTGA	**Rogers, H.J. et al,** 2001. Plant Mol. Biol. 45: 577-585.
HDZIP2ATATHB2	-1290 (-)	TAATMATTA	**Ohgishi, M. et al,** 2001. Plant J. 25: 389-398.
IBOX-	-1154 (+)	GATAAG	**Giuliano, G. et al,** 1988. Proc Natl Acad Sci USA. 85:7089-7093; **Rose, A.** et al, 1999. Plant J. 20, 641-652.
IBOXCORE-	-1292 (+), 1154 (+), -1008 (+), -600 (+), -1298 (-), -698 (-), -566(-)	GATAA	**Terzaghi, W.B. et al,** 1995. Annu. Rev. Plant Physiol. Plant Mol. Biol. 46:445-474.
LTRE1HVBLT49	-657 (+)	CCGAAA	**Dunn, M.A. et al,** 1998. Plant Mol. Biol. 38:551-564.
LTRECOREATCOR15	-239 (+), -115 (+)	CCGAC	**Baker, S.S. et al,** 1994. Plant Mol. Biol. 24:701-713.
MYB2AT	-965 (-)	TAACTG	**Urao, T. et al,** 1993. Plant Cell. 5:1529-1539.

MYBATRD22-	-614 (+)	CTAACCA	**Abe, H. et al,** 1997. Plant Cell. 9:1859-1868.
MYBCORE	-965 (+), -968 (-)	CNGTTR	**Urao, T. et al,** 1993. Plant Cell. 5:1529-1539.
MYBGAHV	-1146 (+)	TAACAAA	**Gubler, F. et al,** 1995. Plant Cell. 7:1879-1891; **Morita A. et al,** 1998. FEBS Lett. 423:81-85.
MYBPLANT-	-612 (+), -744 (-)	MACCWAMC	**Sablowski, RWM et al,** 1994. EMBO J 13:128-137. **Tamagnone, L. et al,** 1998. Plant Cell. 10: 135-154.
MYBPZM	-974 (+), -740 (-), -1155 (+), -601 (+), -697 (-), -565 (-)	CCWACC	**Grotewold, E. et al,** 1994. Cell 76:543-553.
NTBBF1ARROLB	-622 (+), -295 (+), -193 (+), -171 (+), -69 (+), -1275 (-),	ACTTTA	**Baumann, K. et al,** 1999. Plant Cell. 11:323-333.
POLASIG1-	-1141 (+), -733 (+), -678 (+) , -1323 (+), -1181 (+), -1050 (+), -672 (+), -228 (+), -104 (+)	AATAAA	**O'Neill, S.D. et al,** 1990. Mol Gen Genet 221:235-244.
POLLEN1LELAT52	-992 (+), -681 (+), -1356 (-), -1279 (-), -1069 (-), -556 (-),	AGAAA	**Bate, N. and Twell D.** 1998. Plant Mol. Biol. 37:859-869.
PYRIMIDINEBOXHV	-254 (-), -130 (-)	TTTTTTCC	**Cercos, M. et al,** 1999. Plant J. 19: 107-118.
REALPHALGLHCB21	-612 (+), -742 (-)	AACCAA	**Degenhardt, J and Tobin, E.M.** 1996. Plant Cell. 8: 31-41.
ROOTMOTIFTAPOX1	-1128 (+), -1046 (+), -838 (+), -761 (+), -668 (+), -639 (+), -412 (+), -1371 (-), -1129 (-), -1047 (-), -882 (-), -796 (-), -762 (-), -669(-), -640 (-), -585 (-), -519 (-), -247(-), -123 (-)	ATATT	**Elmayan, T. and Tepfer, M.,** 1995. Transgenic Res. 4:388-396.
SEF3MOTIFGM	-972 (+)	AACCCA	**Allen, R.D. et al,** 1989. Plant Cell. 1:623-631.
SEF4MOTIFGM7S	-783 (+), -676 (-)	RTTTTTR	**Lessard, P.A. et al,** 1991, Plant Mol. Biol. 16:397-413.

5 Vectors

5.1 pBluescript SK

f1 (+ /-) origin 6-462 bp
Multiple Cloning Site (MCS) 657-759 bp
***lac* Promoter** 816-938 bp
ColE1 origin 1032-1912 bp
Ampicillin (ORF) 1975-2832 bp

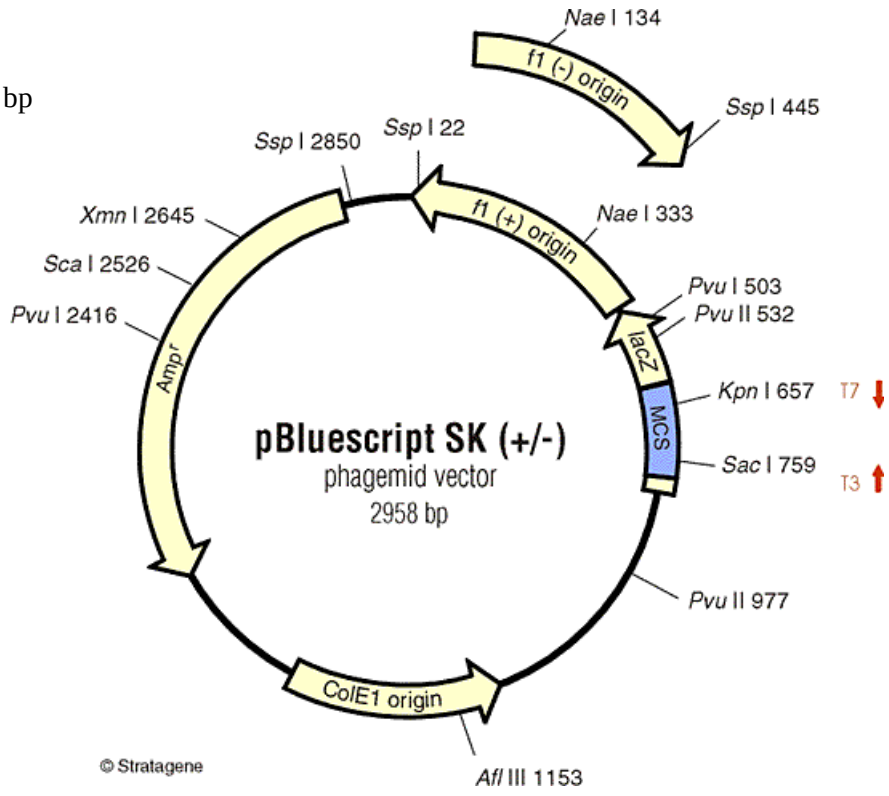

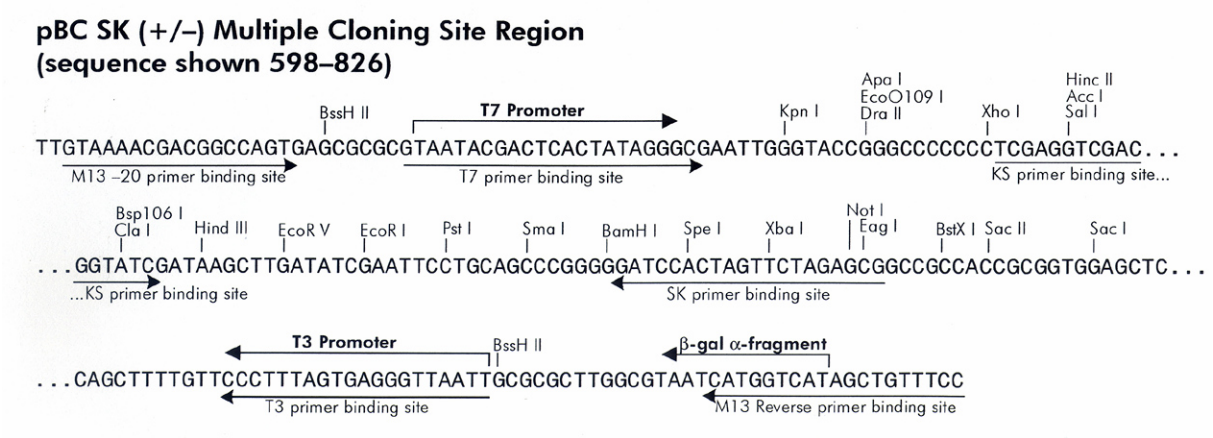

GenBank® #52325 [SK(+)] #52324 [SK(-)]

Source: http://www.stratagene.com

5.2 pCR® 2.1-TOPO

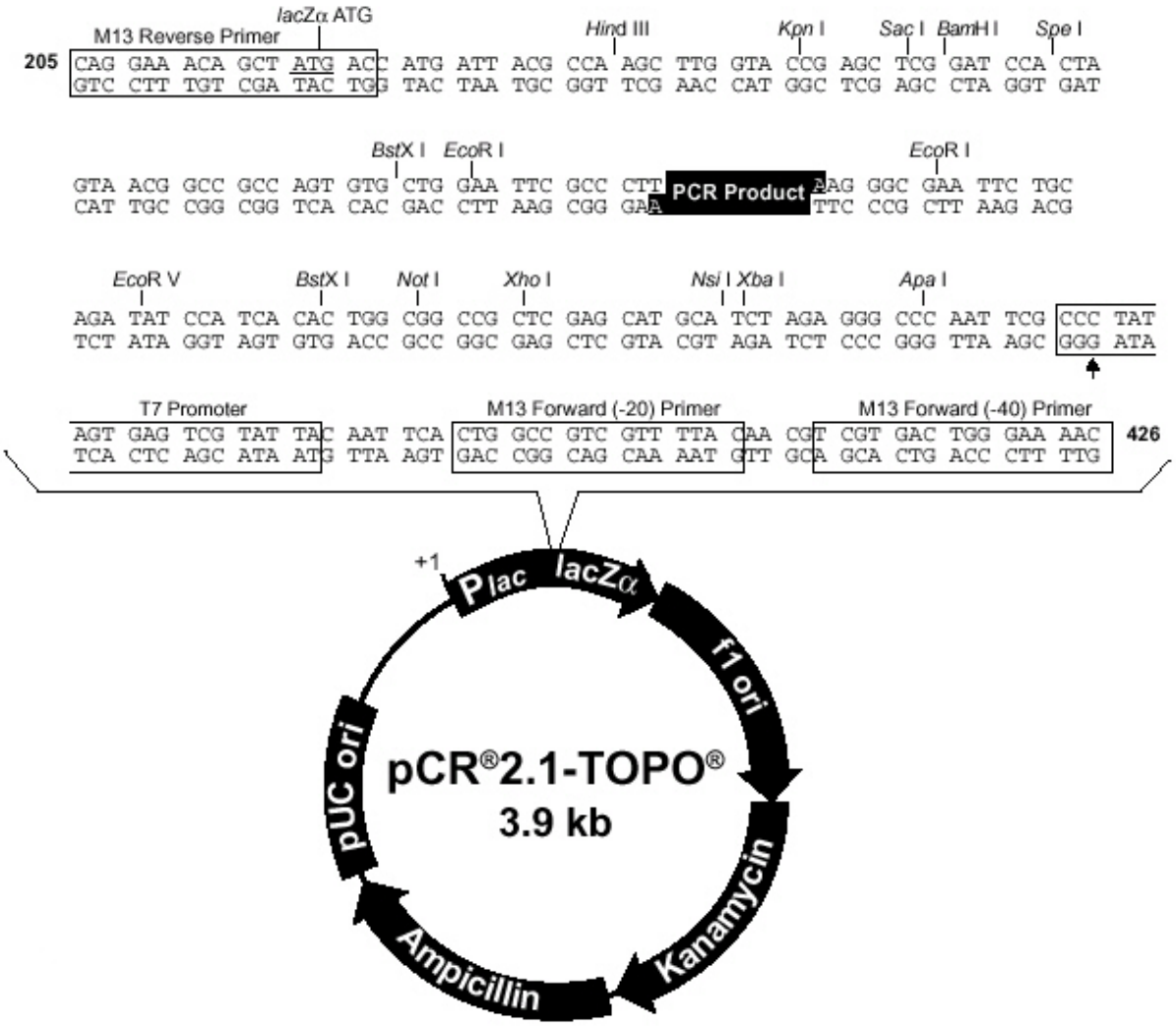

LacZa Fragment 1-571 bp
Multiple Cloning Site 234-357 bp
f1 Origin 548-962 bp
Kanamycin Resistenz ORF 1296-2090 bp
Ampicillin Resistenz ORF 2108-2968 bp
pUC Origin 3113-3786 bp

Source: http://www.invitrogen.com

5.3 pBin HYG-TX

pBin HYG-TX is a pBin19 derivative: pBIB (D.Becker, NAR 18 203 (1991)).

The *Eco*RI-*Hind*III multiple cloning site was exchanged by the Triple x (TX)-Cassette (35S derivative). With that the tetracycline repressor (tetR) controlled expression, inducible by tetracycline, is enabled.

Unique cloning sites in the Cassette: *Hpa* I, *Kpn* I, *Sma* I, *Xba* I, *Sal* I.

Between the left border (LB) and right border (RB) of *Agrobacterium* T-DNA the following regions can be found:

Operator (O) sequence, OCS enhancer sequence, pnos (promoter of nopaline synthase gene) driven hygromycin resistance gene (hpt II) with pAg7-terminator.

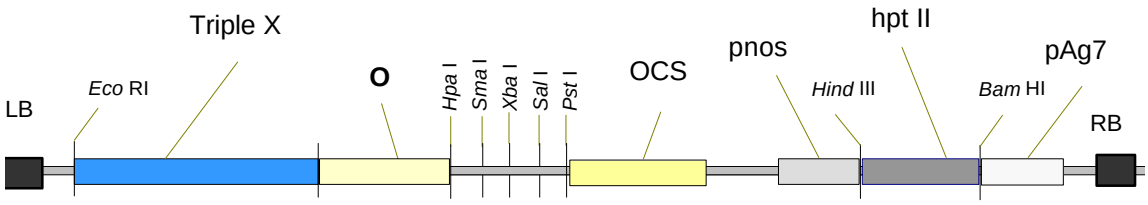

Region of pBin HYG-TX between left border (LB) and right border (RB) of *Agrobacterium* T-DNA.

5.4 pBI221

pBI221 was constructed by cloning the 3.0 kb *Hind* III-*Eco*RI fragment of pBI121 (containing 35SCaMV promoter, β-glucuronidase gene, and nopaline synthetase terminator) into pUC 19.

It refers kanamycin resistance (neomycin resistance gene, nptII).

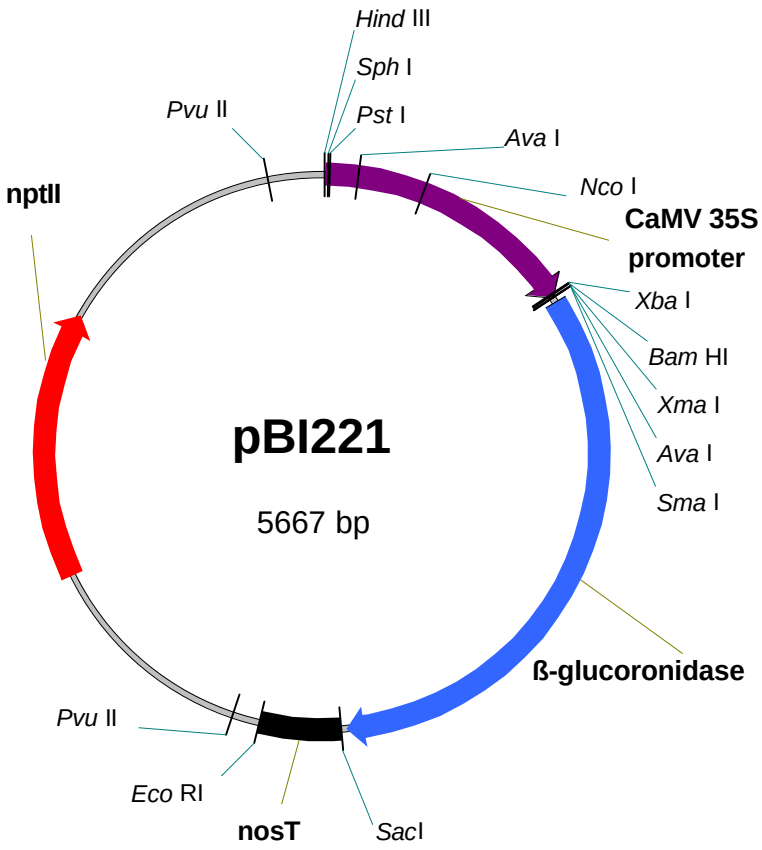

Further description: http://www.clontech.com

5.5 pGPTV

pGPTV-KAN is a binary vector conferring kanamycin (npt II) resistance, including β-glucuronidase gene with a nopaline synthetase terminator.

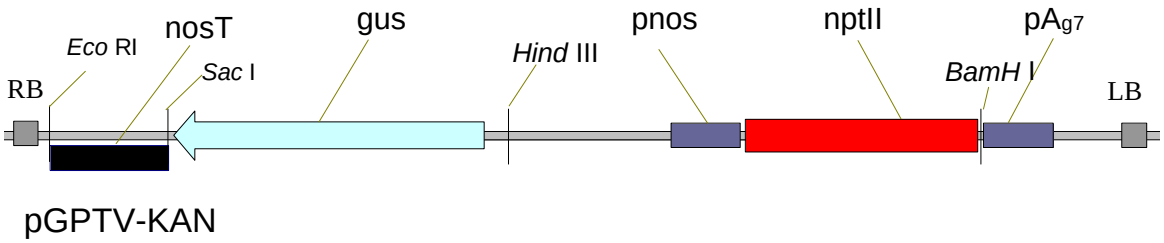

pGPTV-KAN

5.6 pUC 18

pUC18 is a relatively small cloning vector conferring ampicillin resistance.

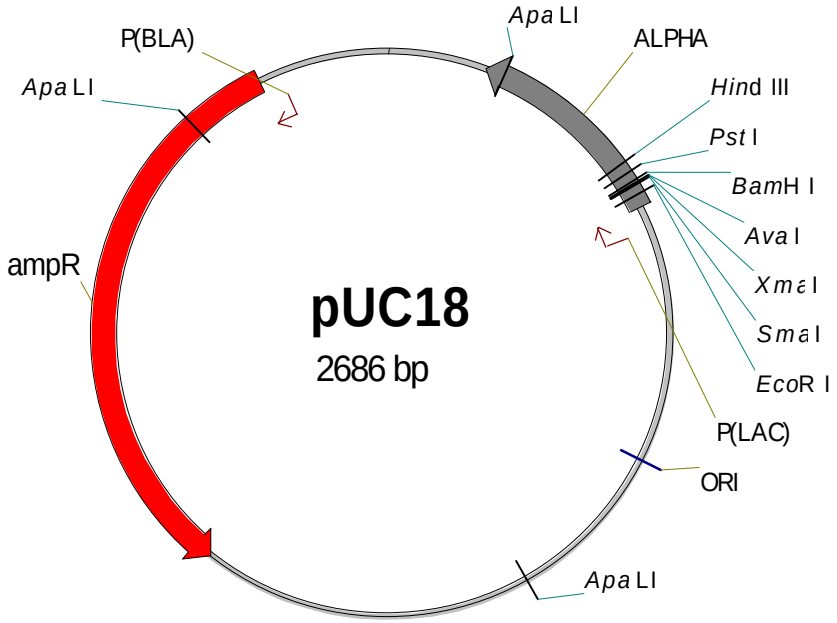

PUBLICATION LIST

Siefritz, F., Tyree, M.T., Lovisolo, C., Schubert, A., Kaldenhoff, R. (2002). PIP1 plasma membrane aquaporins in Nicotiana tabacum: From cellular effects to the function in plants. *The Plant Cell.* **14**, 869-876.

Siefritz, F., Biela, A., Eckert, M., Otto, B., Uehlein, N., Kaldenhoff, R. (2001). The tobacco plasma membrane aquaporin *Nt*AQP1. *Journal of Experimental Botany.* **52** (363), 1953-1957.

Abd-El Baki, G.K., Siefritz, F., Man, H.M., Weiner, H., Kaldenhoff, R., Kaiser, W.M. (2000). Nitrate reductase in *Zea mays* L. under salinity. *Plant Cell and Environment.* **23**, (5), 515-521.

Eckert, M., Biela, A., Siefritz, F., Kaldenhoff, R. (1999). New aspects of plant aquaporin regulation and specificity. *Journal of Experimental Botany.* **50** (339), 1541-1545.

Printed conference contributions:

Kaldenhoff, R., Otto, B., Biela, A., Siefritz, F., Eckert, M. (2000). Expression, location and function of a plasma membrane and chloroplast located aquaporin from tobacco. In: Hohmann, S.and Nielsen, S., editor. Molecular biology and physiology of water and solute transport. Dodrecht, New York. 43: Kluwer Academics/Plenum Publishers, 2000:43.

Presentations:

Rhein-Main-Kolloquium der Botanischen Institute, Gießen 2001. How important are aquaporins for the water transport in plants?

contributed:

Water relations of *Nt*AQP1-Aquaporin-Antisense Tobacco plants. XL congresso annuale della societa`italiana di fisiologia vegetale-SIFV, 2001

Poster presentations:

International Meeting on "Universal Principles of Pro- and Eukaryotic Membrane Transport Systems". Osnabrück 1999. Activity, selectivity and mercury-sensitivity of plant plasma membrane aquaporins.

Final Symposium des Sonderforschungsbereich 251:"Ökologie, Physiology und Biochemie pflanzlicher und tierischer Leistungen unter Stress", 2000, Retzbach.

Plant Biology 2001, Providence, R.I, USA. How important are aquaporins for plants?

CURRICULUM VITAE

Persönliche Daten

Name	Franka Siefritz
Geburtsdatum	07. Februar 1974
Geburtsort	Schweinfurt, Deutschland
Familienstand	ledig
Staatsangehörigkeit	deutsch

Schulausbildung

1980-1984	Grundschule in Gochsheim
1984-1993	Besuch des Alexander-von-Humboldt-Gymnasiums Schweinfurt
Juli 1993	Allgemeine Hochsschulreife

Hochschulstudium

1993-1995	Grundstudium der Biologie an der Julius-Maximillians-Universität Würzburg, Vordiplom
Juni/Juli 1996	Praktikum am Max-Planck-Institut für Biochemie Martinsried, bei Prof. Dr. Wolfram Zillig. Thema: Charakterisierung zweier neuer Viren von *Sulfolobus islandicus* und die Natur der UV-Induzierbarkeit der SSV1-verwandten genetischen Elemente.
1996-1997	Auslandsstudium an der State University of New York (SUNY) Albany, USA. Partnerschaftsprogramm der Universität Würzburg, DAAD-Stipendium. Laborpraktikum: Ph.D Dmitry A. Belostotsky, Assistant Professor, Molecular Plantgenetics.
1997-1998	Studium der Biologie an der Julius-Maximillians-Universität Würzburg
1998	Diplomarbeit am Lehrstuhl Molekulare Pflanzenphysiologie und Biophysik bei Prof. Dr. Ralf Kaldenhoff, Julius-von-Sachs-Institut für Biowissenschaften, Universität Würzburg. Thema: Identifikation und Analyse des *Nt*AQP1 Aquaporingen-Promotors aus *Nicotiana tabacum*.
ab Januar 1999	Wissenschaftliche Mitarbeiterin am Lehrstuhl für Molekulare Pflanzenphysiologie und Biophysik der Universität Würzburg.

Promotion

Februar 1999	Promotionsstudium am Lehrstuhl Molekulare Pflanzenphysiologie und Biophysik bei Prof. Dr. Ralf Kaldenhoff, Julius-von-Sachs-Institut für Biowissenschaften, Universität Würzburg.
Mai/Juni2000	Druckmesssonden-Seminar bei Prof. Dr. Steudle, Universität Bayreuth.
Juli 2000	Gaswechsel Studien an *Nt*AQP1-Antisense Tabak, Universität Turin, Italien.
Januar 2001	Tabak-NMR Studien, Universität Wageningen, Niederlande.

ERKLÄRUNG

Hiermit erkläre ich, dass ich die vorliegende Dissertation in allen Teilen selbst angefertigt und keine anderen als die angegebenen Quellen und Hilfsmittel verwendet habe.

Ich habe die Dissertation weder in gleicher noch in ähnlicher Form in anderen Prüfungsverfahren vorgelegt.

Ich erkläre weiterhin, dass ich bislang noch keine weiteren akademischen Grade erworben oder zu erwerben versucht habe.

Werneck, April 2002

.....